Digital Beamforming and MIMO-SAR Systems

Gerhard Krieger

German Aerospace Center - DLR

Microwaves and Radar Institute

Oberpfaffenhofen

Future SAR Systems: Motivation

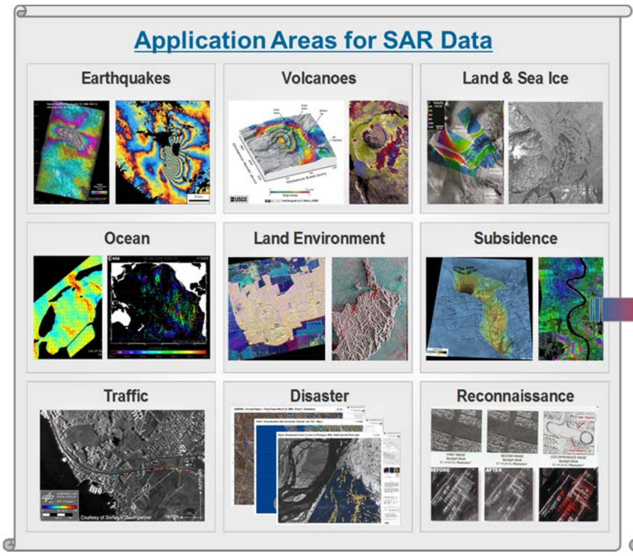

Future Demands

- *wider coverage and shorter revisit times*
- *higher geometric and radiometric resolution*
- *new data products from coherent combinations of SAR images:*
  - *Delta-DEMs (ice mass balance, ...)*
  - *3-D volume imaging (forest structure, ...)*
  - *4-D tomography (biomass dynamics, ...)*
- *reliable data supply*
- *cost efficiency*

Future SAR Systems: Motivation

New SAR Techniques and Technologies

Digital Beamforming | MIMO-SAR | Hybrid & Adaptive SAR

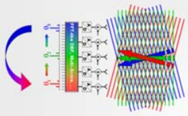

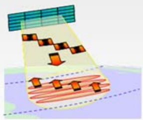

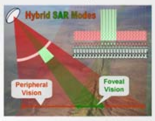

New Data Acquisition Concepts

GEO - MEO - LEO | Sparse Satellite Arrays | Novel Platforms

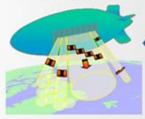

New Retrieval Algorithms and Products

Object Dynamics | 3-D & 4-D Structure | Data Fusion

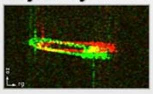

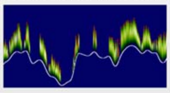

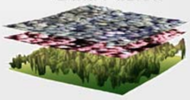

Future Demands

- *wider coverage and shorter revisit times*
- *higher geometric and radiometric resolution*
- *new data products from coherent combinations of SAR images:*
  - *Delta-DEMs (ice mass balance, ...)*
  - *3-D volume imaging (forest structure, ...)*
  - *4-D tomography (biomass dynamics, ...)*
- *reliable data supply*
- *cost efficiency*

DLR

SAR System Design Constraints

DLR

Limitations of Conventional SAR Sensors

SAR is the ideal sensor for the observation of dynamic processes on the Earth surface, but ...

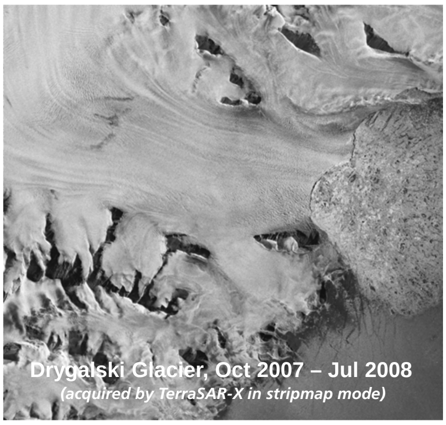

	Imaging Mode (Single Pol.)		
	ScanSAR	Stripmap	Spotlight
Resolution	16 m	3 m	1 m
Swath Width	100 km	30 km	10 km
Duty Cycle	3 minutes / orbit		

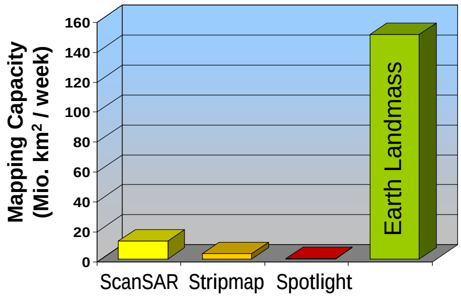

DLR

SAR Systems: State of the Art and Future Requirements

State of the Art (TerraSAR-X)	Imaging Mode (**single pol.**)		
	ScanSAR	Stripmap	Spotlight
Resolution	**16 m**	**3 m**	**1 m**
Swath Width	**100 km**	**30 km**	**10 km**
Orbit Duty Cycle	**3 minutes per orbit**		

Resolution ⟷ Swath Width ⟷ Repeat Cycle

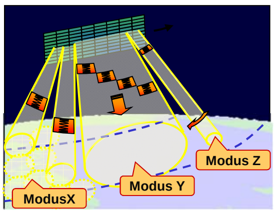

Future Requirements	Imaging Mode (**quad pol.**)		
	Mode X	Mode Y	Mode Z
Resolution	**5 m**	**2 m**	**1 m**
Swath Width	**500 km**	**200 km**	**100 km**
Orbit Duty Cycle	**> 50 minutes per orbit**		

DLR

SAR Systems: State of the Art and Future Requirements

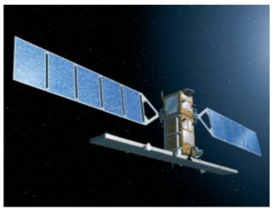

State of the Art (Sentinel-1)	Imaging Mode (**single/dual pol.**)		
	EW	IW	SM
Resolution	**40 m**	**20 m**	**5 m**
Swath Width	**400 km**	**250 km**	**80 km**
Orbit Duty Cycle	**25 minutes per orbit**		

Resolution ⟷ Swath Width ⟷ Repeat Cycle

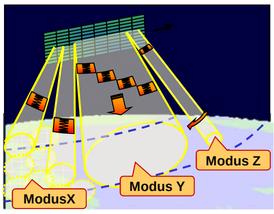

Future Requirements	Imaging Mode (**quad pol.**)		
	Mode X	Mode Y	Mode Z
Resolution	**5 m**	**2 m**	**1 m**
Swath Width	**500 km**	**200 km**	**100 km**
Orbit Duty Cycle	**> 50 minutes per orbit**		

SAR System Design Constraints (1)

high azimuth resolution

- high azimuth resolution δa requires long synthetic aperture L:

$$\delta a = \frac{\lambda \cdot r}{2\,L} = \frac{d_{ant}}{2}$$

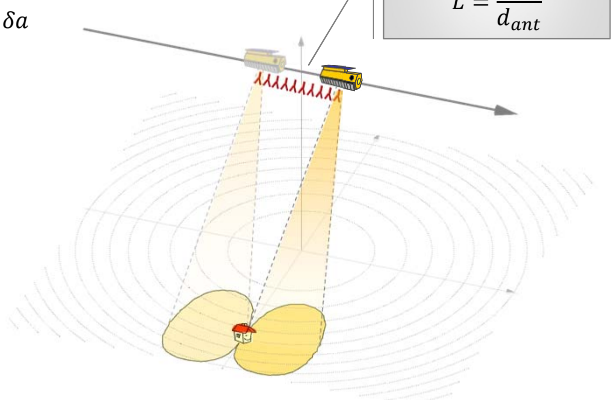

synthetic aperture

$$L = \frac{\lambda \cdot r}{d_{ant}}$$

SAR System Design Constraints (2)

high azimuth resolution

↓

large Doppler bandwidth

- long synthetic aperture is provided by short antenna with broad azimuth beam
- large azimuth beamwidth implies wide Doppler spectrum:

$$B = \frac{2 \cdot v}{d_{ant}} = \frac{v}{\delta a}$$

$$f_{Dop} = \frac{2 \cdot v}{\lambda} \cdot \cos \vartheta$$

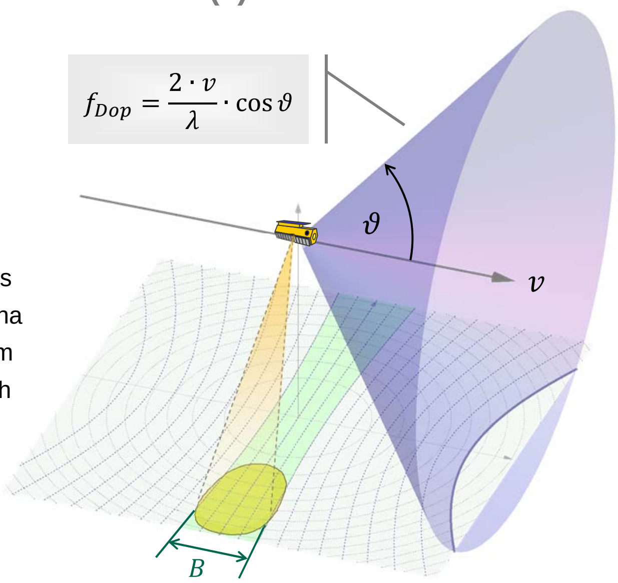

DLR

SAR System Design Constraints (3)

high azimuth resolution

↓

large Doppler bandwidth

↓

high PRF

Azimut Ambiguity-to-Signal Ratio (AASR):

$$AASR = \frac{\sum_{i \neq 0} \int_{-B_{proc}/2}^{B_{proc}/2} G^2(f + i \cdot PRF) \cdot df}{\int_{-B_{proc}/2}^{B_{proc}/2} G^2(f) \cdot df}$$

G: antenna gain

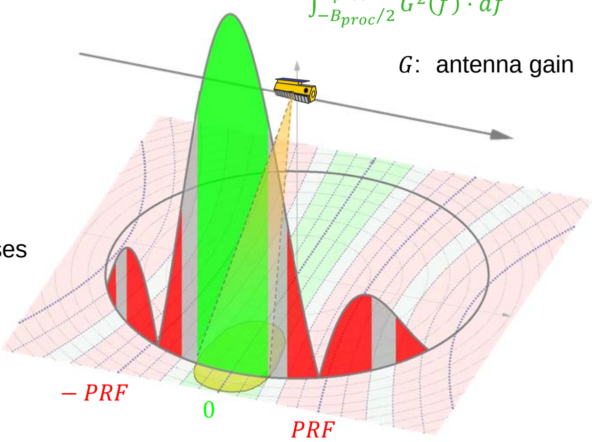

- sampling with PRF causes ambiguities (AASR)
- low AASR requires high PRF:

$$PRF > B = \frac{v}{\delta a}$$

DLR

Azimuth Ambiguities: Example

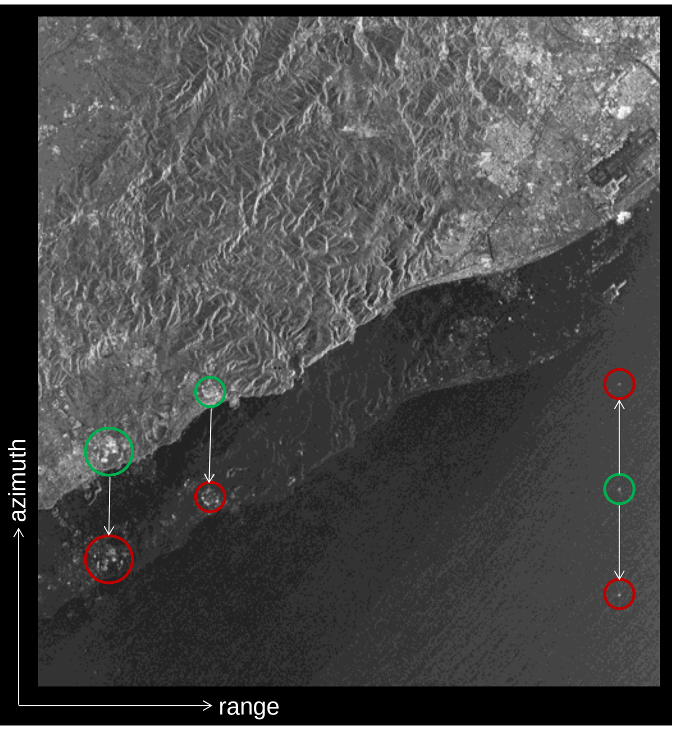

SAR System Design Constraints (4)

high azimuth resolution

↓

large Doppler bandwidth

↓

high PRF

↓

range ambiguities

- high PRF causes range ambiguities

Range Ambiguity-to-Signal Ratio (RASR):

$$RASR = \frac{\sum_{i\neq 0} \sigma^0(\theta_i)\cdot G^2(\theta_i)/\left(r_i^3\sin(\theta_i)\right)}{\sigma^0(\theta_0)\cdot G^2(\theta_0)/\left(r_0^3\sin(\theta_0)\right)}$$

G: antenna gain
σ^0: backscatter coefficient
r: range
θ: incident angle

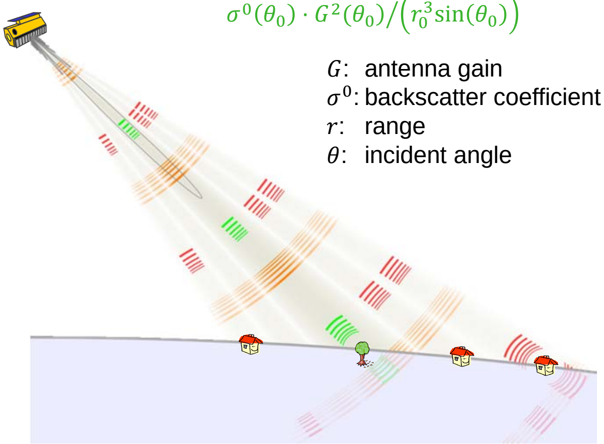

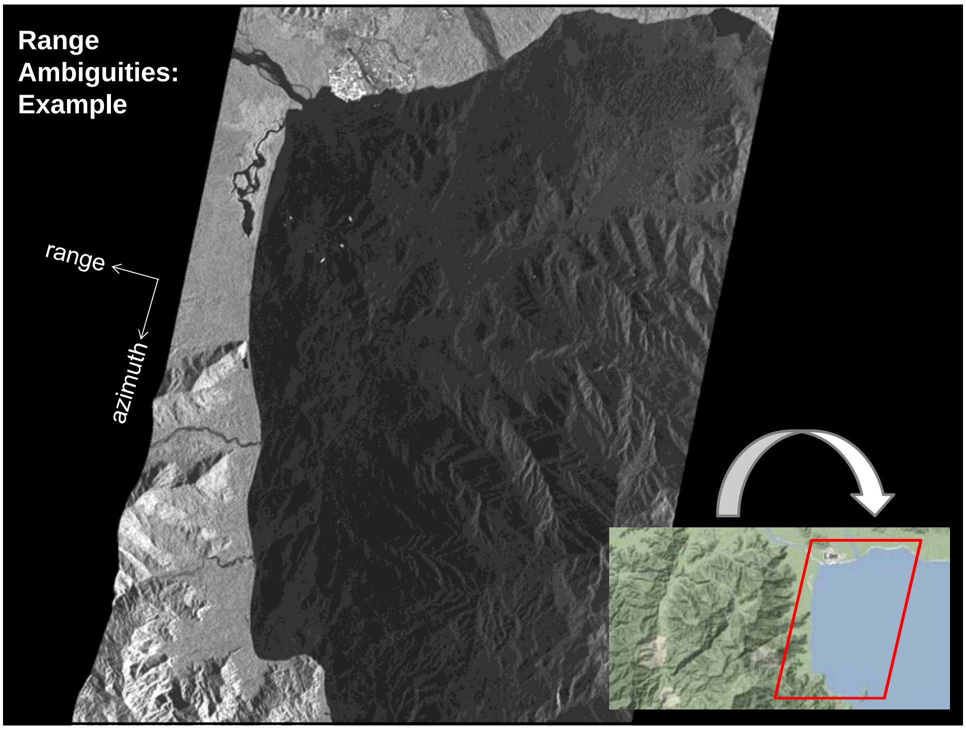
Range
Ambiguities:
Example
range
azimuth

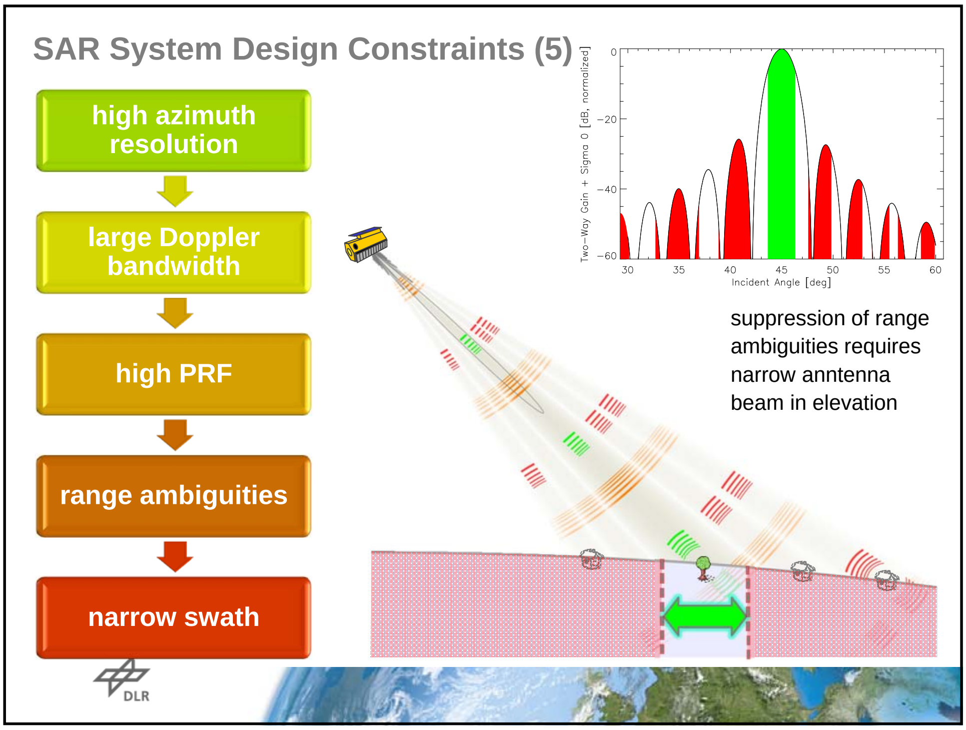
SAR System Design Constraints (5)
high azimuth resolution
large Doppler bandwidth
high PRF
range ambiguities
narrow swath
Two-Way Gain + Sigma 0 [dB, normalized]
0
-20
-40
-60
30
35
40
45
50
55
60
Incident Angle [deg]
suppression of range ambiguities requires narrow anntenna beam in elevation
DLR

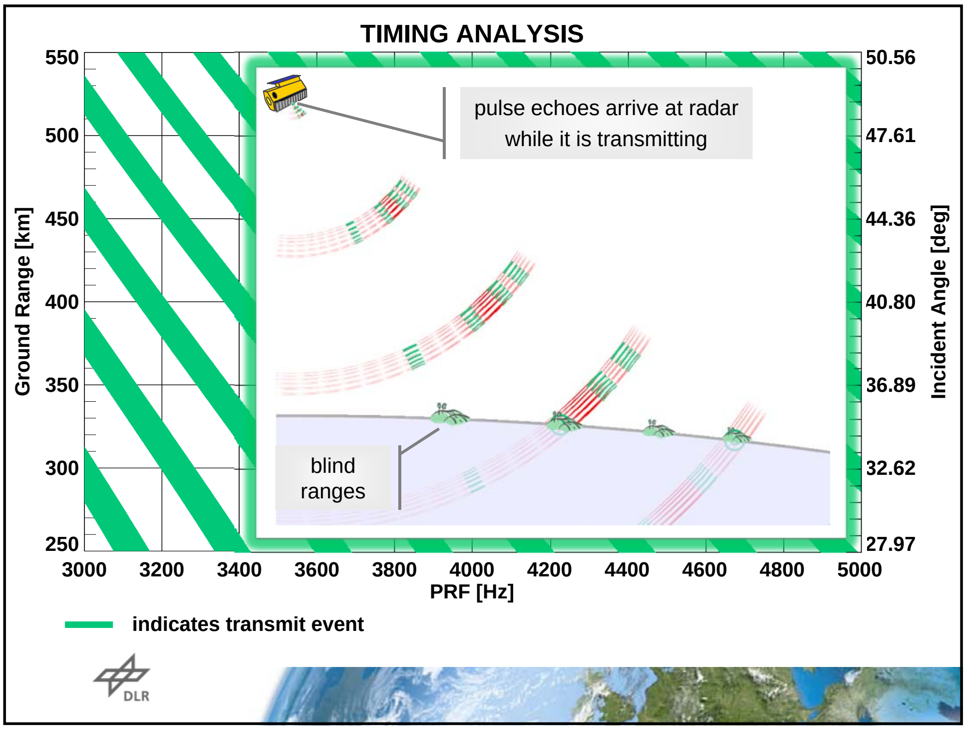
TIMING ANALYSIS
pulse echoes arrive at radar
while it is transmitting
blind
ranges
Ground Range [km]
Incident Angle [deg]
550
500
450
400
350
300
250
50.56
47.61
44.36
40.80
36.89
32.62
27.97
3000 3200 3400 3600 3800 4000 4200 4400 4600 4800 5000
PRF [Hz]
indicates transmit event
DLR

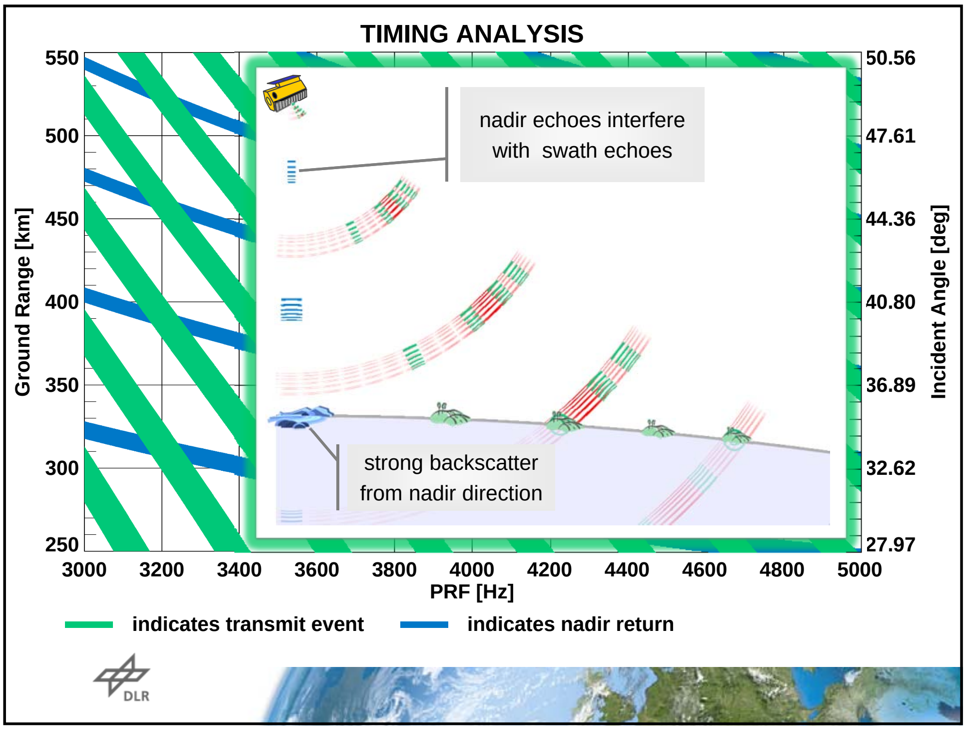
TIMING ANALYSIS
nadir echoes interfere
with swath echoes
strong backscatter
from nadir direction
Ground Range [km]
Incident Angle [deg]
550
500
450
400
350
300
250
50.56
47.61
44.36
40.80
36.89
32.62
27.97
3000 3200 3400 3600 3800 4000 4200 4400 4600 4800 5000
PRF [Hz]
indicates transmit event
indicates nadir return
DLR

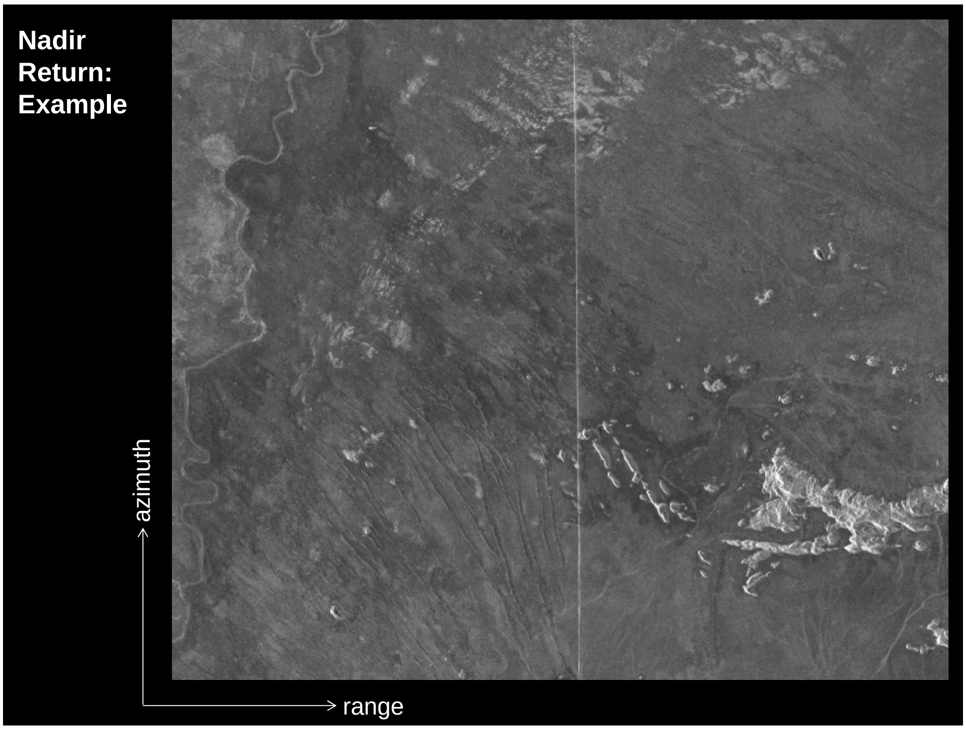

Nadir Return: Example
azimuth
range

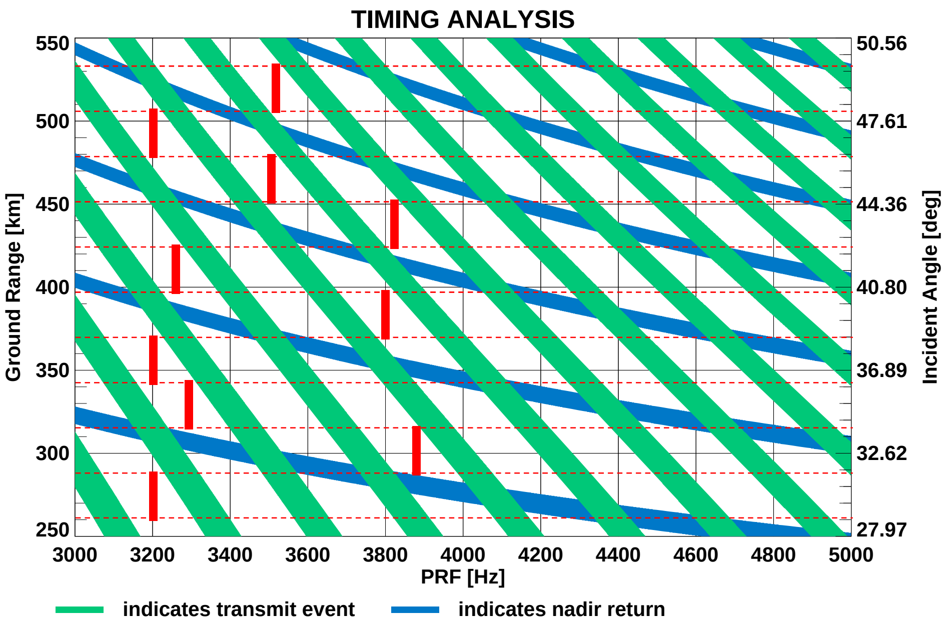

TIMING ANALYSIS
Ground Range [km]
Incident Angle [deg]
550
500
450
400
350
300
250
50.56
47.61
44.36
40.80
36.89
32.62
27.97
3000
3200
3400
3600
3800
4000
4200
4400
4600
4800
5000
PRF [Hz]
indicates transmit event
indicates nadir return

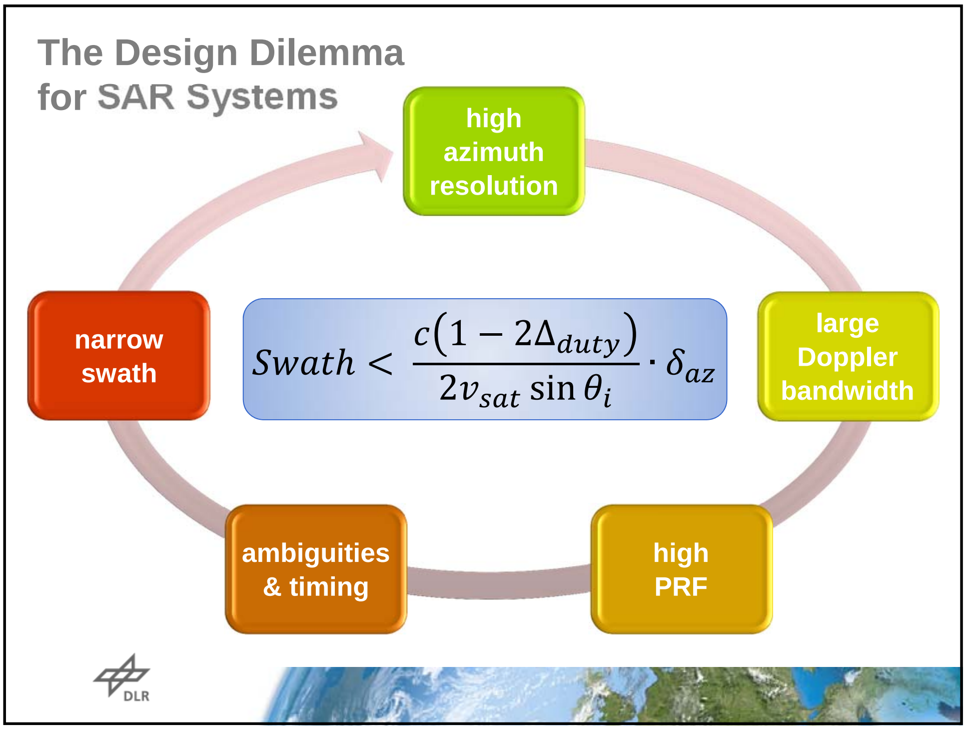
The Design Dilemma
for SAR Systems
high
azimuth
resolution
narrow
swath
$Swath < \frac{c(1-2\Delta_{duty})}{2v_{sat}\sin\theta_i}\cdot\delta_{az}$
large
Doppler
bandwidth
ambiguities
& timing
high
PRF
DLR

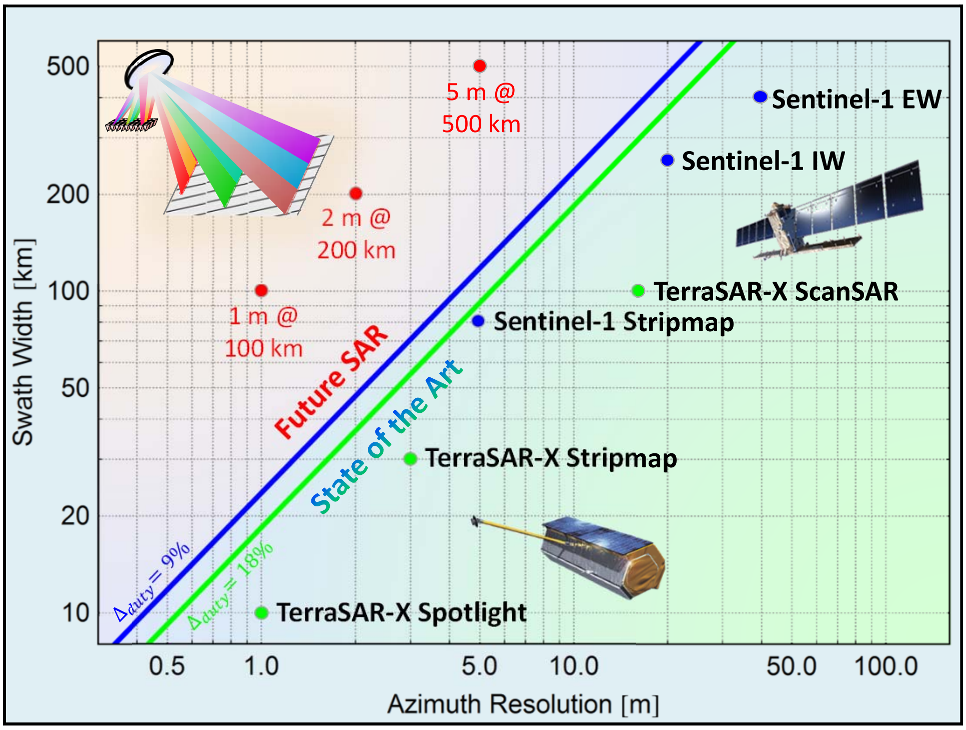
500
200
100
50
20
10
Swath Width [km]
0.5
1.0
5.0
10.0
50.0
100.0
Azimuth Resolution [m]
5 m @
500 km
2 m @
200 km
1 m @
100 km
Sentinel-1 EW
Sentinel-1 IW
TerraSAR-X ScanSAR
Sentinel-1 Stripmap
TerraSAR-X Stripmap
TerraSAR-X Spotlight
Future SAR
State of the Art
$\Delta_{duty} = 9\%$
$\Delta_{duty} = 18\%$

Digital Beamforming for SAR

Digital Beamforming / Multichannel SAR

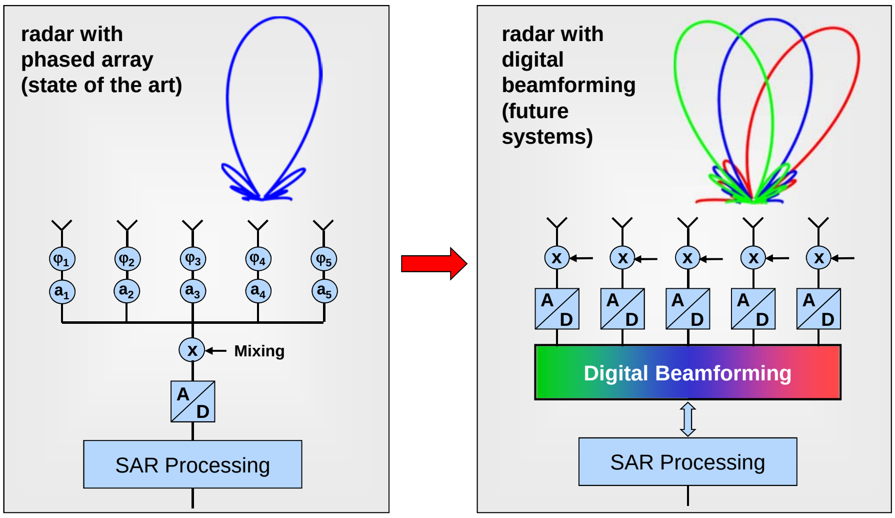

DBF-SAR Systems with Planar Arrays

Scan-On-Receive	Digital Beamforming in Elevation

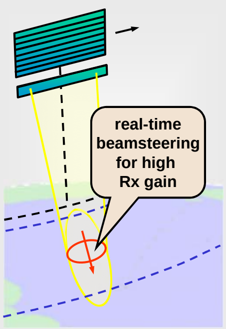

- high sensitivity and less pattern losses at swath border
- improved range ambiguity suppression

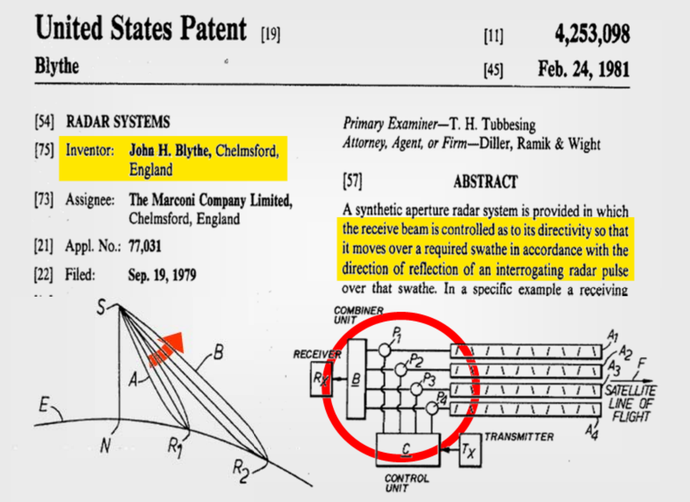

United States Patent [19] Blythe

[11] 4,253,098

[45] Feb. 24, 1981

[54] RADAR SYSTEMS

[75] Inventor: John H. Blythe, Chelmsford, England

[73] Assignee: The Marconi Company Limited, Chelmsford, England

[21] Appl. No.: 77,031

[22] Filed: Sep. 19, 1979

Primary Examiner—T. H. Tubbesing

Attorney, Agent, or Firm—Diller, Ramik & Wight

[57] ABSTRACT

A synthetic aperture radar system is provided in which the receive beam is controlled as to its directivity so that it moves over a required swathe in accordance with the direction of reflection of an interrogating radar pulse over that swathe. In a specific example a receiving

J.H. Blythe, Radar Systems, US Patent 4253098, 1981.

DBF-SAR Systems with Planar Arrays

Scan-On-Receive	Digital Beamforming in Elevation

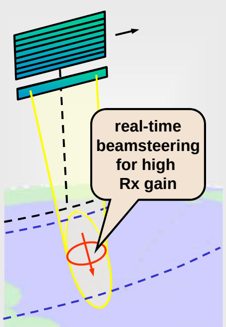

- high sensitivity and less pattern losses at swath border
- improved range ambiguity suppression

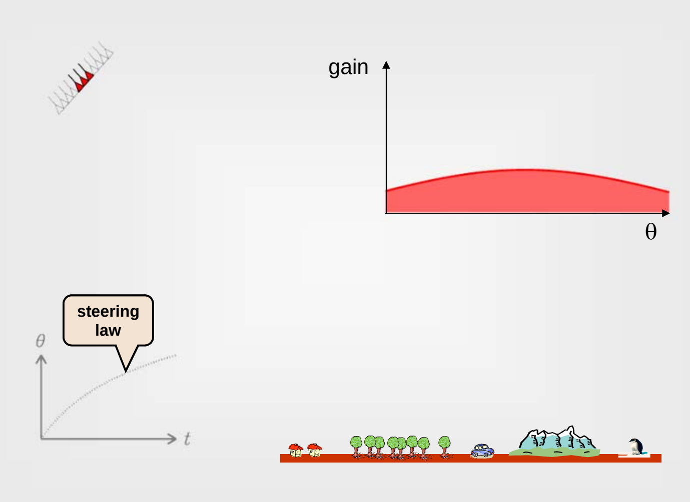

DBF-SAR Systems with Planar Arrays

Scan-On-Receive | **Digital Beamforming in Elevation**

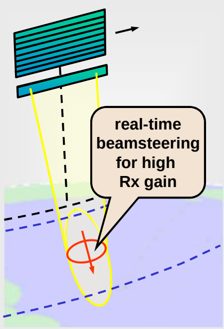

- high sensitivity and less pattern losses at swath border
- improved range ambiguity suppression

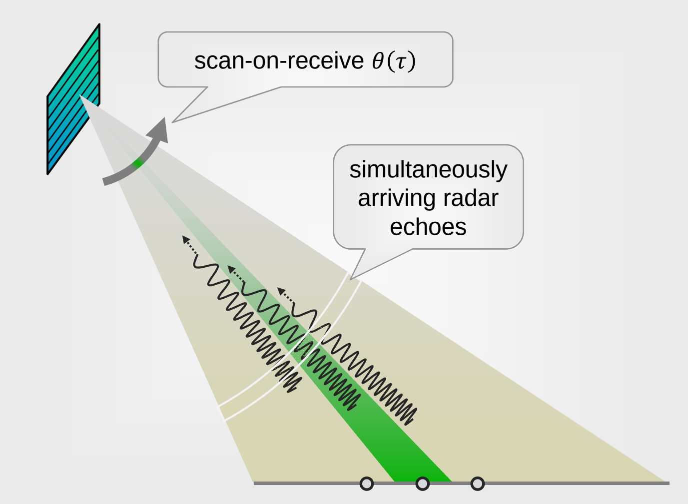

DBF-SAR Systems with Planar Arrays

Scan-On-Receive | **Digital Beamforming in Elevation**

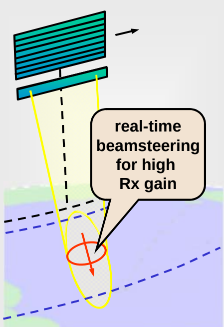

- high sensitivity and less pattern losses at swath border
- improved range ambiguity suppression

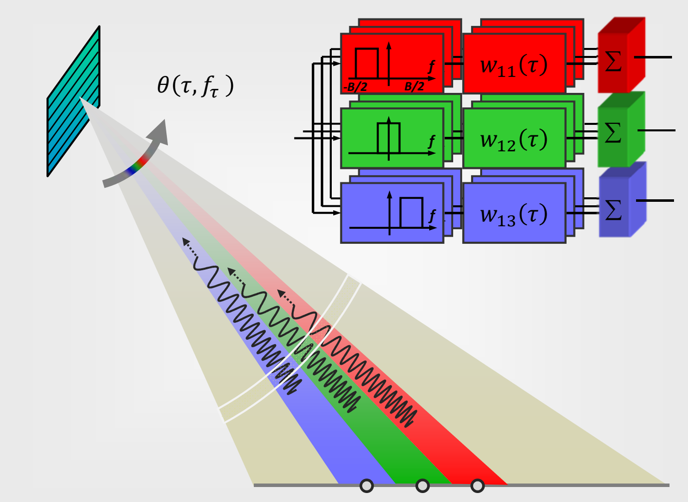

DBF-SAR Systems with Planar Arrays

Scan-On-Receive | **Digital Beamforming in Elevation**

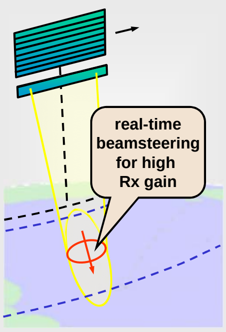

- high sensitivity and less pattern losses at swath border
- improved range ambiguity suppression

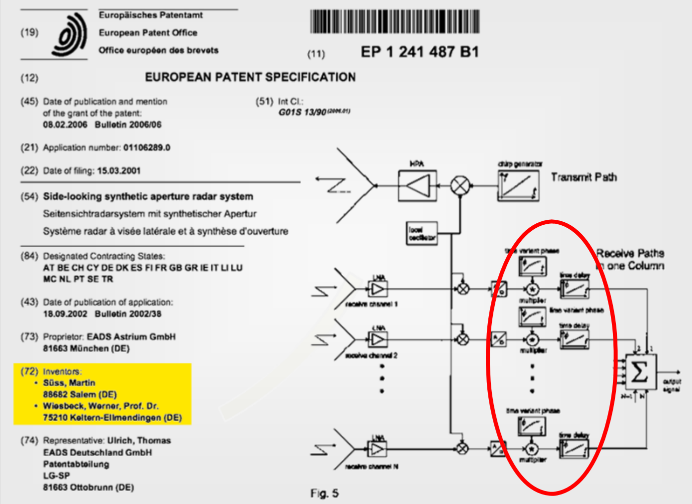

(19) Europäisches Patentamt
European Patent Office
Office européen des brevets

(11) EP 1 241 487 B1

(12) EUROPEAN PATENT SPECIFICATION

(45) Date of publication and mention of the grant of the patent:
08.02.2006 Bulletin 2006/06

(51) Int Cl.:
G01S 13/90

(21) Application number: 01106289.0

(22) Date of filing: 15.03.2001

(54) Side-looking synthetic aperture radar system
Seitensichtradarsystem mit synthetischer Apertur
Système radar à visée latérale et à synthèse d'ouverture

(84) Designated Contracting States:
AT BE CH CY DE DK ES FI FR GB GR IE IT LI LU MC NL PT SE TR

(43) Date of publication of application:
18.09.2002 Bulletin 2002/38

(73) Proprietor: EADS Astrium GmbH
81663 München (DE)

(72) Inventors:
- Süss, Martin
88682 Salem (DE)
- Wiesbeck, Werner, Prof. Dr.
75210 Keltern-Ellmendingen (DE)

(74) Representative: Ulrich, Thomas
EADS Deutschland GmbH
Patentabteilung
LG-SP
81663 Ottobrunn (DE)

M. Suess et al., A novel high resolution, wide swath SAR system, Proc. IGARSS, pp. 1013-15, 2001.

DLR

DBF-SAR Systems with Planar Arrays

Scan-On-Receive | **Digital Beamforming in Elevation**

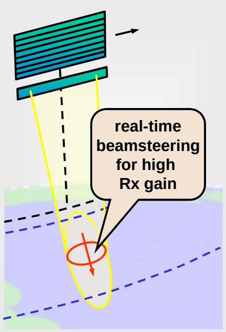

- high sensitivity and less pattern losses at swath border
- improved range ambiguity suppression

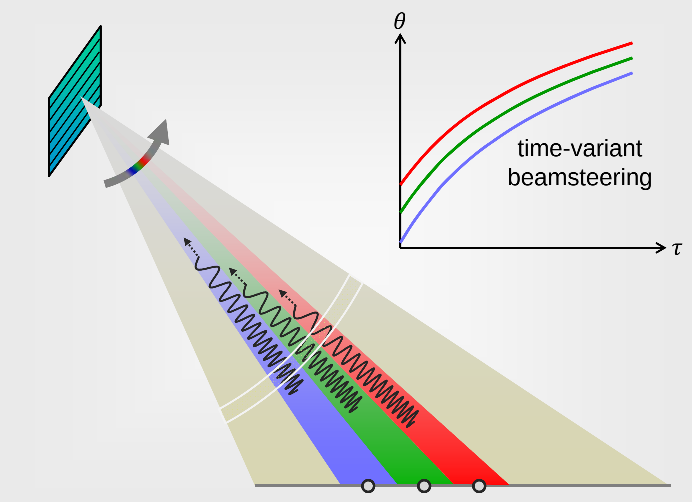

DLR

DBF-SAR Systems with Planar Arrays

Scan-On-Receive

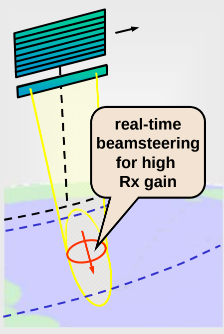

- high sensitivity and less pattern losses at swath border
- improved range ambiguity suppression

Digital Beamforming in Elevation

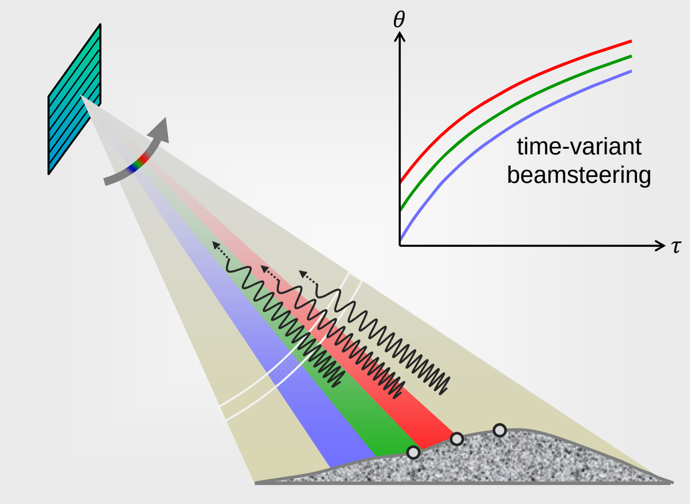

Losses from Beam Mispointing due to Topography (X-Band)

$h_{ant} = 1$ m	$h_{ant} = 2$ m	$h_{ant} = 3$ m

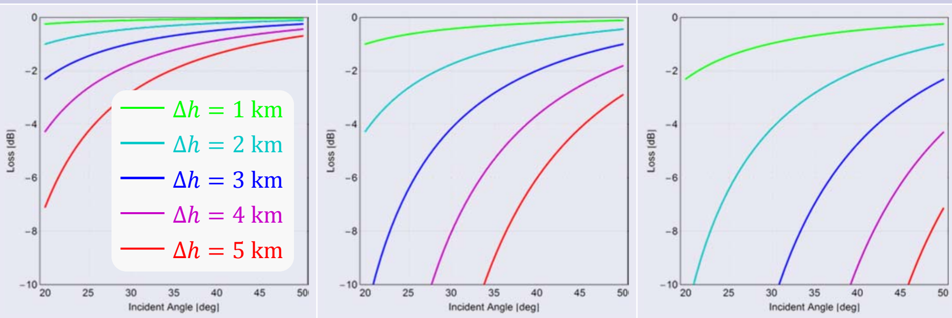

$$h_{orbit} = 700\text{ km},\ \theta_{ant} = 35°,\ \lambda = 3.1\text{ cm}$$

1. high antenna requires a beam steering law in accordance with topography (either via coarse onboard DEM or appropriate commanding from ground)
2. topography variations within a wide azimuth beam must also be considered
3. additional mispointing due to range cell migration (for high res. & ScanSAR)

Losses from Beam Mispointing due to Topography (L-Band)

$h_{ant} = 5$ m	$h_{ant} = 7.5$ m	$h_{ant} = 10$ m

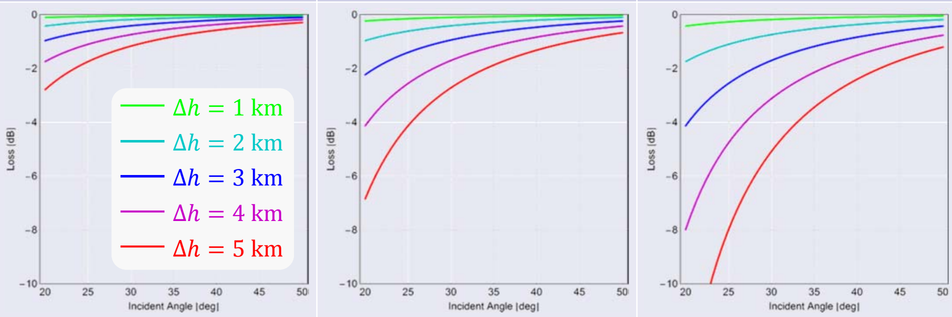

$h_{orbit} = 700$ km, $\theta_{ant} = 35°$, $\lambda = 23.6$ cm

1. high antenna requires a beam steering law in accordance with topography (either via coarse onboard DEM or appropriate commanding from ground)
2. topography variations within a wide azimuth beam must also be considered
3. additional mispointing due to range cell migration (for high res. & ScanSAR)

DLR

DBF-SAR Systems with Planar Arrays

Scan-On-Receive	Digital Beamforming in Elevation
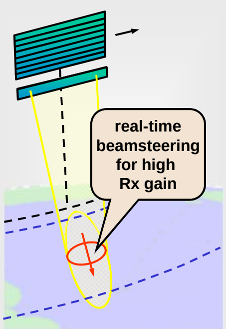	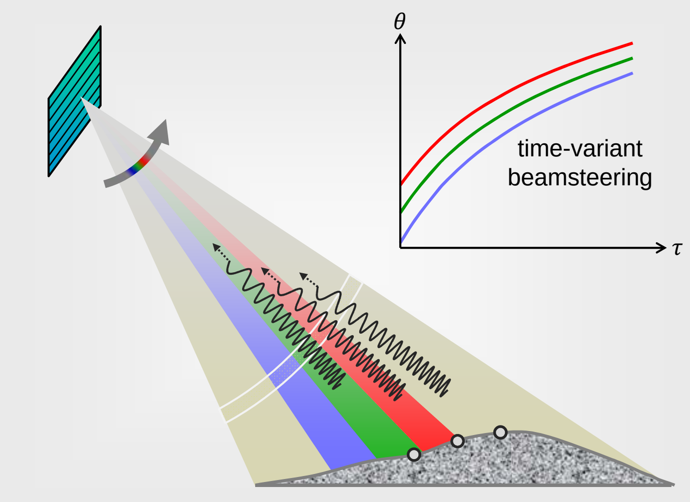
▪ high sensitivity and less pattern losses at swath border ▪ improved range ambiguity suppression	

DLR

DBF-SAR Systems with Planar Arrays

Scan-On-Receive	Digital Beamforming in Elevation

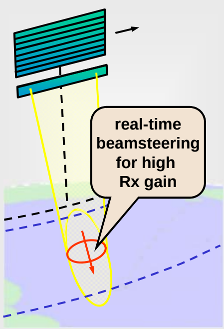

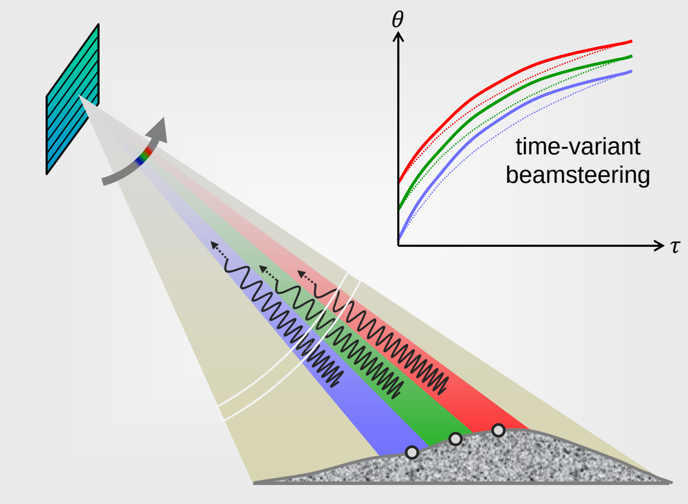

- high sensitivity and less pattern losses at swath border
- improved range ambiguity suppression

DLR

DBF-SAR Systems with Planar Arrays

DPCA	Multiple Rx Apertures in Azimuth

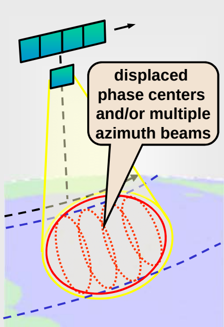

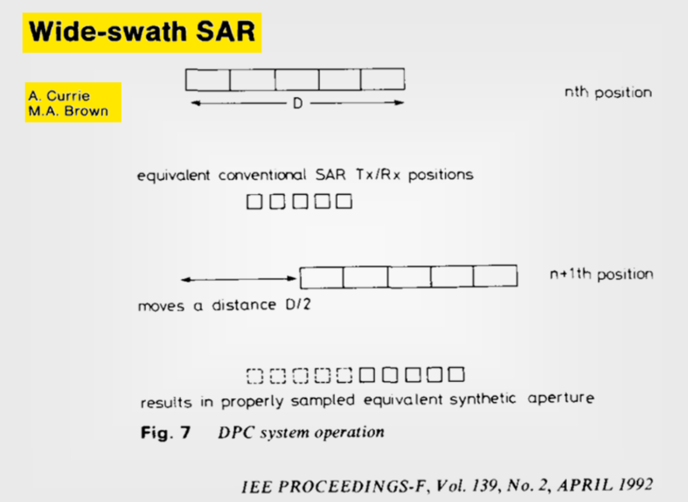

- enables high azimuth resolution and wide swath
- requires dedicated multichannel SAR processing

DLR

A. Currie et al., Wide-swath SAR, IEE Proc. F – Radar and Signal Processing, Vol. 139, pp. 122-135, 1992.

DBF-SAR Systems with Planar Arrays

DPCA	Multiple Rx Apertures in Azimuth
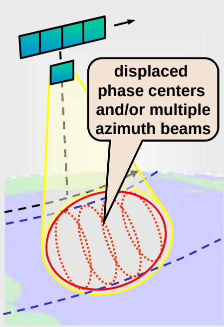	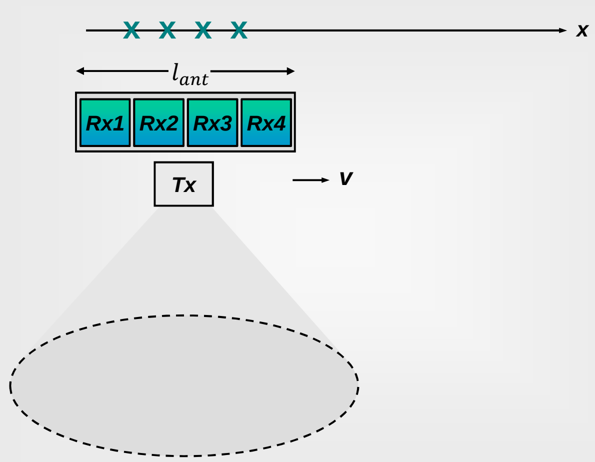
▪ enables high azimuth resolution and wide swath ▪ requires dedicated multichannel SAR processing	

DLR

DBF-SAR Systems with Planar Arrays

DPCA	Multiple Rx Apertures in Azimuth
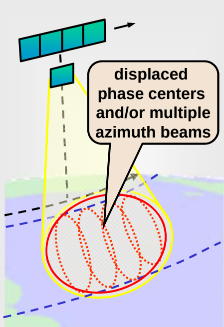	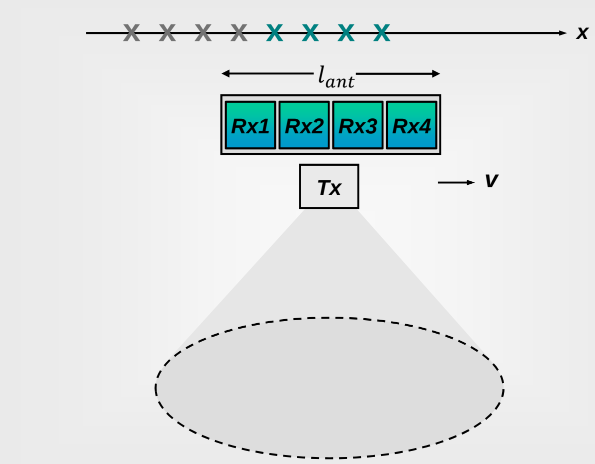
▪ enables high azimuth resolution and wide swath ▪ requires dedicated multichannel SAR processing	

DLR

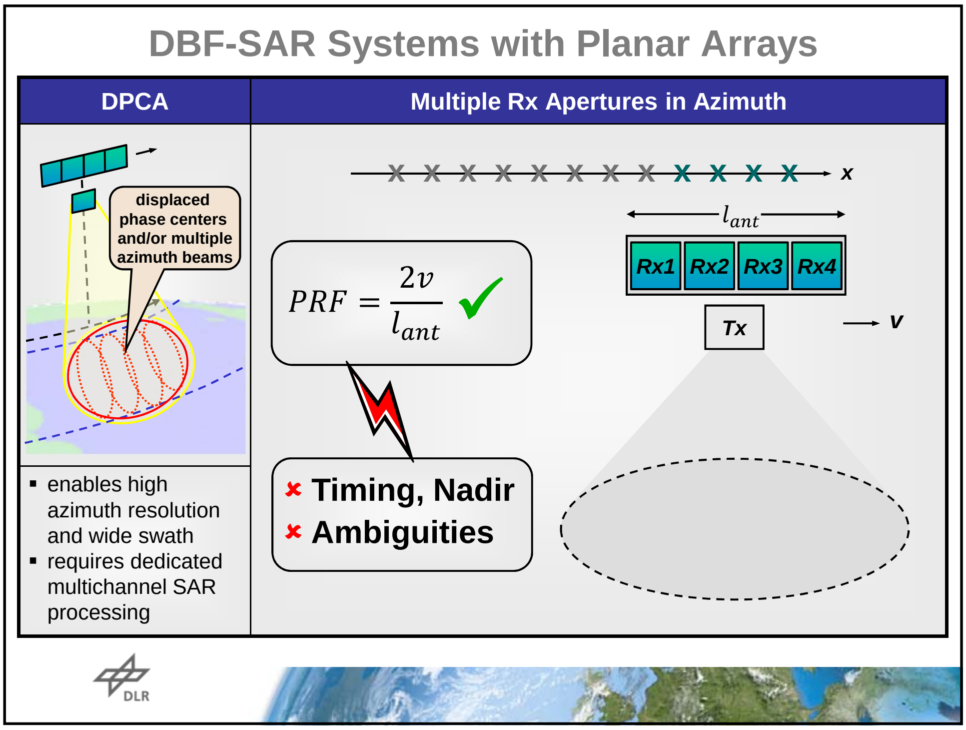
DBF-SAR Systems with Planar Arrays
DPCA
Multiple Rx Apertures in Azimuth
displaced phase centers and/or multiple azimuth beams
enables high azimuth resolution and wide swath
requires dedicated multichannel SAR processing
x
l_{ant}
Rx1
Rx2
Rx3
Rx4
Tx
v
$PRF = \frac{2v}{l_{ant}}$
Timing, Nadir
Ambiguities
DLR

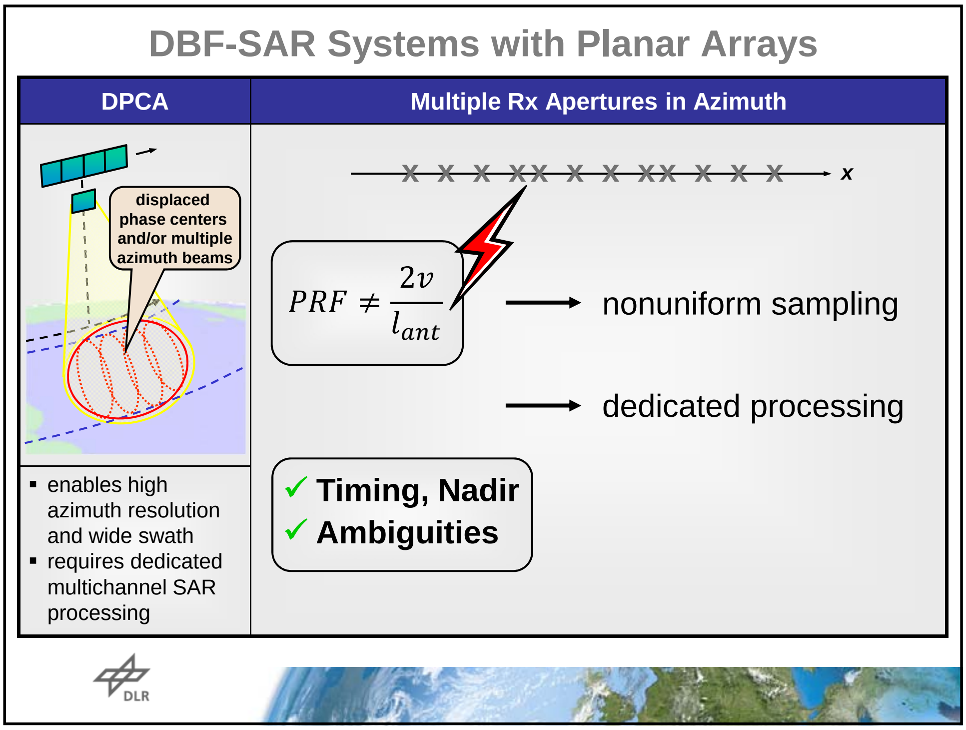
DBF-SAR Systems with Planar Arrays
DPCA
Multiple Rx Apertures in Azimuth
displaced phase centers and/or multiple azimuth beams
enables high azimuth resolution and wide swath
requires dedicated multichannel SAR processing
x
$PRF \neq \frac{2v}{l_{ant}}$
nonuniform sampling
dedicated processing
Timing, Nadir
Ambiguities
DLR

DBF-SAR Systems with Planar Arrays

DPCA

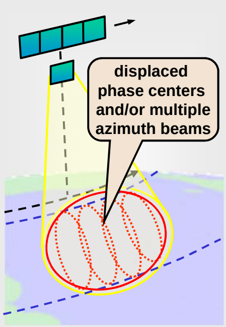

- enables high azimuth resolution and wide swath
- requires dedicated multichannel SAR processing

Multiple Rx Apertures in Azimuth

System Model:

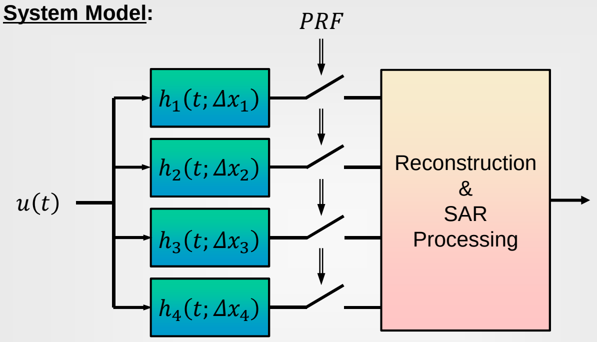

Bistatic Azimuth Impulse Response:

$$h_i(t;\Delta x_i) \cong A_{Tx}(vt)\cdot A_{Rx,i}(vt-\Delta x_i)\cdot \exp\left[-j\frac{2\pi}{\lambda}\left(r_{Tx}(vt)+r_{Rx}(vt-\Delta x_i)\right)\right]$$

G. Krieger et al., Unambiguous SAR signal reconstruction from nonuniform displaced phase center sampling, IEEE Geosci. Remote Sens. Letters, Vol. 1, pp. 260-264, 2004.

Coherent Reconstruction

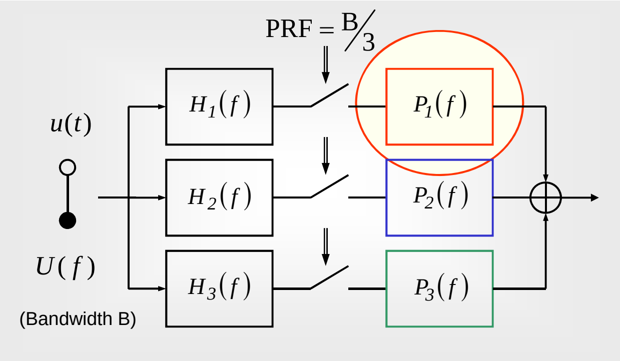

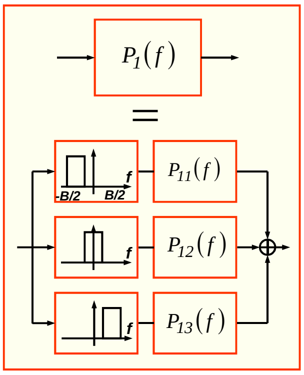

$$\mathbf{A(f)} = \begin{bmatrix} H_1(f) & H_2(f) & H_3(f) \\ H_1(f+B/3) & H_2(f+B/3) & H_3(f+B/3) \\ H_1(f+2B/3) & H_2(f+2B/3) & H_3(f+2B/3) \end{bmatrix} \longrightarrow \mathbf{A}^{-1}\mathbf{(f)} = \begin{bmatrix} P_{11}(f) & P_{12}(f+B/3) & P_{13}(f+2B/3) \\ P_{21}(f) & P_{22}(f+B/3) & P_{23}(f+2B/3) \\ P_{31}(f) & P_{32}(f+B/3) & P_{33}(f+2B/3) \end{bmatrix}$$

G. Krieger et al., Unambiguous SAR signal reconstruction from nonuniform displaced phase center sampling, IEEE Geosci. Remote Sens. Letters, Vol. 1, pp. 260-264, 2004.

DBF-SAR Systems with Planar Arrays

DPCA	Multiple Rx Apertures in Azimuth

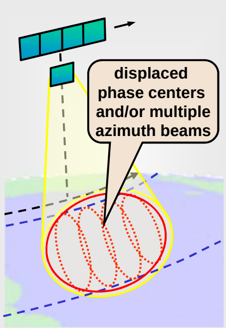

- enables high azimuth resolution and wide swath
- requires dedicated multichannel SAR processing

Reconstruction in Frequency Domain:

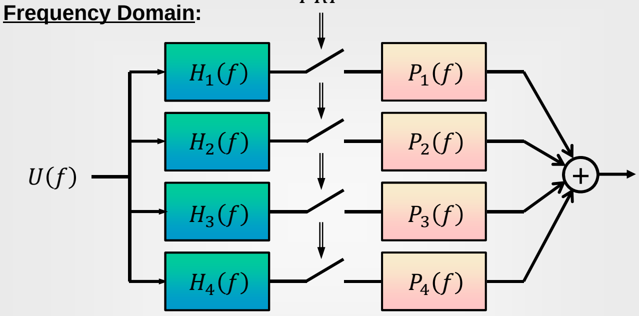

Reconstruction by sum of linear filters $\sum P_i(f)$ can also be interpreted as a frequency dependent linear beamformer

DLR

G. Krieger et al., Unambiguous SAR signal reconstruction from nonuniform displaced phase center sampling, IEEE Geosci. Remote Sens. Letters, Vol. 1, pp. 260-264, 2004.

DBF-SAR Systems with Planar Arrays

DPCA	Multiple Rx Apertures in Azimuth

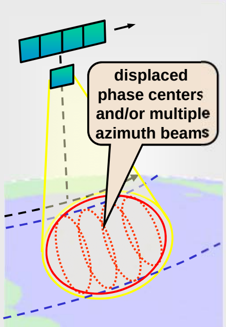

- enables high azimuth resolution and wide swath
- requires dedicated multichannel SAR processing

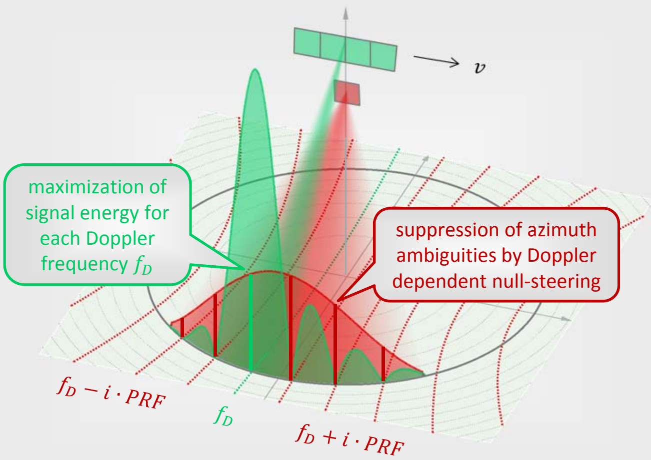

DLR

DBF-SAR Systems with Planar Arrays

DPCA	Multiple Rx Apertures in Azimuth
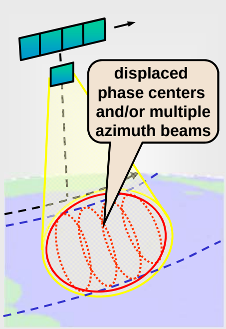	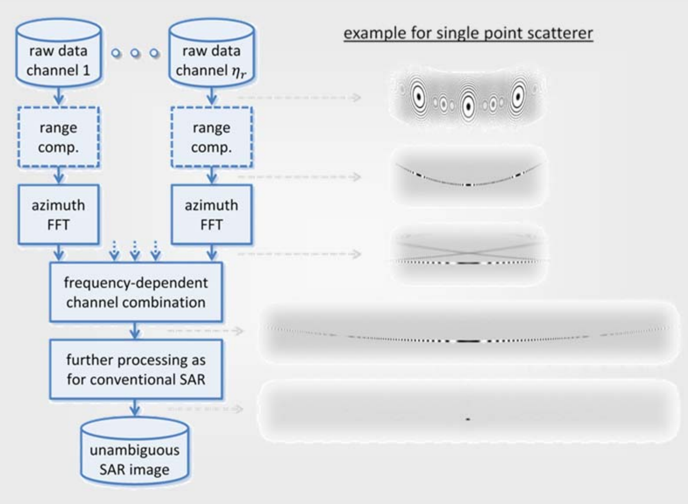
▪ enables high azimuth resolution and wide swath ▪ requires dedicated multichannel SAR processing	

Reconstruction from Nonuniform DPCA Sampling

Single-Channel Image	Demonstration with TerraSAR-X
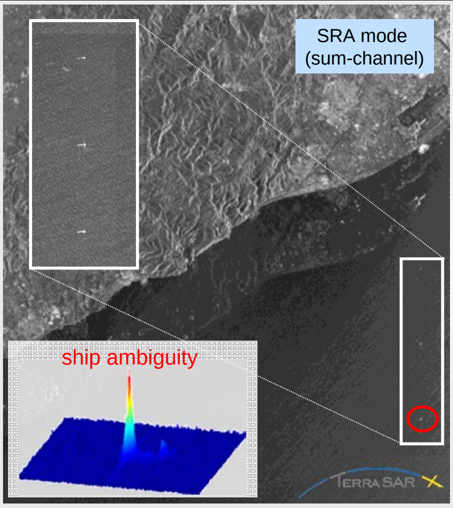	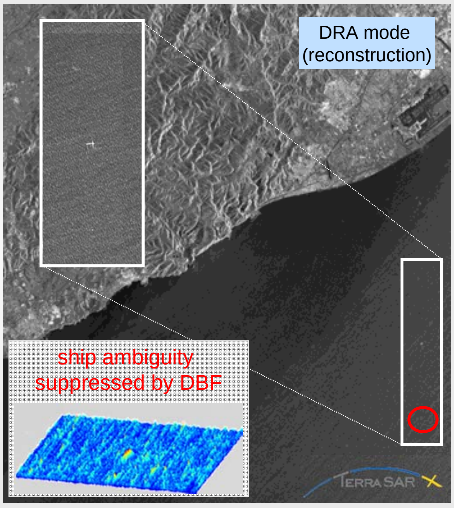

J. H. Kim et al., First Spaceborne Demonstration of Digital Beamforming for Azimuth Ambiguity Suppression, IEEE Trans. Geosci. Remote Sensing, Vol. 51, pp. 579-590, 2013.

Pulse-to-Pulse Antenna Phase Center Variation

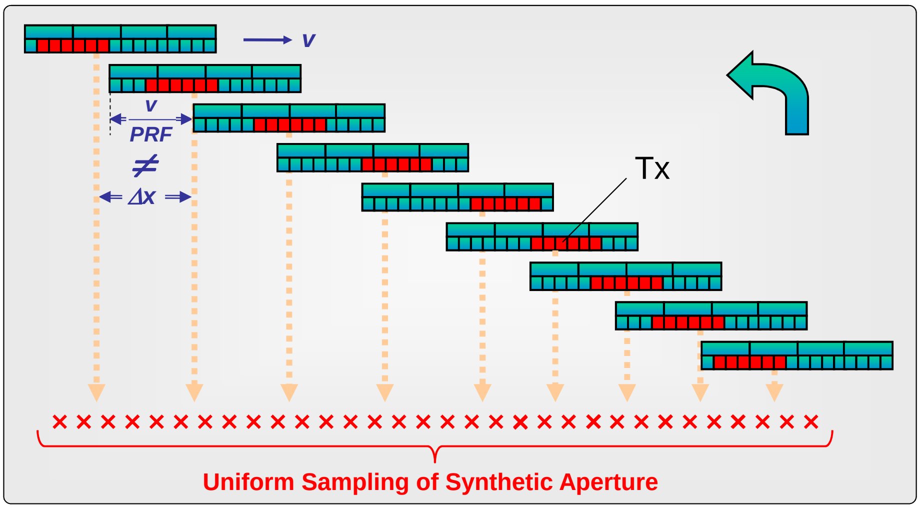

N. Gebert et al., Azimuth Phase Center Adaptation on Transmit for High-Resolution Wide-Swath SAR Imaging, IEEE Geosci. Remote Sens. Letters, Vol. 6, pp. 782-786, 2009.

DBF-SAR Systems with Planar Arrays

HRWS	Combination of Scan on Receive with DPCA
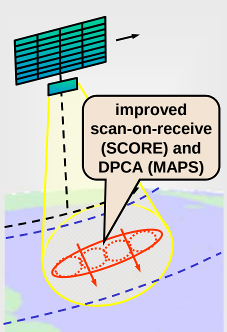	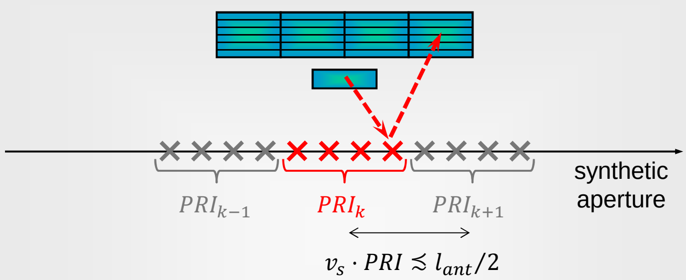
▪ scan-on-receive with dispersive beam for high Rx gain ▪ DPCA for improved azimuth resolution in stripmap mode	

M. Suess et al., A novel high resolution, wide swath SAR system, Proc. IGARSS, pp. 1013-15, 2001.

DBF-SAR Systems with Planar Arrays

HRWS	Combination of Scan on Receive with DPCA

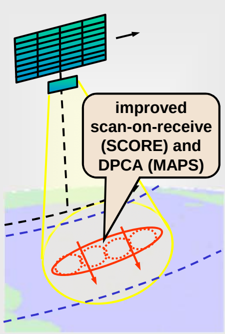

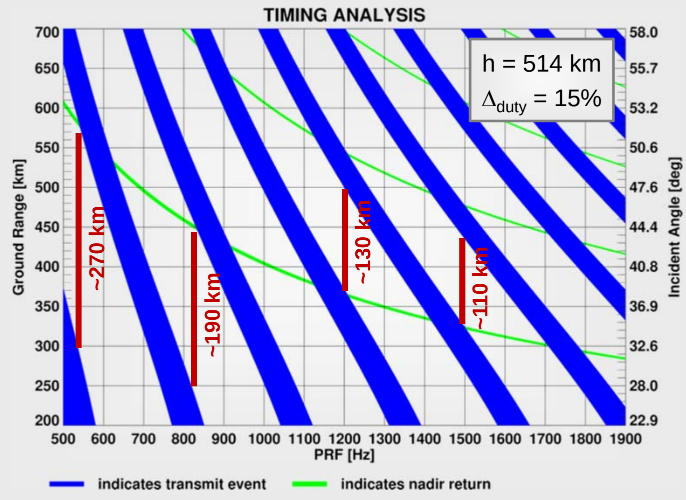

- scan-on-receive with dispersive beam for high Rx gain
- DPCA for improved azimuth resolution in stripmap mode

M. Suess et al., A novel high resolution, wide swath SAR system, Proc. IGARSS, pp. 1013-15, 2001.

DBF-SAR Systems with Planar Arrays

HRWS	Combination of Scan on Receive with DPCA

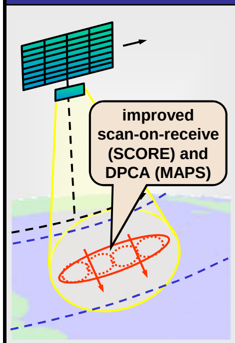

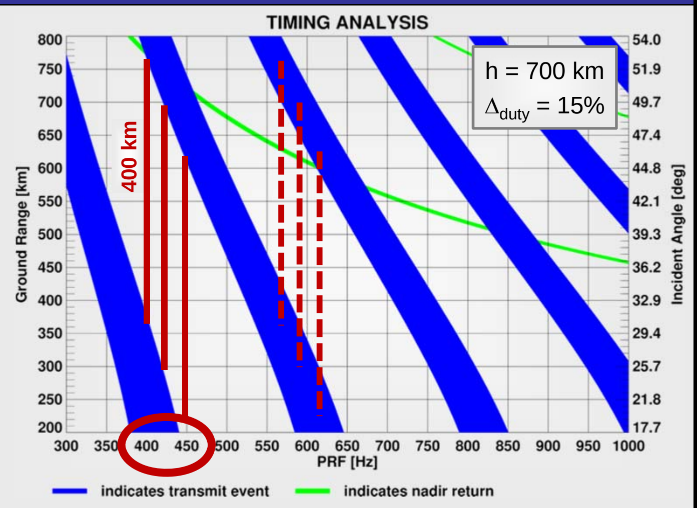

- scan-on-receive with dispersive beam for high Rx gain
- DPCA for improved azimuth resolution in stripmap mode

M. Suess et al., A novel high resolution, wide swath SAR system, Proc. IGARSS, pp. 1013-15, 2001.

DBF-SAR Systems with Planar Arrays

HRWS	Combination of Scan on Receive with DPCA

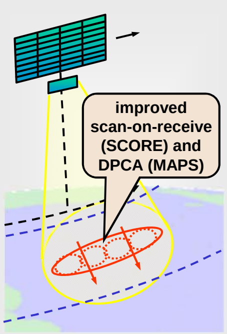

- scan-on-receive with dispersive beam for high Rx gain
- DPCA for improved azimuth resolution in stripmap mode

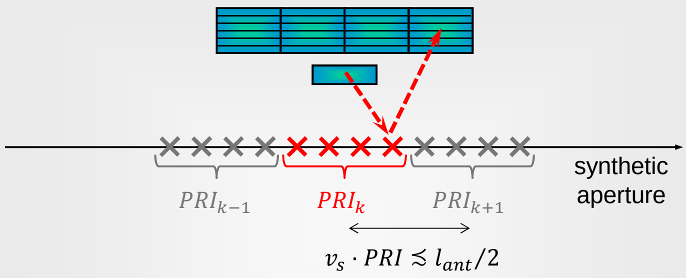

Swath	PRF	l_{ant}
100 km	≲ 1.6 kHz	≳ 10 m
200 km	≲ 800 Hz	≳ 20 m
400 km	≲ 400 Hz	≳ 40 m

$$l_{ant} \gtrsim \frac{2 \cdot v_s}{PRF}$$

DLR

M. Suess et al., A novel high resolution, wide swath SAR system, Proc. IGARSS, pp. 1013-15, 2001.

DBF-SAR Systems with Planar Arrays

Quad Array SAR	Suppression of Range Ambiguities by Null Steering

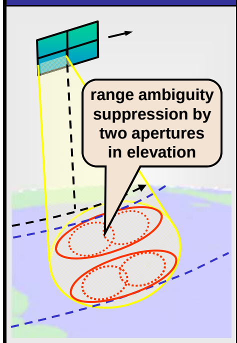

- good azimuth resolution
- compact antenna
- range gap in the middle of the swath

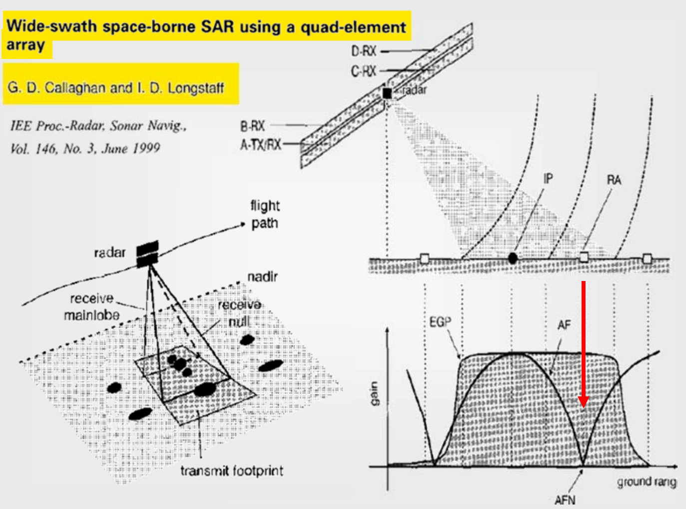

DLR

G.D. Callaghan et al., Wide-swath space-borne SAR using a quad-element array, IEE Proceedings for Radar, Sonar and Navigation, Vol. 146, pp. 159-165, 1999.

DBF-SAR Systems with Planar Arrays

Burst-DBF-SAR	DPCA in Burst Mode Operation

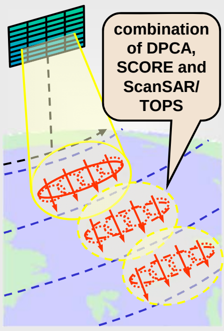

- enables mapping of ultra-wide swaths with high resolution
- suggested as Sentinel-1 successor system

- Minimum PRF is determined by antenna length:

$$PRF \gtrsim \frac{2 \cdot v_s}{l_{ant}}$$

l_{ant}	PRF
10 m	≳ 1500 Hz
12.5 m	≳ 1200 Hz
15 m	≳ 1000 Hz

- Minimum burst number is determined from timing

ScanSAR with Planar Array

Burst-DBF-SAR	DPCA in Burst Mode Operation

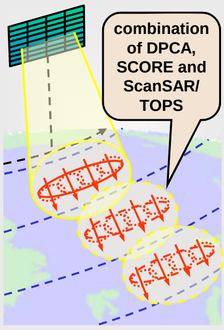

- enables mapping of ultra-wide swaths with high resolution
- suggested as Sentinel-1 successor system

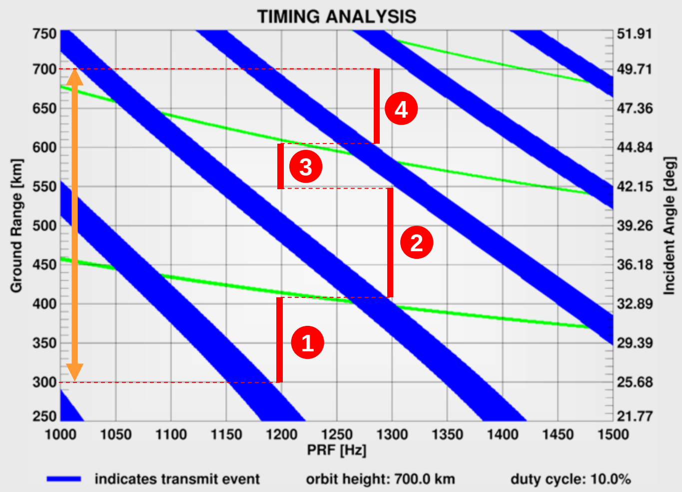

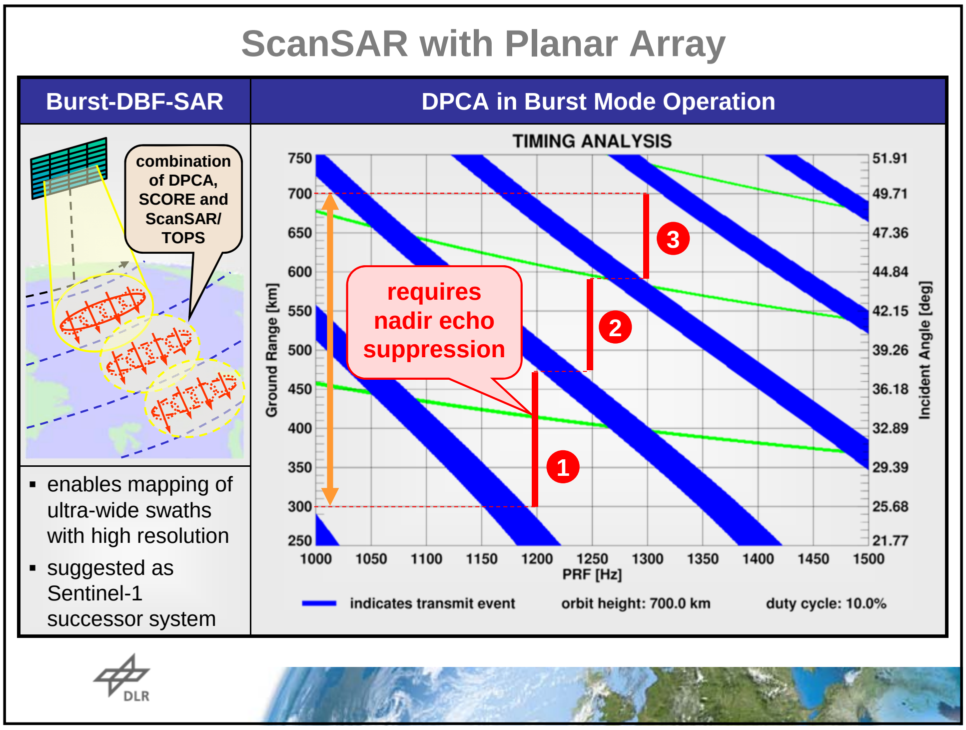
ScanSAR with Planar Array
Burst-DBF-SAR
DPCA in Burst Mode Operation
combination of DPCA, SCORE and ScanSAR/ TOPS
enables mapping of ultra-wide swaths with high resolution
suggested as Sentinel-1 successor system
TIMING ANALYSIS
Ground Range [km]
Incident Angle [deg]
PRF [Hz]
requires nadir echo suppression
1
2
3
indicates transmit event
orbit height: 700.0 km
duty cycle: 10.0%
DLR

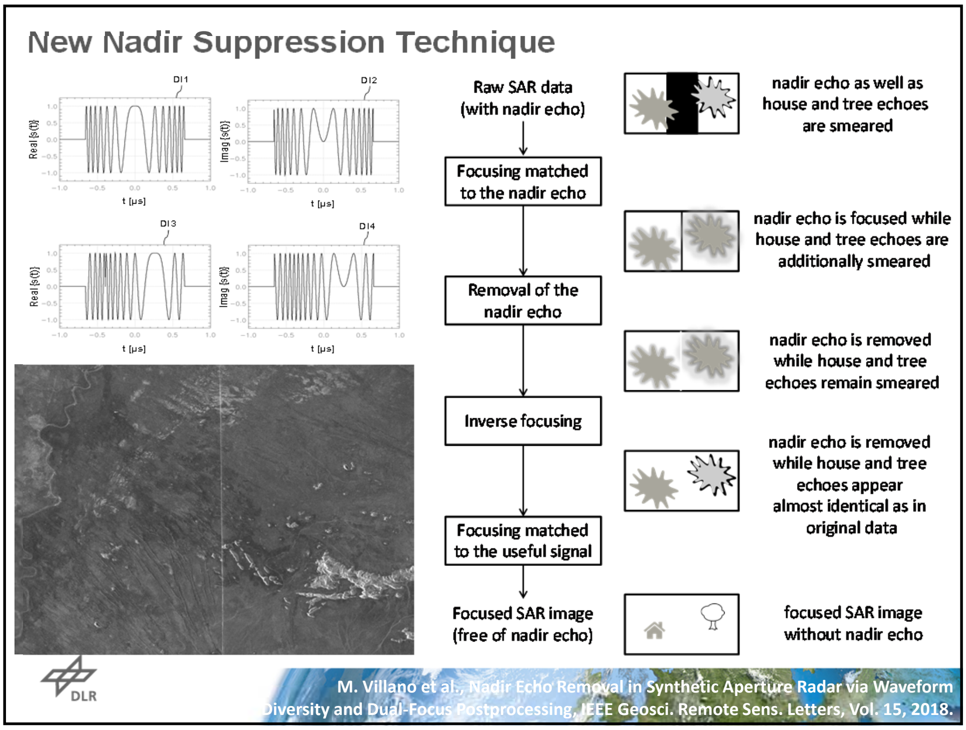
New Nadir Suppression Technique
Raw SAR data (with nadir echo)
Focusing matched to the nadir echo
Removal of the nadir echo
Inverse focusing
Focusing matched to the useful signal
Focused SAR image (free of nadir echo)
nadir echo as well as house and tree echoes are smeared
nadir echo is focused while house and tree echoes are additionally smeared
nadir echo is removed while house and tree echoes remain smeared
nadir echo is removed while house and tree echoes appear almost identical as in original data
focused SAR image without nadir echo
M. Villano et al., Nadir Echo Removal in Synthetic Aperture Radar via Waveform Diversity and Dual-Focus Postprocessing, IEEE Geosci. Remote Sens. Letters, Vol. 15, 2018.
DLR

DBF-SAR Systems with Planar Arrays

Burst-DBF-SAR	DPCA in Burst Mode Operation

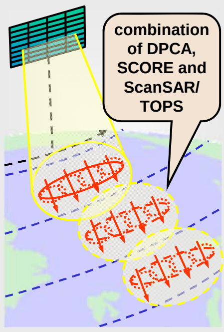

- enables mapping of ultra-wide swaths with high resolution
- suggested as Sentinel-1 successor system

- Minimum PRF is determined by antenna length:

$$PRF \gtrsim \frac{2 \cdot v_s}{l_{ant}} \rightarrow$$

l_{ant}	PRF
10 m	≳ 1500 Hz
12.5 m	≳ 1200 Hz
15 m	≳ 1000 Hz

- Minimum burst number is determined from timing:

$$PRF \gtrsim 1200\ Hz \rightarrow \begin{cases} N_{burst} = 4 \text{ (with nadir)} \\ N_{burst} = 3 \text{ (w/o nadir)} \end{cases}$$

- Minimum number of azimuth channels from az. resolution:

$$N_{az} \gtrsim \frac{l_{ant}}{2\delta_{az}} \cdot (N_{burst} + 1) \xrightarrow[l_{ant} = 12.5 \text{ m}]{N_{burst} = 4} N_{az} \gtrsim 7$$

DLR

DBF-SAR Systems with Planar Arrays

Burst-DBF-SAR	DPCA in Burst Mode Operation

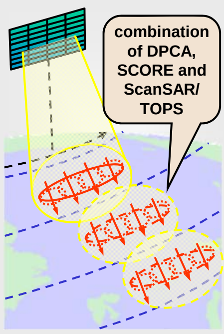

- enables mapping of ultra-wide swaths with high resolution
- suggested as Sentinel-1 successor system

- The high-resolution wide-swath ScanSAR mode may imply a notable squint angle change at the burst borders:

Mode	Bursts	N_{az}	Δ Squint Angle ($\Delta\psi$)		
			L-band	C-band	X-band
5 m @ 400 km	4	7	5.1°	1.2°	0.66°

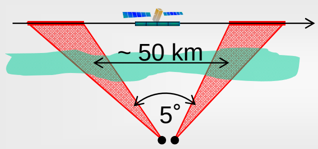

$$\Delta\psi \approx \frac{N_{burst}}{2\delta_{az}} \cdot \lambda$$

<u>Challenges:</u>
- azimuth scalloping (AASR, NESZ)
- line-of-sight variation (interferometry)
- atmospheric discontinuities (ionosphere)

DLR

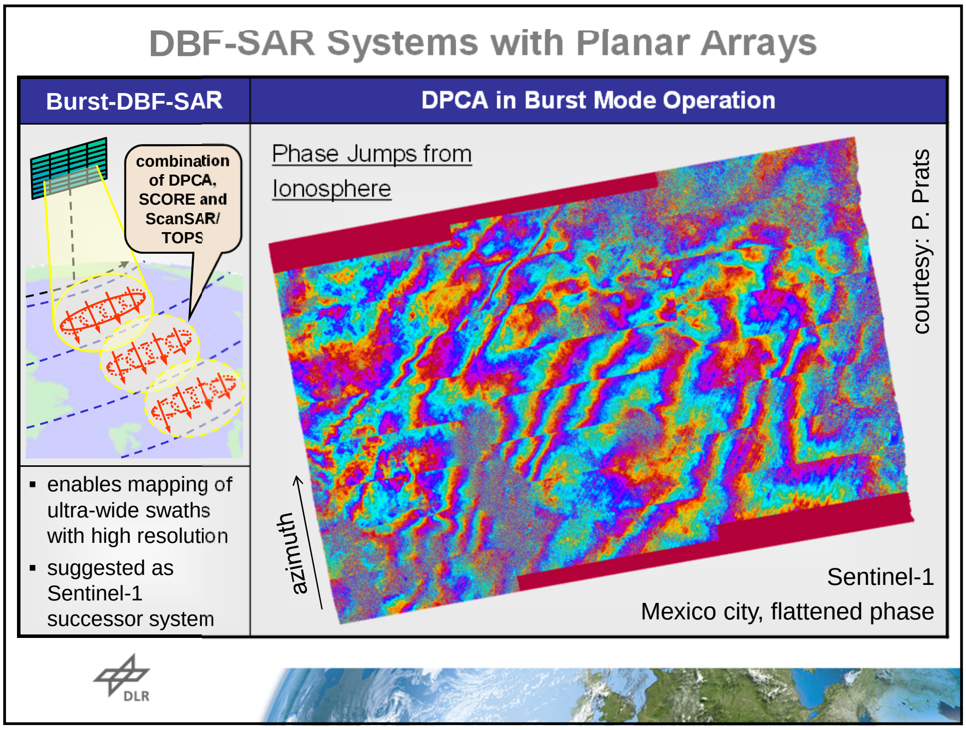
DBF-SAR Systems with Planar Arrays
Burst-DBF-SAR
DPCA in Burst Mode Operation
combination of DPCA, SCORE and ScanSAR/ TOPS
enables mapping of ultra-wide swaths with high resolution
suggested as Sentinel-1 successor system
Phase Jumps from Ionosphere
courtesy: P. Prats
azimuth
Sentinel-1
Mexico city, flattened phase
DLR

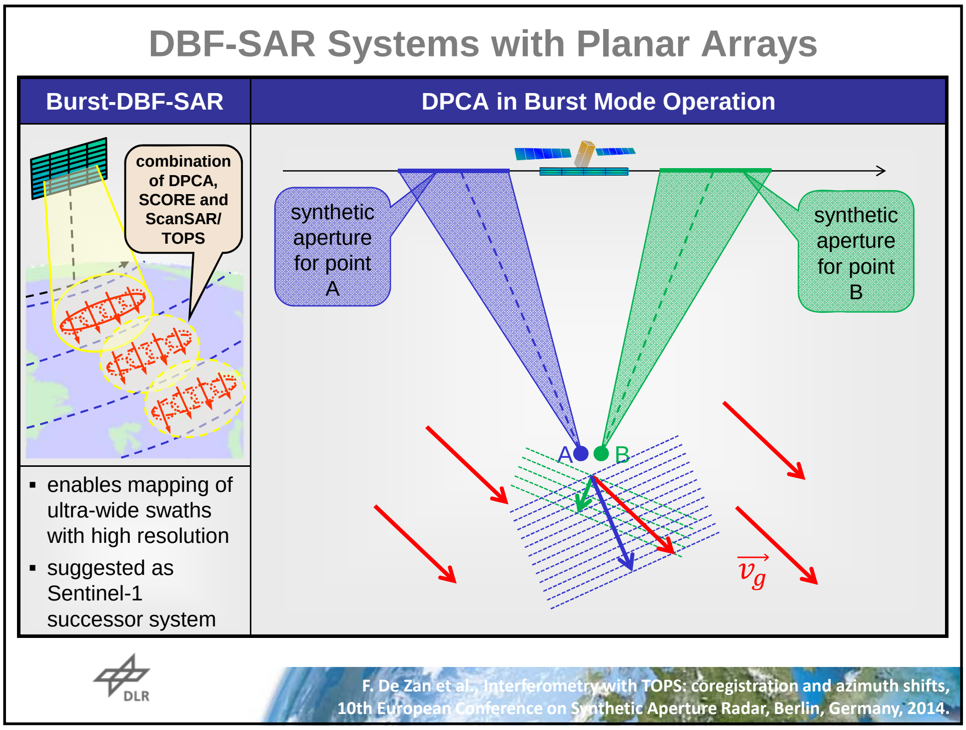
DBF-SAR Systems with Planar Arrays
Burst-DBF-SAR
DPCA in Burst Mode Operation
combination of DPCA, SCORE and ScanSAR/ TOPS
enables mapping of ultra-wide swaths with high resolution
suggested as Sentinel-1 successor system
synthetic aperture for point A
synthetic aperture for point B
A
B
$\vec{v}_g$
DLR
F. De Zan et al., Interferometry with TOPS: coregistration and azimuth shifts, 10th European Conference on Synthetic Aperture Radar, Berlin, Germany, 2014.

DBF-SAR Systems with Planar Arrays

Burst-DBF-SAR	DPCA in Burst Mode Operation

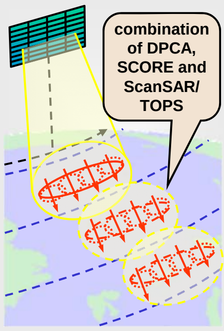

- enables mapping of ultra-wide swaths with high resolution
- suggested as Sentinel-1 successor system

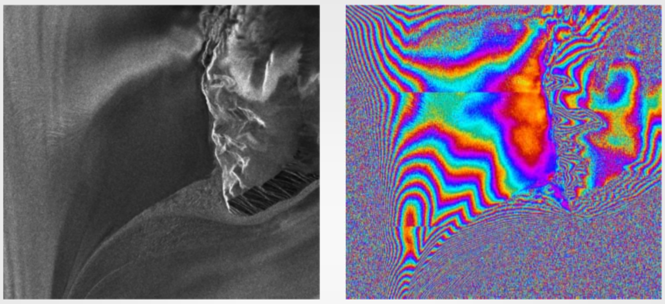

11-day TSX TOPS interferogram over the Lambert glacier, Antarctica. (Left) Reflectivity image and (right) flattened interferogram. The images show three consecutive bursts (9 km per burst in azimuth), where the top-right part is a stable rocky area showing no phase jumps at burst edges. The glacier, on the other hand, shows clear jumps at burst edges. The jumps are legitimate and correspond to the projection of the motion in the LOS direction, being the latter azimuth-dependent. At burst edges the LOS vectors have opposite azimuth directions, and therefore the jumps can be clearly seen. Range is horizontal and azimuth is vertical (from F. De Zan et al, EUSAR 2014).

DLR

F. De Zan et al., Interferometry with TOPS: coregistration and azimuth shifts, 10th European Conference on Synthetic Aperture Radar, Berlin, Germany, 2014.

DBF-SAR Systems with Planar Arrays

Burst-DBF-SAR	DPCA in Burst Mode Operation

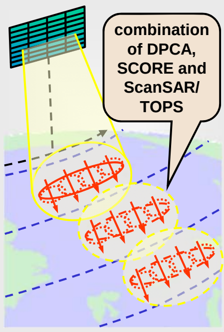

- enables mapping of ultra-wide swaths with high resolution
- suggested as Sentinel-1 successor system

Scalloping in Multichannel ScanSAR mode

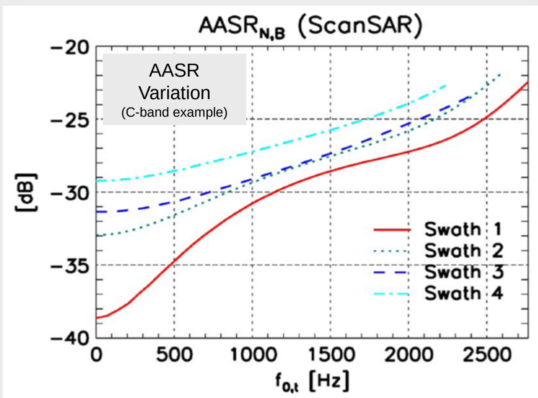

DLR

N. Gebert et al., Multichannel Azimuth Processing in ScanSAR and TOPS Mode Operation, IEEE Trans. Geosci. Remote Sens., Vol. 48, pp. 2994-3008, 2010.

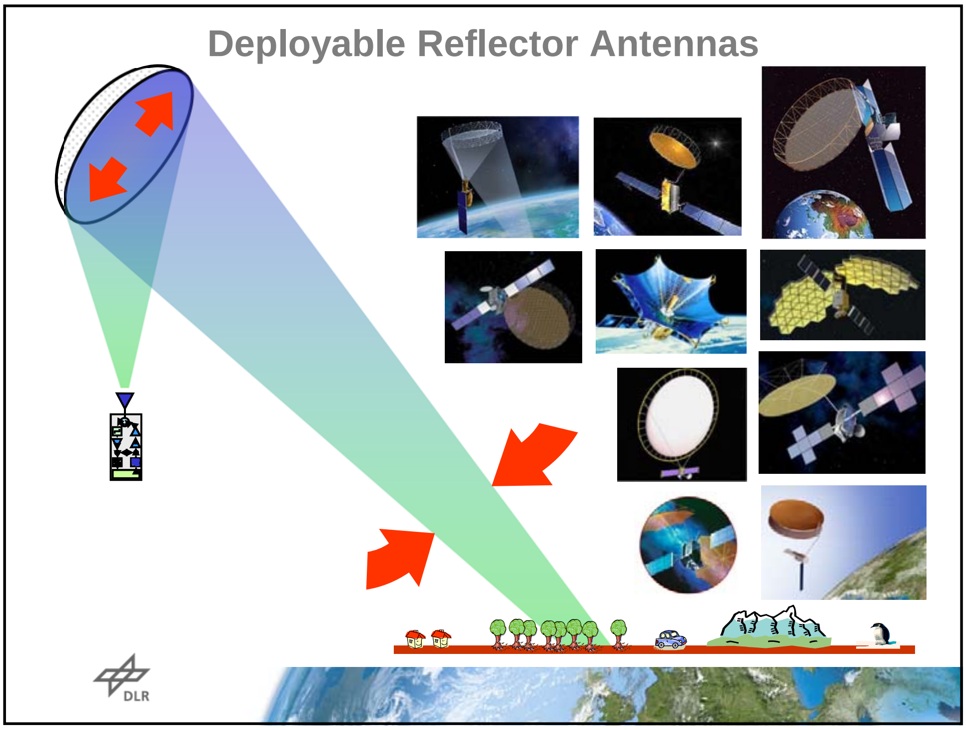

Deployable Reflector Antennas
DLR

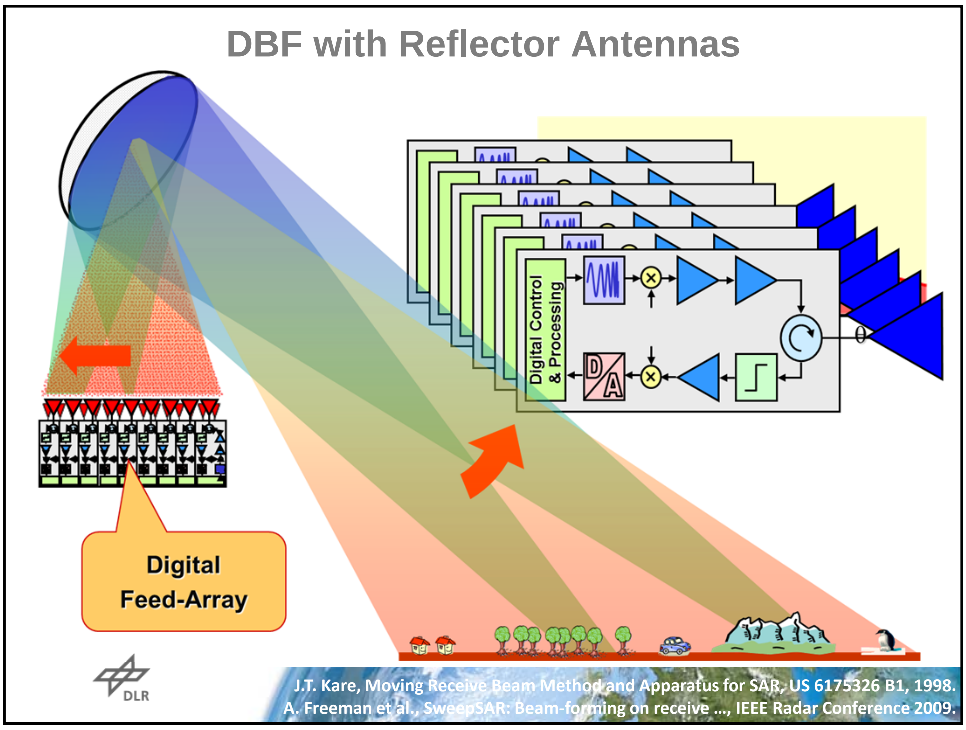

DBF with Reflector Antennas
Digital Control & Processing
D/A
Digital Feed-Array
DLR
J.T. Kare, Moving Receive Beam Method and Apparatus for SAR, US 6175326 B1, 1998.
A. Freeman et al., SweepSAR: Beam-forming on receive ..., IEEE Radar Conference 2009.

DBF with Reflector Antennas

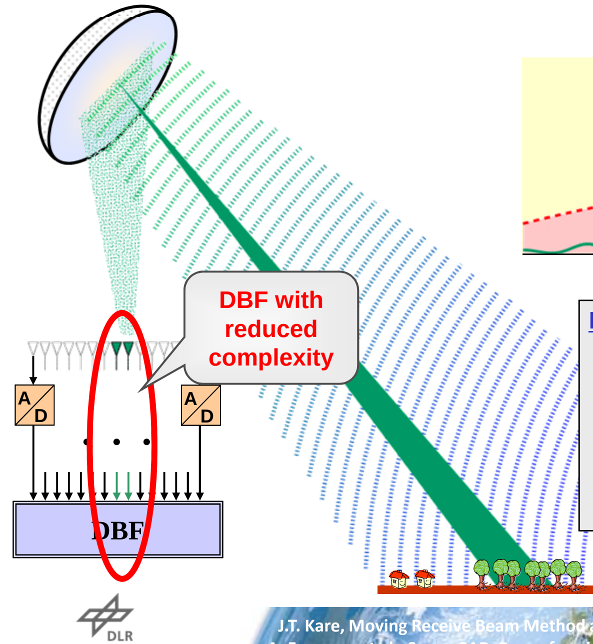

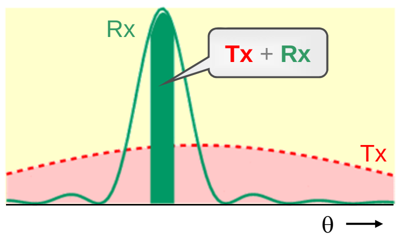

Large reflector enables:

- high sensitivity also at low frequencies
- improved ambiguity suppression
- innovative SAR modes
- multiple frequency SAR

J.T. Kare, Moving Receive Beam Method and Apparatus for SAR, US 6175326 B1, 1998.
A. Freeman et al., SweepSAR: Beam-forming on receive ..., IEEE Radar Conference 2009.

DBF-Reflector-SAR: Challenges and Solutions

Variable Antenna Gain from Element Switching

Frequency Dependence of Antenna Patterns

Feed Blockage & Multipath

Redundancy Against Tx/Rx Module Failure

Modulation for Long Transmit Pulses

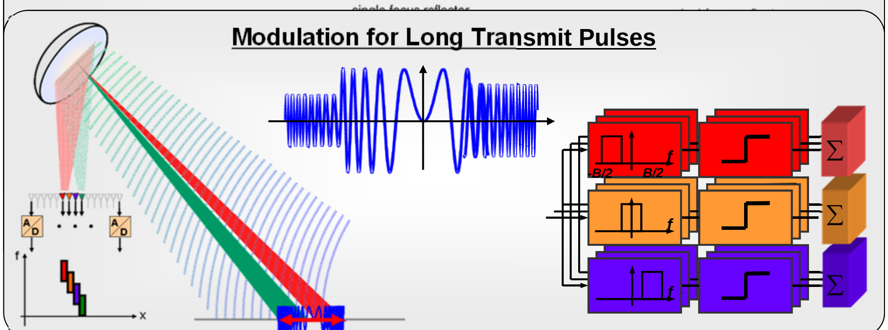

S. Huber et al., Spaceborne Reflector SAR Systems with Digital Beamforming, IEEE Transactions on Aerospace and Electronic Systems, Vol. 48, pp. 3473-3493, 2012.

Synthetic Aperture Radar

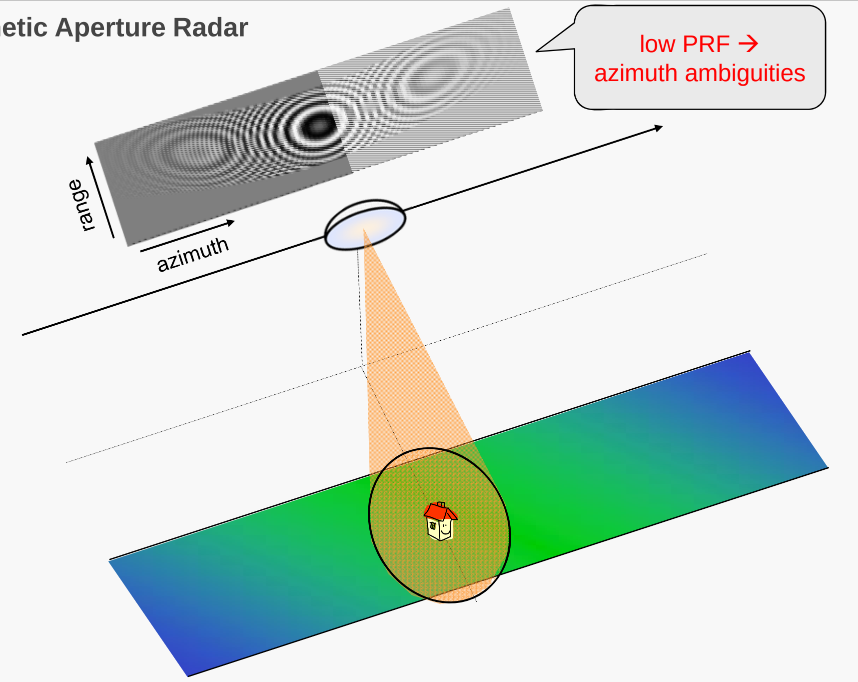

Multiple Swath Mapping

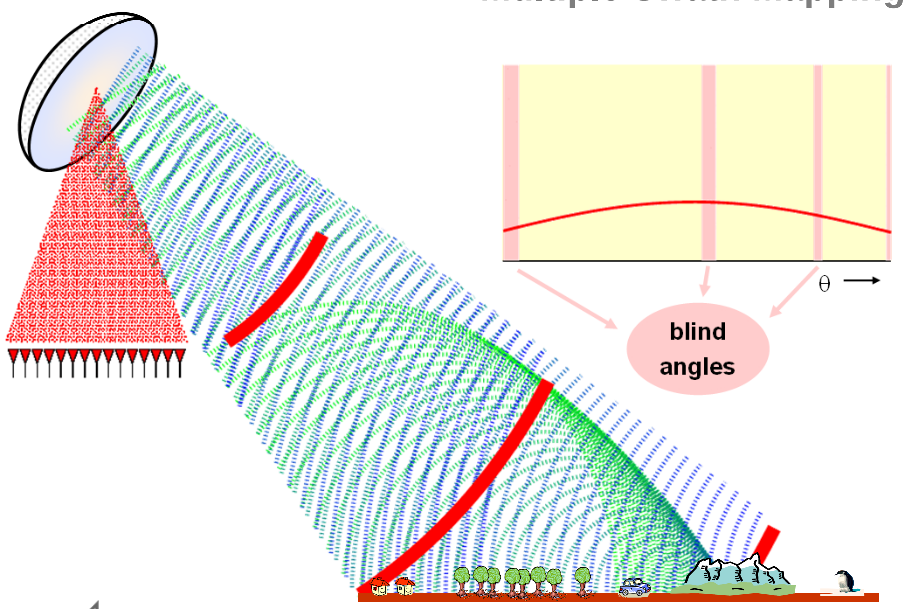

G. Krieger et al., Advanced Concepts for Ultra-Wide-Swath SAR Imaging, European Conference on Synthetic Aperture Radar, Friedrichshafen, Germany, 2008.

Multiple Swath Mapping

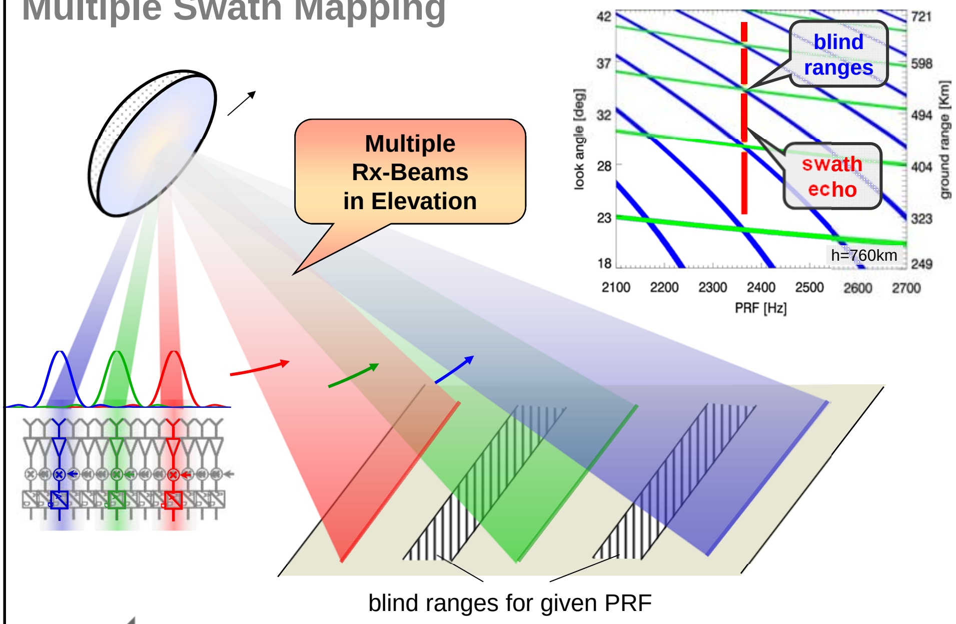

G. Krieger et al., Advanced Concepts for Ultra-Wide-Swath SAR Imaging, European Conference on Synthetic Aperture Radar, Friedrichshafen, Germany, 2008.

Multiple Swath Mapping

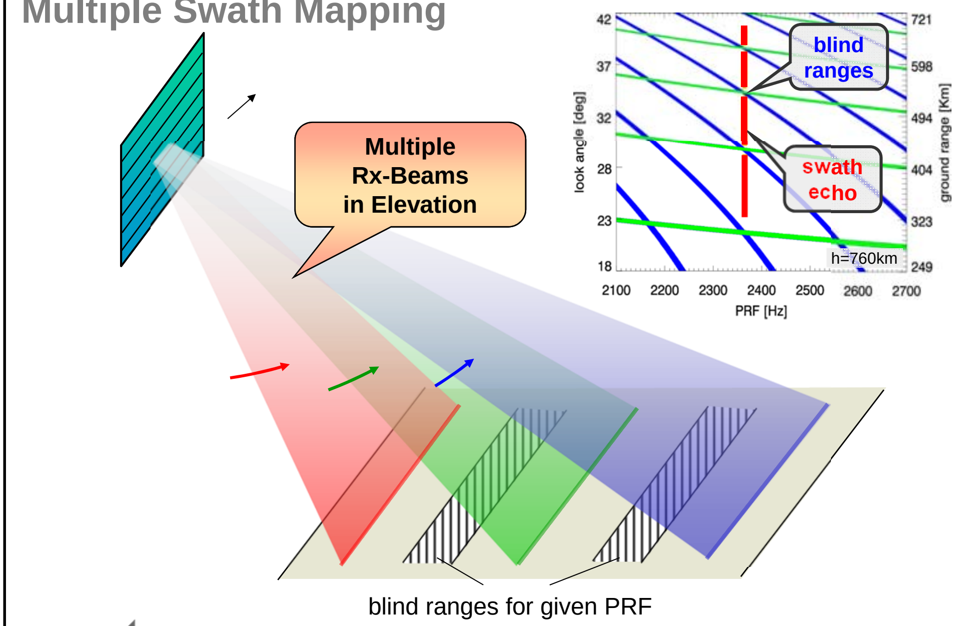

H. D. Griffiths et al., Ambiguity Suppression In SARs Using Adaptive Array Techniques, International Geoscience and Remote Sensing Symposium, pp. 1015-1018, 1991.

Multiple Swath Mapping

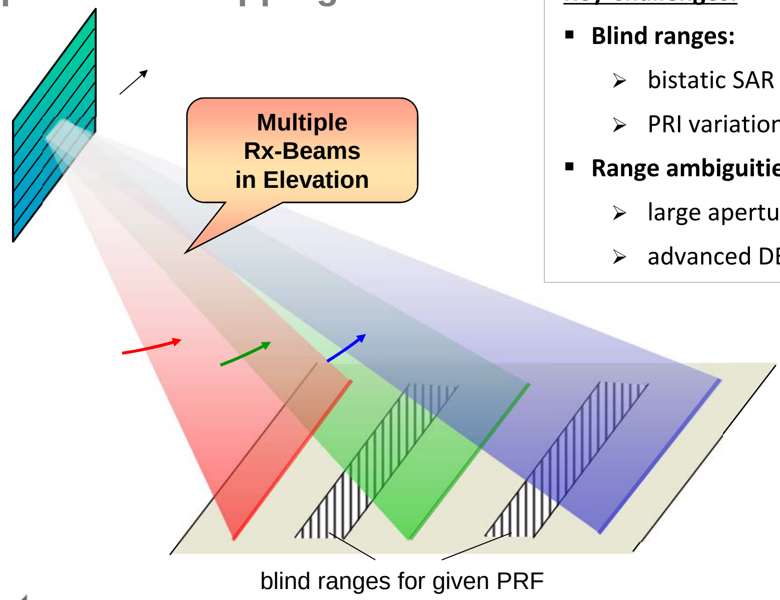

Key Challenges:

- **Blind ranges:**
  - bistatic SAR
  - PRI variation
- **Range ambiguities:**
  - large aperture
  - advanced DBF

DLR

H. D. Griffiths et al., Ambiguity Suppression In SARs Using Adaptive Array Techniques, International Geoscience and Remote Sensing Symposium, pp. 1015-1018, 1991.

Range Ambiguity Suppression by Null-Steering

- null-steering requires sufficient antenna height to avoid losses:

$$h_{\text{ant}} \gtrsim \frac{2\lambda \cdot r_{far} \cdot \tan(\theta_{inc,max})}{c \cdot PRI}$$

- null-steering is sensitive to
  - antenna phase errors
  - topography
  - satellite mispointing
  - squint/Doppler variation
- possible mitigations
  - larger antenna & tapered beams
  - advanced beamforming (e.g. real-time DBF with broad “nulls”)
  - cross elevation beam range ambiguity suppression (CEBRAS)

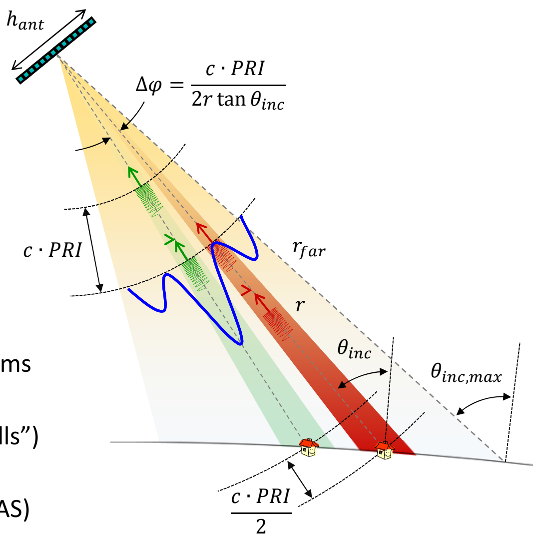

DLR

Minimum Antenna Height ($\theta_{i,max} = 50°$, $h_{sat} = 700$ km)

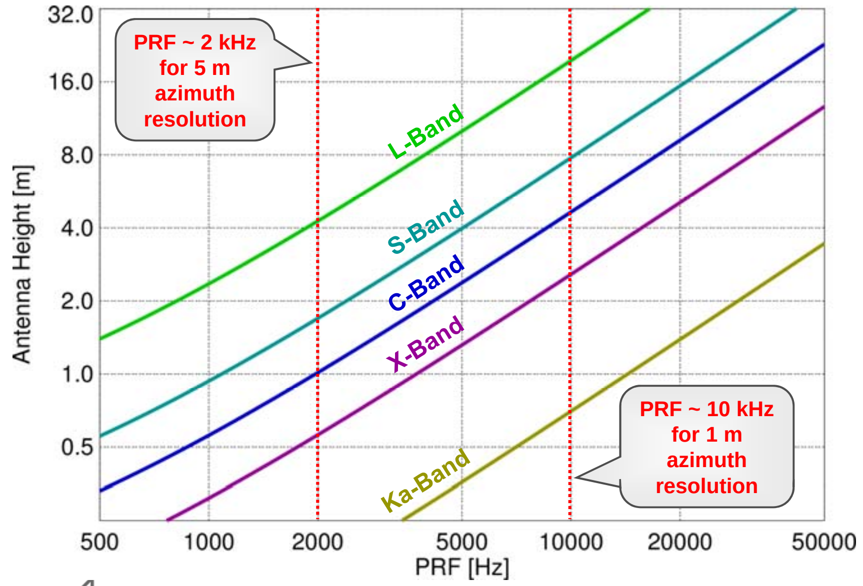

G. Krieger et al., SIMO and MIMO System Architectures and Modes for High-Resolution Ultra-Wide-Swath SAR Imaging, EUSAR 2016.

Tx-Rx Separation (Bistatic System)

- Simultaneous transmission and reception avoids blind ranges
- Direct signal can be suppressed by
  - Doppler filter
  - additional mitigation by waveform diversity and/or PRI variation
- Advantages
  - ultra-wide swaths with high resolution
  - compact antennas and satellites
  - no Tx/Rx switches, less losses, FMCW, ...
- Drawbacks
  - requires two satellites (3 for single-pass InSAR)
  - requires accurate time and phase synchronisation

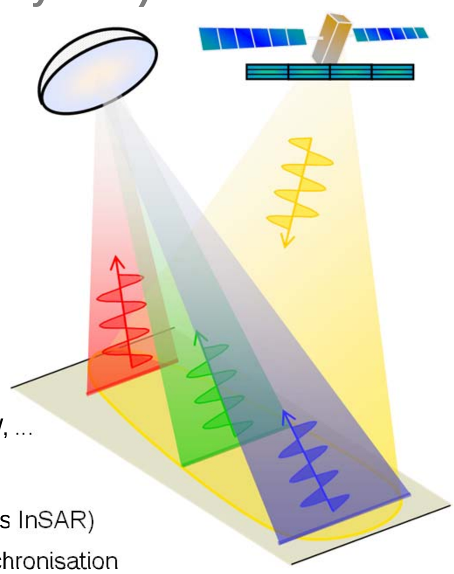

G. Krieger et al., Potential of digital beamforming in bi- and multistatic SAR, IEEE International Geoscience and Remote Sensing Symposium, pp. 527-529, 2003.

Tx-Rx Separation (Bistatic System)

- Simultaneous transmission and reception avoids blind ranges
- Example:

Parameter	Value
Swath	500 km
Azimuth Resolution	3 m
Orbit Height	800 km
PRF	3.5 kHz
Tx Antenna Length	5 m
Tx Antenna Height	> 0.8 m (L-band) > 0.1 m (X-band)
Rx Antenna Length	5 m
Rx Antenna Height	> 5.6 m (L-band) > 0.7 m (X-band)

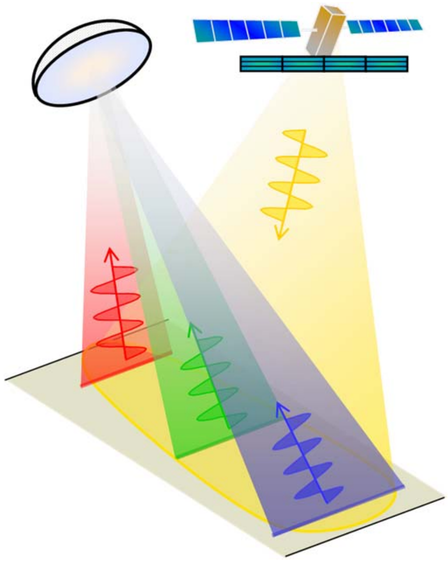

Multi-Beam Concepts for Ultra-Wide-Swath Imaging

- Strategies for Elimination of Blind Ranges -

Continuous PRI Variation

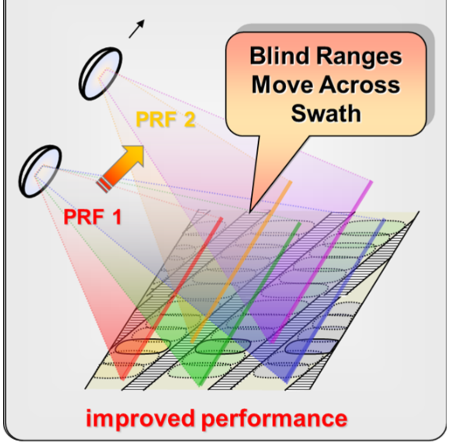

Multiple-Beam ScanSAR

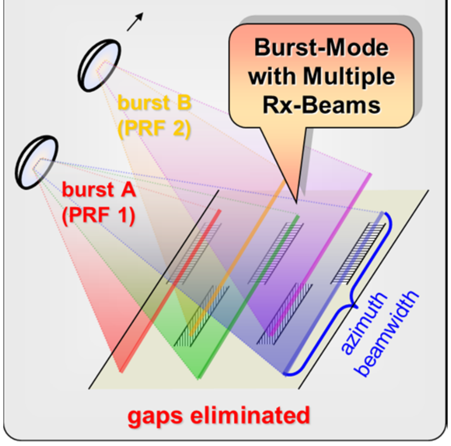

Systematic Shift of Blind Ranges

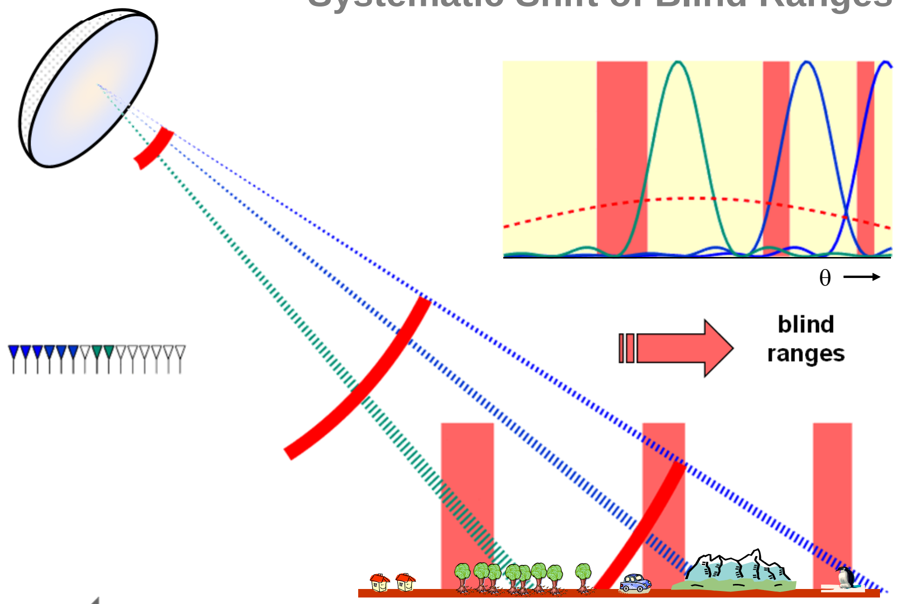

G. Krieger et al., Advanced Concepts for Ultra-Wide-Swath SAR Imaging, EUSAR 2008.
B. Grafmueller et al., High Resolution SAR Device and Antenna, US 2009/0079621 A1.

Timing Options for SAR with Variable PRI

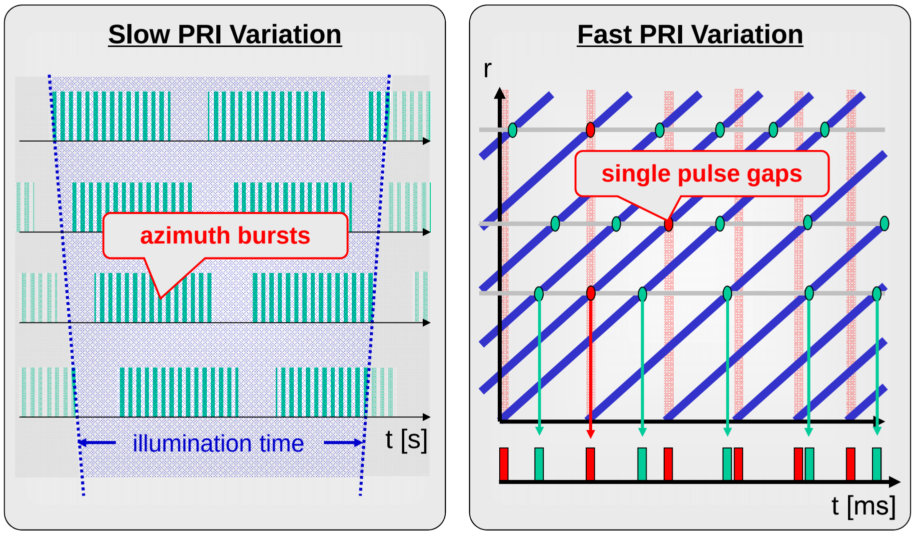

Multiple Elevation Beam SAR with Slow PRI Variation

System Parameters

wavelength	λ	0.236 m
satellite height	h_{sat}	773 km
incident angles	θ_{inc}	24°- 47.2°
swath width	Δs	400 km
reflector diameter	D	12 m
focal length	F	12 m
reflector offset	O	7.2 m
azimuth elements	N_{az}	5 (0.6 λ)
elevation channels	N_{el}	45 (0.6 λ)
minimum PRF	PRF_{min}	3300 Hz
maximum PRF	PRF_{max}	3444 Hz
cycle time	T_{cycle}	3.54 s
Tx duty cycle	Δ_{cycle}	4%
burst length	T_{burst}	> 3.35 s

Range-Dependent Burst Positions

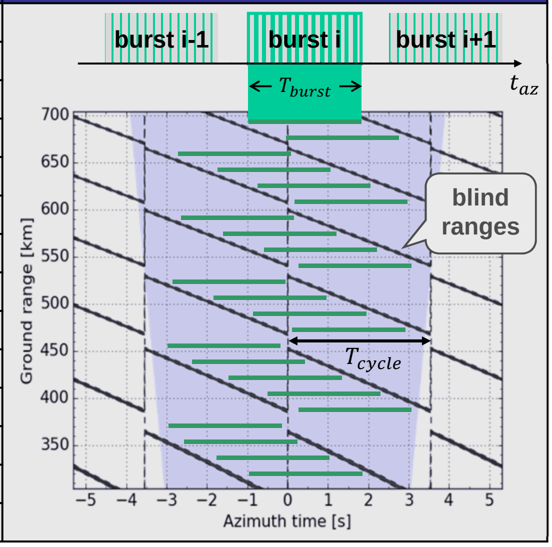

G. Krieger et al., SIMO and MIMO System Architectures and Modes for High-Resolution Ultra-Wide-Swath SAR Imaging, EUSAR 2016.

SAR with Slow PRI Variation

Parameter	Value
Wavelength	0.236 m (L-Band)
Azimuth Resolution	5 m
Antenna diameter	12 m
Feed size	6.4 m x 0.71 m
Orbital altitude	773 km
Average Tx power (for NESZ = -25 dB)	883 W (610 W)

NESZ

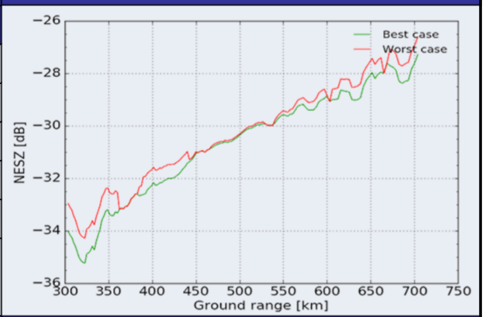

Range Ambiguities (RASR)

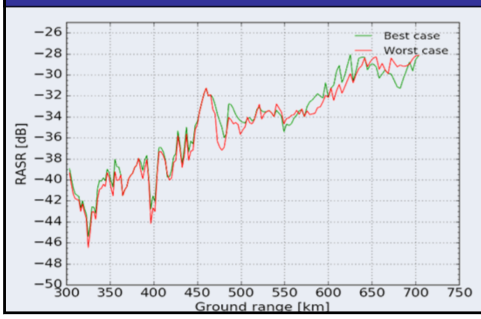

Azimuth Ambiguities (AASR)

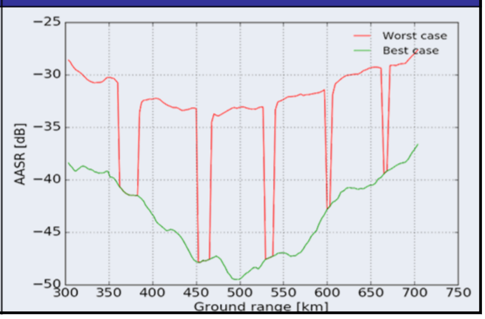

Multiple Elevation Beam SAR with Slow PRI Variation

System Parameters		
wavelength	λ	0.236 m
satellite height	h_{sat}	773 km
incident angles	θ_{inc}	24°- 47.2°
swath width	Δs	400 km
reflector diameter	D	12 m
focal length	F	12 m
reflector offset	O	7.2 m
azimuth elements	N_{az}	5 (0.6 λ)
elevation channels	N_{el}	45 (0.6 λ)
minimum PRF	PRF_{min}	3300 Hz
maximum PRF	PRF_{max}	3444 Hz
cycle time	T_{cycle}	3.54 s
Tx duty cycle	Δ_{cycle}	4%
burst length	T_{burst}	> 3.35 s

Range-Dependent Burst Positions

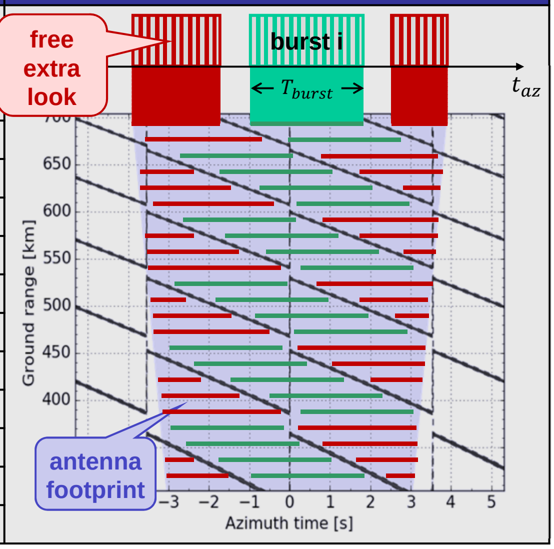

Extra Looks

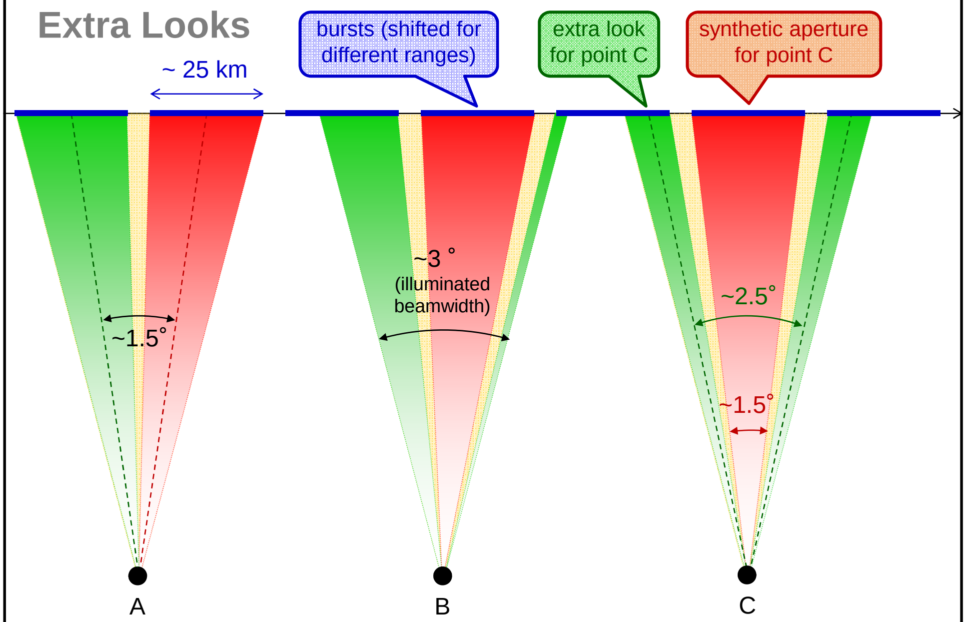

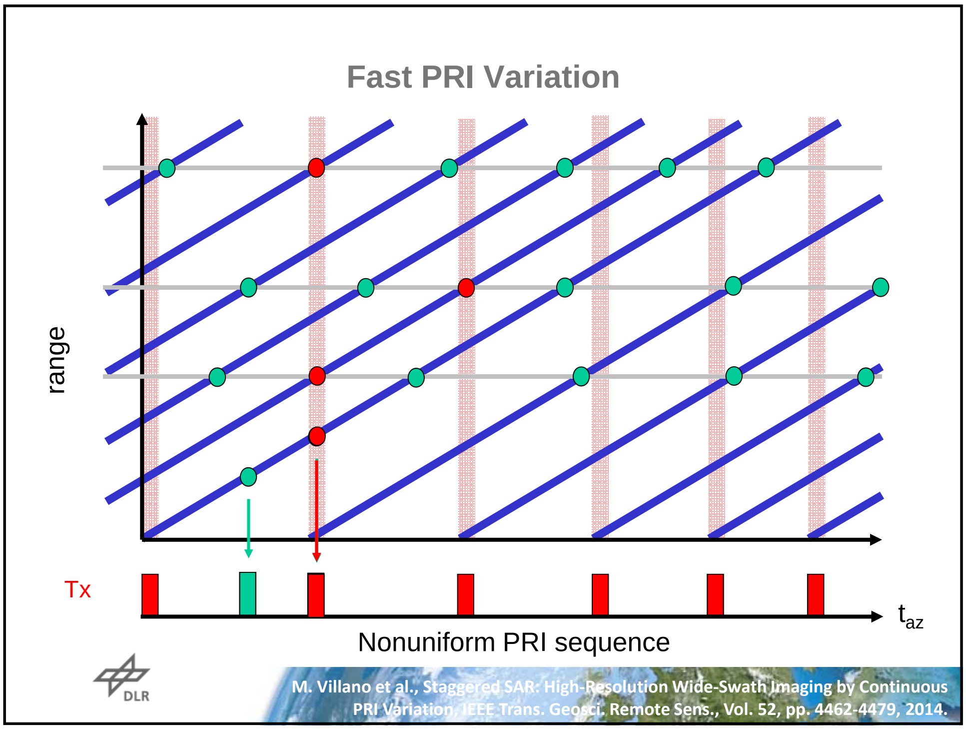

Fast PRI Variation
range
Tx
t_{az}
Nonuniform PRI sequence
DLR
M. Villano et al., Staggered SAR: High-Resolution Wide-Swath Imaging by Continuous PRI Variation, IEEE Trans. Geosci. Remote Sens., Vol. 52, pp. 4462-4479, 2014.

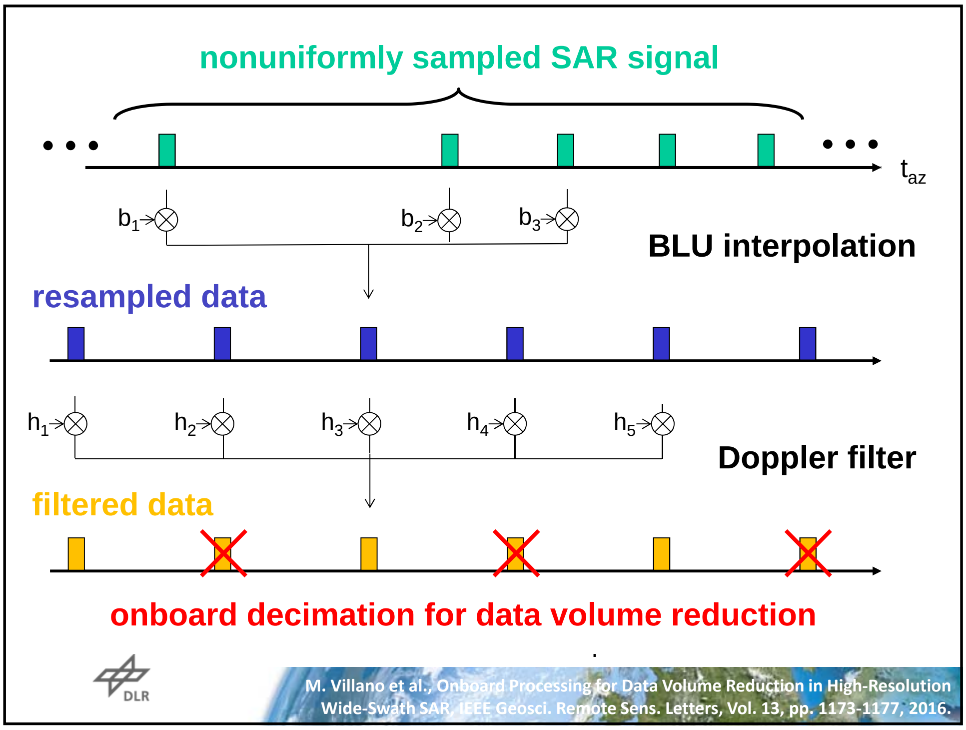

nonuniformly sampled SAR signal
t_{az}
b_1
b_2
b_3
BLU interpolation
resampled data
h_1
h_2
h_3
h_4
h_5
Doppler filter
filtered data
onboard decimation for data volume reduction
DLR
M. Villano et al., Onboard Processing for Data Volume Reduction in High-Resolution Wide-Swath SAR, IEEE Geosci. Remote Sens. Letters, Vol. 13, pp. 1173-1177, 2016.

Staggered SAR (400 km Single-Pol)

Parameter	Value
Wavelength	0.236 m (L-Band)
Antenna diameter	15 m
Feed size	7.15 m x 0.86 m
Orbital altitude	773 km
Tx duty cycle	6%
Average Tx power	306 W
Polarisation	single-pol (400 km)

NESZ

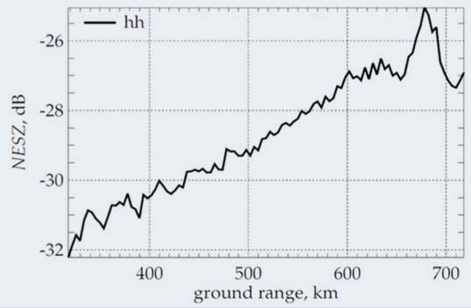

Range Ambiguities (RASR)

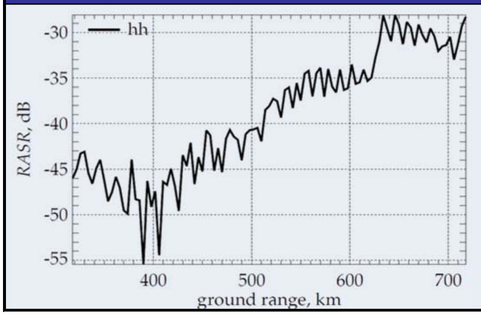

Azimuth Ambiguities (AASR)

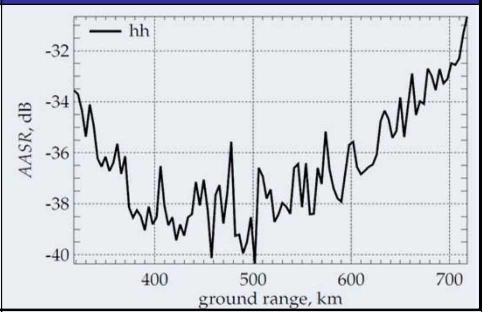

Staggered SAR (200 km Quad-Pol)

Parameter	Value
Wavelength	0.236 m (L-Band)
Antenna diameter	15 m
Feed size	7.15 m x 0.86 m
Orbital altitude	773 km
Tx duty cycle	2 x 3%
Average Tx power	177 W
Polarisation	quad-pol (200 km)

NESZ

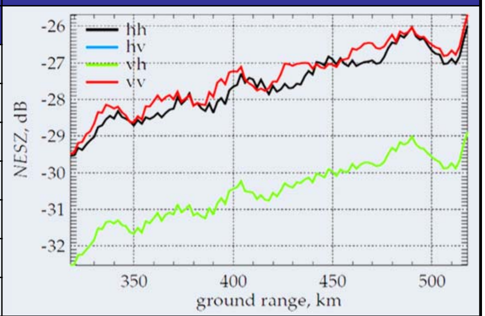

Range Ambiguities (RASR)

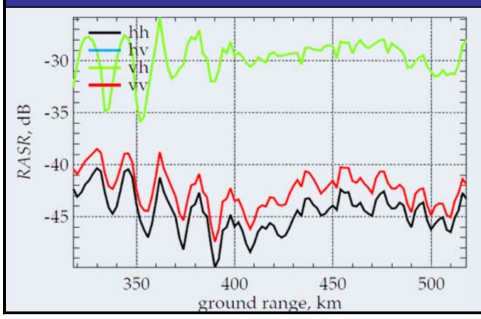

Azimuth Ambiguities (AASR)

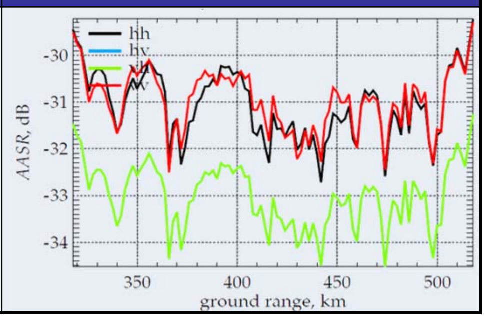

Smearing of Azimuth Ambiguities in Staggered SAR

Simulation to demonstrate the additional benefits from azimuth ambiguity smearing for a staggered-SAR system, based on a TerraSAR-X image, acquired over Barcelona, Spain. (a) Original image with accentuated azimuth ambiguities. (b) Simulated staggered-SAR image using the more elaborated sequence and best linear interpolation (BLU). (From Villano et al., *Staggered SAR: High-Resolution Wide-Swath Imaging by Continuous PRI Variation*, IEEE Transactions on Geoscience and Remote Sensing, July 2013).

DLR

M. Villano et al., Staggered SAR: Performance Analysis and Experiments With Real Data, IEEE Trans. Geosci. Remote Sens., Vol. 55, pp. 6617-6638, 2017.

Tandem-L

Systematic Monitoring of Earth System Dynamics

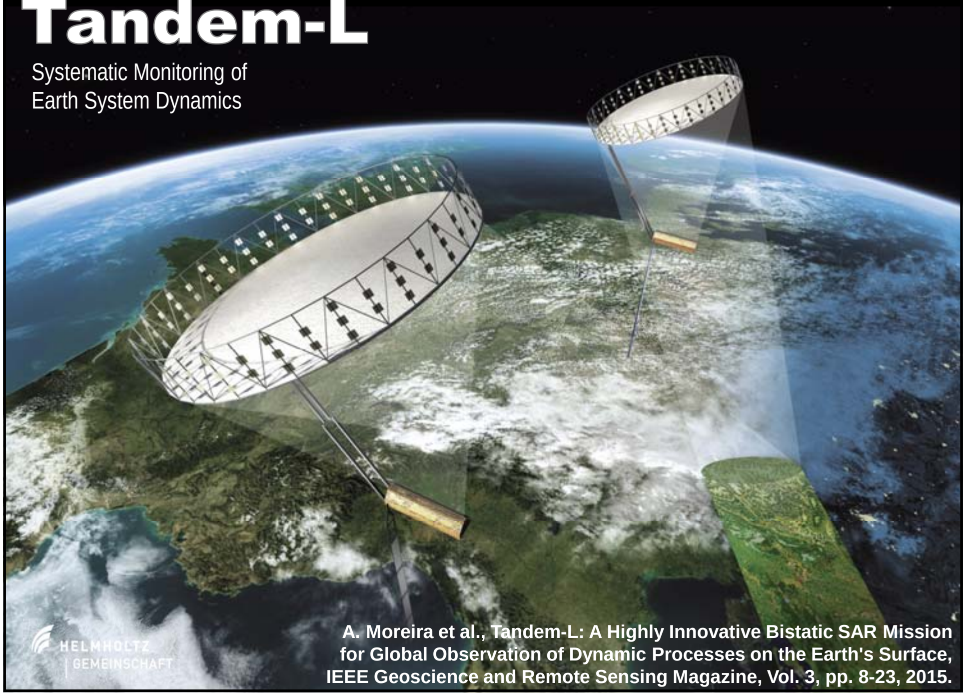

HELMHOLTZ GEMEINSCHAFT

A. Moreira et al., Tandem-L: A Highly Innovative Bistatic SAR Mission for Global Observation of Dynamic Processes on the Earth's Surface, IEEE Geoscience and Remote Sensing Magazine, Vol. 3, pp. 8-23, 2015.

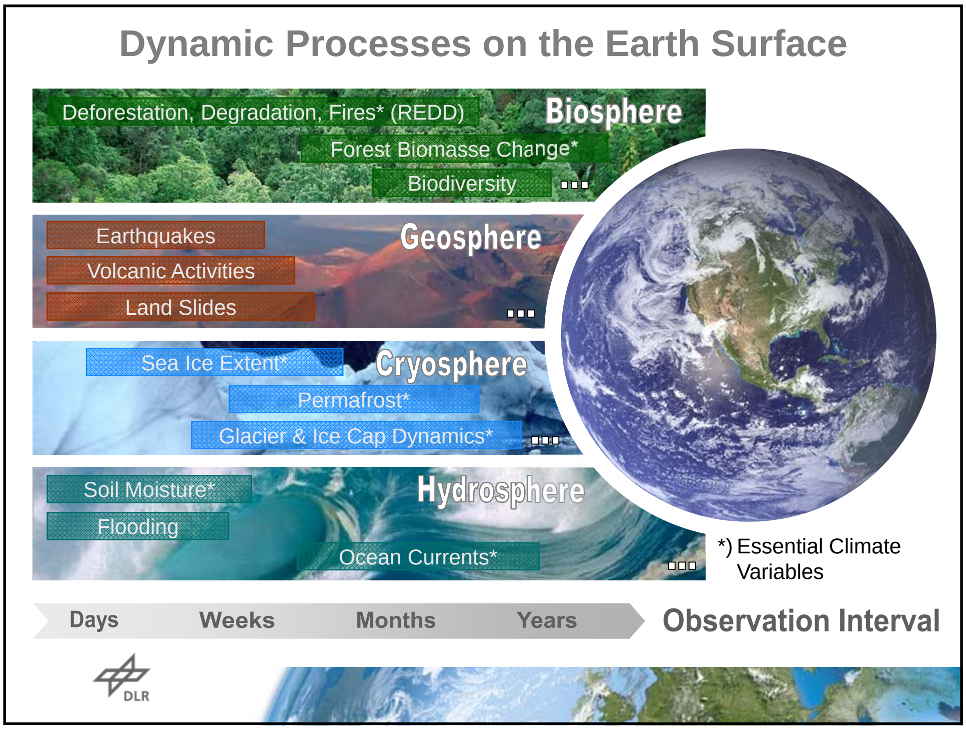

Dynamic Processes on the Earth Surface
Deforestation, Degradation, Fires* (REDD)
Biosphere
Forest Biomasse Change*
Biodiversity
Earthquakes
Volcanic Activities
Land Slides
Geosphere
Sea Ice Extent*
Cryosphere
Permafrost*
Glacier & Ice Cap Dynamics*
Soil Moisture*
Flooding
Hydrosphere
Ocean Currents*
*) Essential Climate Variables
Days
Weeks
Months
Years
Observation Interval
DLR

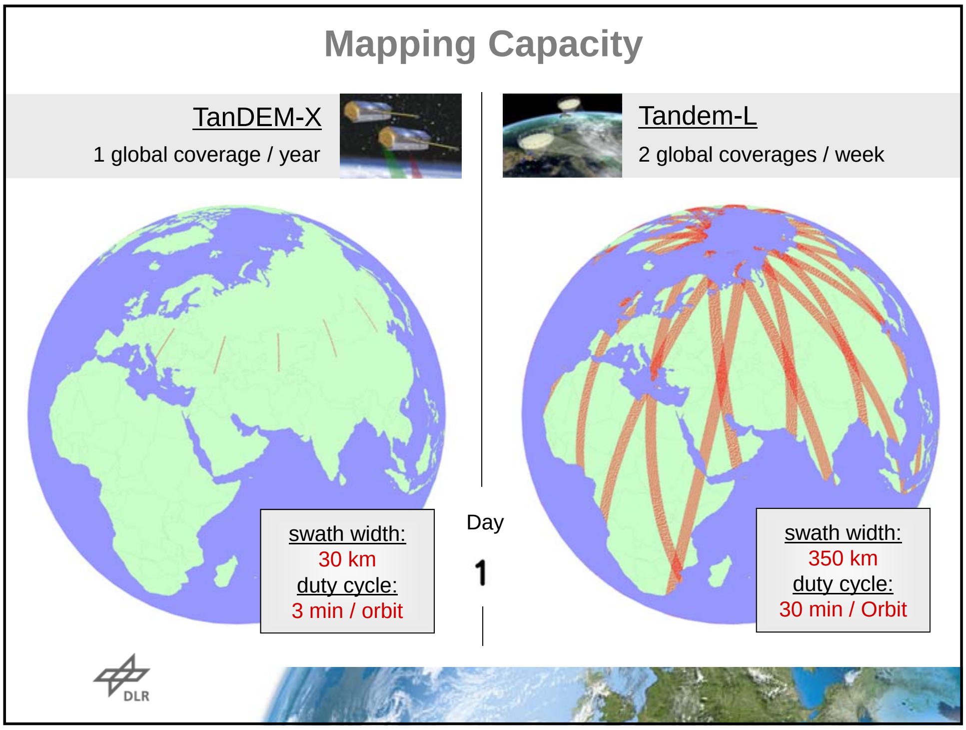

Mapping Capacity
TanDEM-X
1 global coverage / year
Tandem-L
2 global coverages / week
swath width:
30 km
duty cycle:
3 min / orbit
Day
1
swath width:
350 km
duty cycle:
30 min / Orbit
DLR

Staggered SAR with Multiple Azimuth Channels

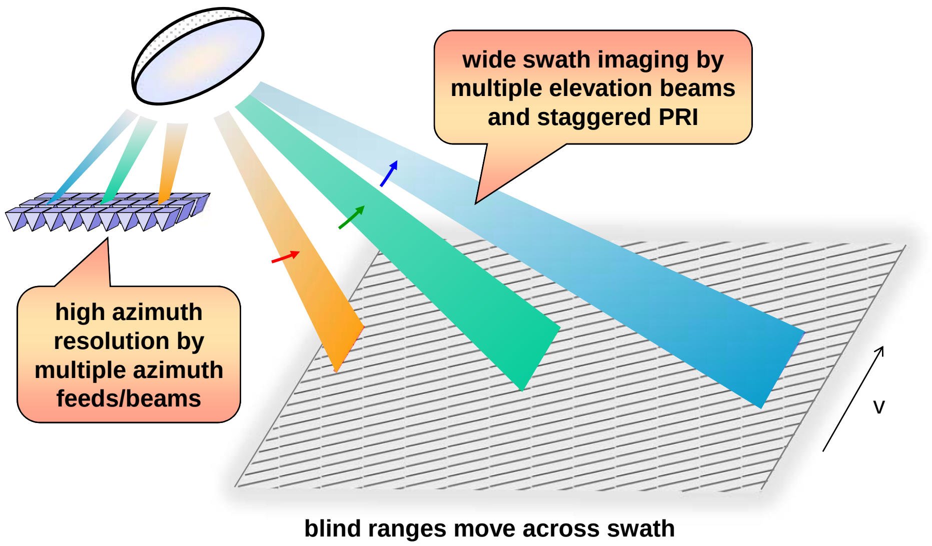

Staggered SAR with Multiple Azimuth Channels

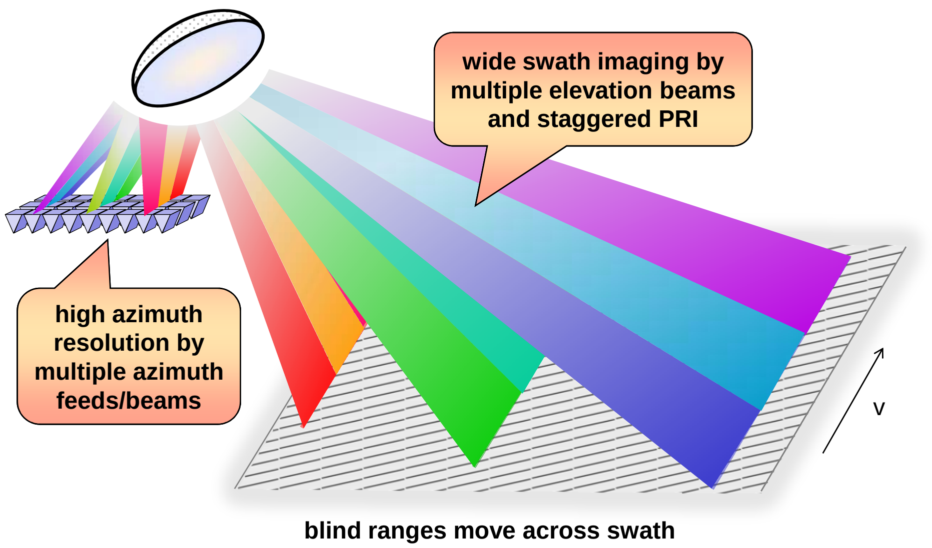

Staggered SAR with Multiple Azimuth Channels

- Requires combination of
  - multi-channel reconstruction
  - staggered SAR interpolation
- Novel virtual beam synthesis technique
- Key idea: multichannel SAR signal resampling to uniform grid using
  - multiple Rx pulses (time-variant interpolation)
  - adaptive beams (time-variant aperture tapering)

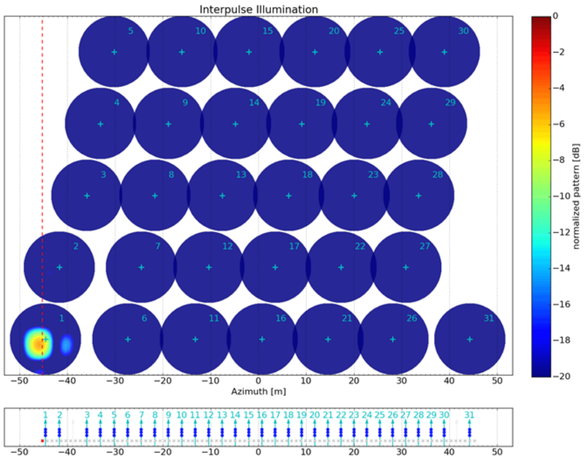

F. Queiroz de Almeida et al, “Multichannel staggered SAR azimuth sample regularization”, Proc. EUSAR, June 2016 (TGRS paper in print)

DLR

F. Queiroz de Almeida et al., Multichannel Staggered SAR Azimuth Processing, IEEE Trans. Geosci. Remote Sens., Vol. 56, pp. 2772-2788, 2018.

Multichannel Staggered SAR	
Parameter	**Value**
Wavelength	0.236 m (L-Band)
Antenna diameter	18 m
Feed size	9.3 m x 0.76 m
Orbital altitude	773 km
Azimuth channels	4
Average Tx power	302 W
Polarisation	quad-pol (400 km)

NESZ

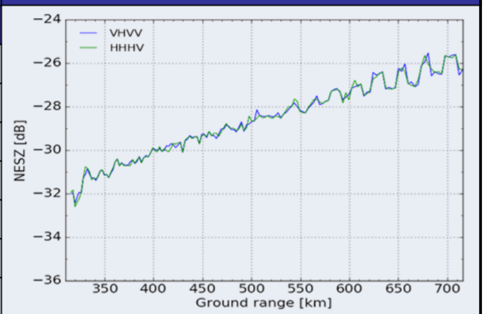

Range Ambiguities (RASR)

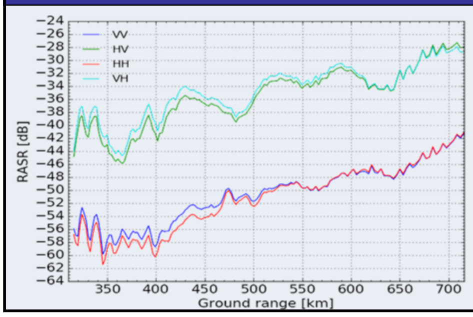

Azimuth Ambiguities (AASR)

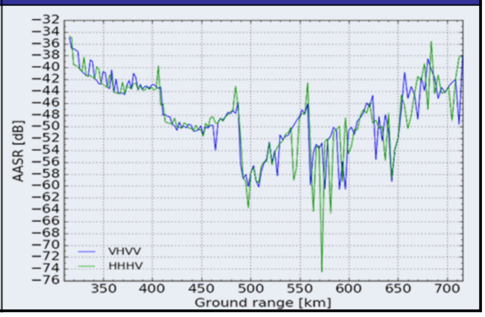

MIMO SAR

Spatiotemporally Non-Separable Waveform Encoding

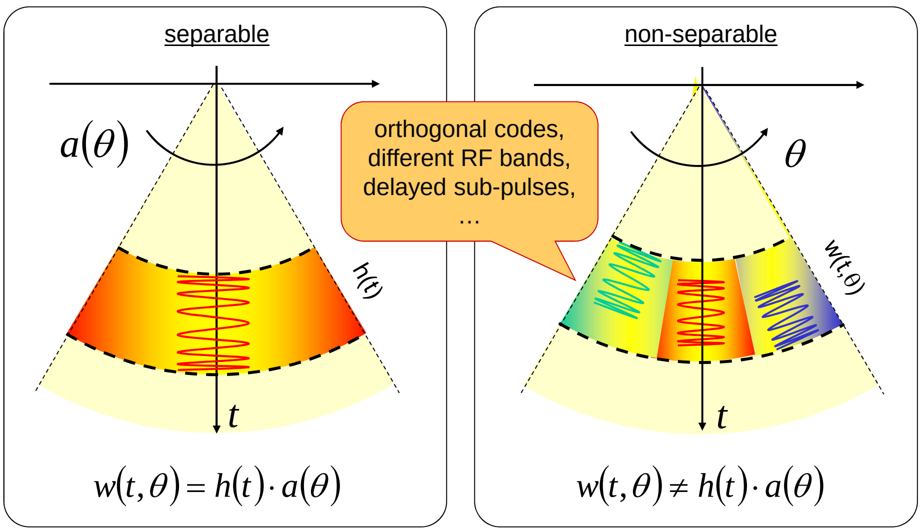

G. Krieger et al., Multidimensional Waveform Encoding: A New DBF Technique for SAR Remote Sensing, IEEE Trans. Geosci. Remote Sens., Vol. 46, pp. 31-46, 2008.

Multidimensional Waveforms: Possible Implementation

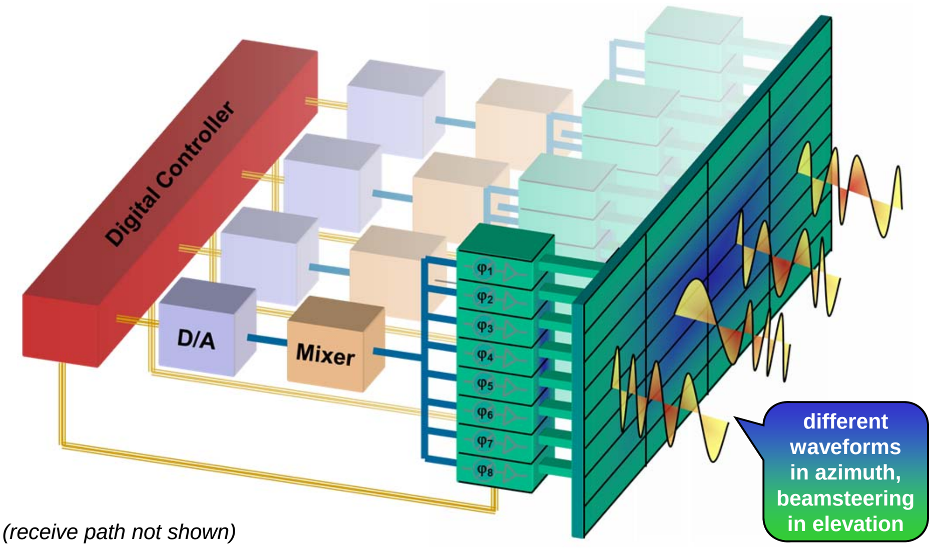

(receive path not shown)

Non-Separable Waveform: Example with 3 Sub-Pulses

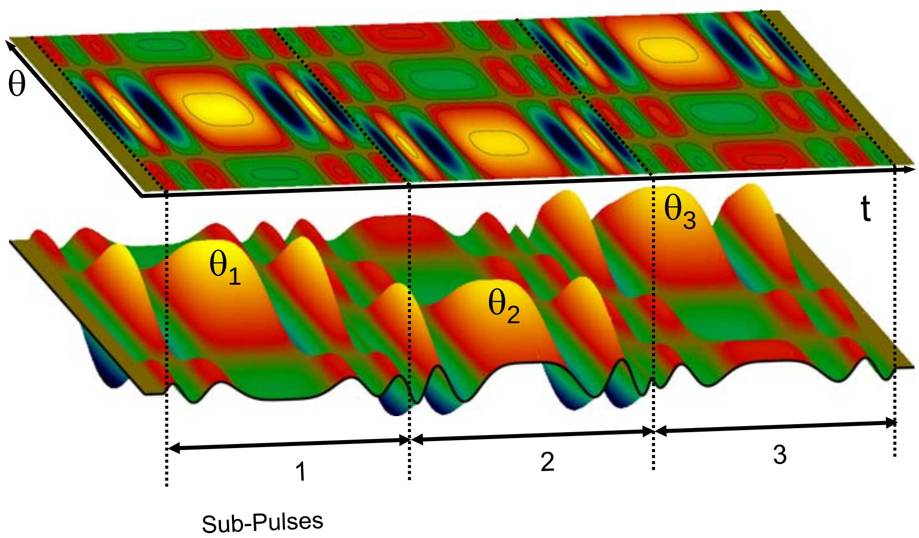

High-Resolution Wide-Swath SAR Imaging (X-Band)

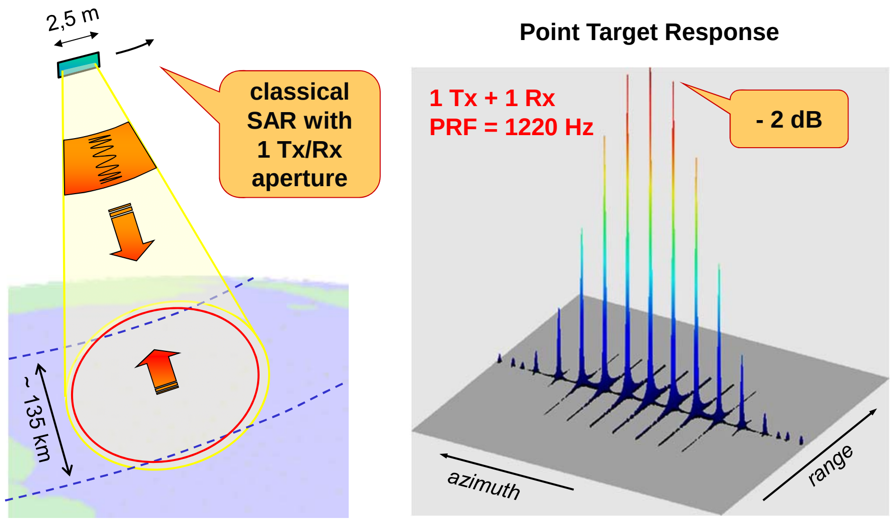

DLR

G. Krieger et al., Multidimensional Waveform Encoding: A New DBF Technique for SAR Remote Sensing, IEEE Trans. Geosci. Remote Sens., Vol. 46, pp. 31-46, 2008.

Displaced Phase Center Antenna (DPCA) Technique

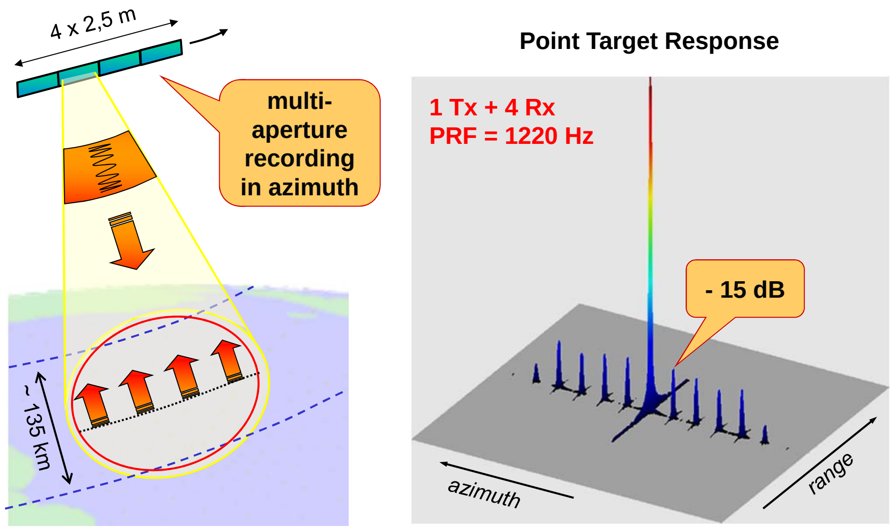

DLR

G. Krieger et al., Multidimensional Waveform Encoding: A New DBF Technique for SAR Remote Sensing, IEEE Trans. Geosci. Remote Sens., Vol. 46, pp. 31-46, 2008.

Multidimensional Waveform Encoding (MIMO SAR)

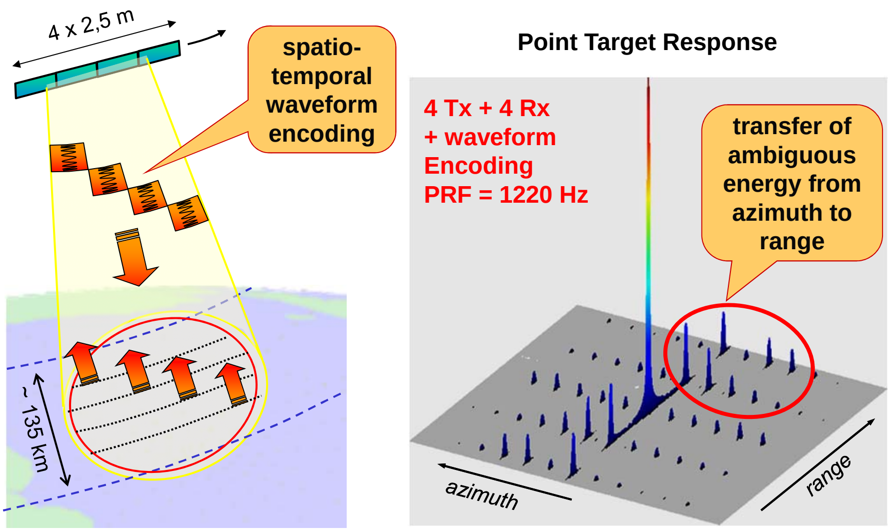

DLR

G. Krieger et al., Multidimensional Waveform Encoding: A New DBF Technique for SAR Remote Sensing, IEEE Trans. Geosci. Remote Sens., Vol. 46, pp. 31-46, 2008.

Multidimensional Waveform Encoding (MIMO SAR)

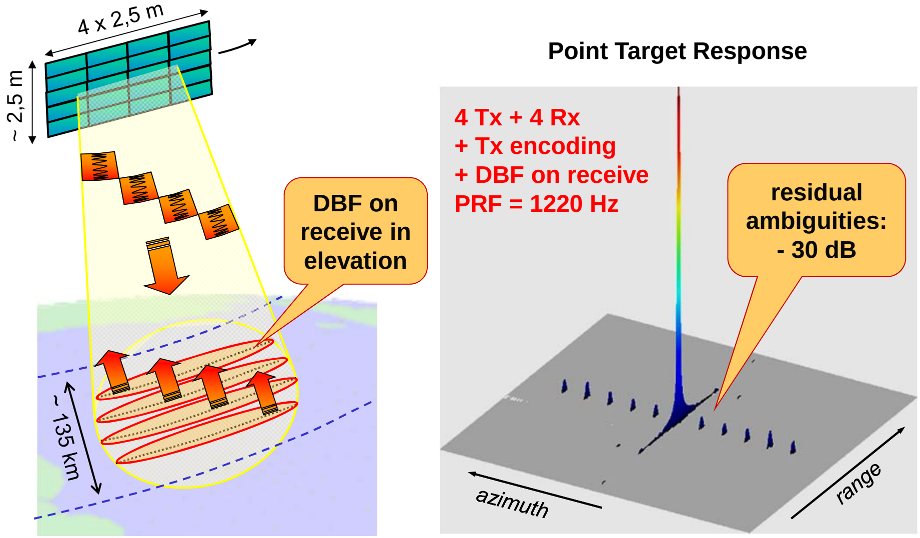

DLR

G. Krieger et al., Multidimensional Waveform Encoding: A New DBF Technique for SAR Remote Sensing, IEEE Trans. Geosci. Remote Sens., Vol. 46, pp. 31-46, 2008.

MIMO-SAR with Reflector Antennas

Direct Radiating Arrays	Reflectors with Digital Feed Array

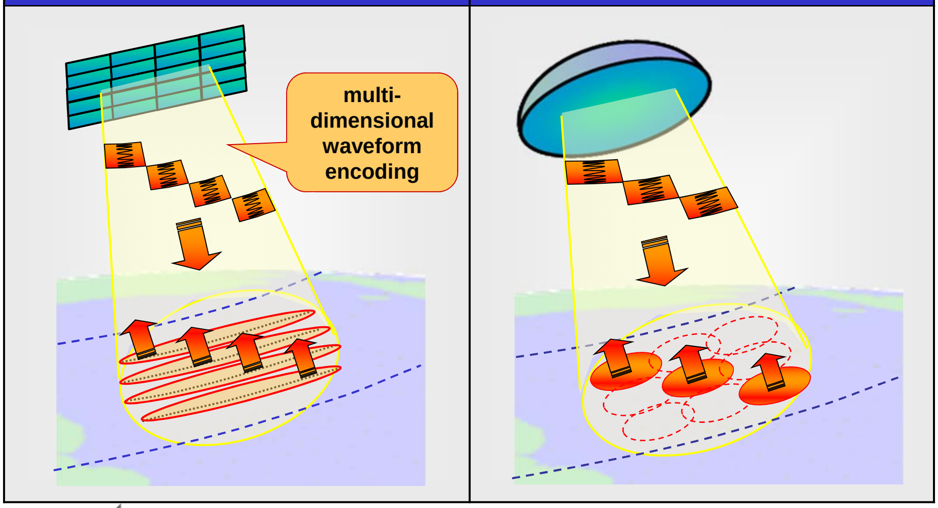

Additional Azimuth Phase Centers for Improved SAR Imaging & GMTI

Classic HRWS

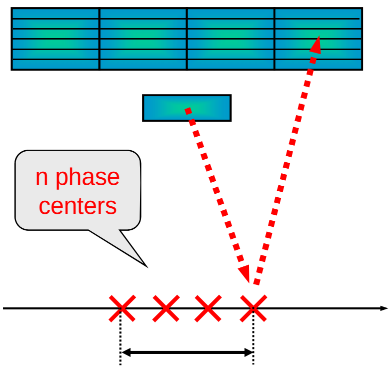

$$d_{\max} = \frac{n-1}{2} \cdot d_{ant}$$

Waveform Encoding

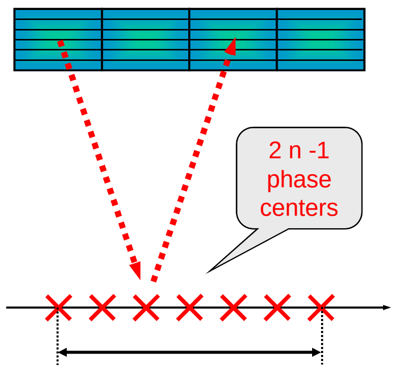

$$d_{\max} = (n-1) \cdot d_{ant}$$

G. Krieger et al., Multidimensional Waveform Encoding: A New DBF Technique for SAR Remote Sensing, IEEE Trans. Geosci. Remote Sens., Vol. 46, pp. 31-46, 2008.

Fully Polarimetric Waveform Encoding

- transmit two sub-pulses with H and V → two polarisations in each Tx pulse !
- receive radar echo in two polarisations
- use DBF to separate Tx polarisations
- **no increase of PRF → full swath width !**

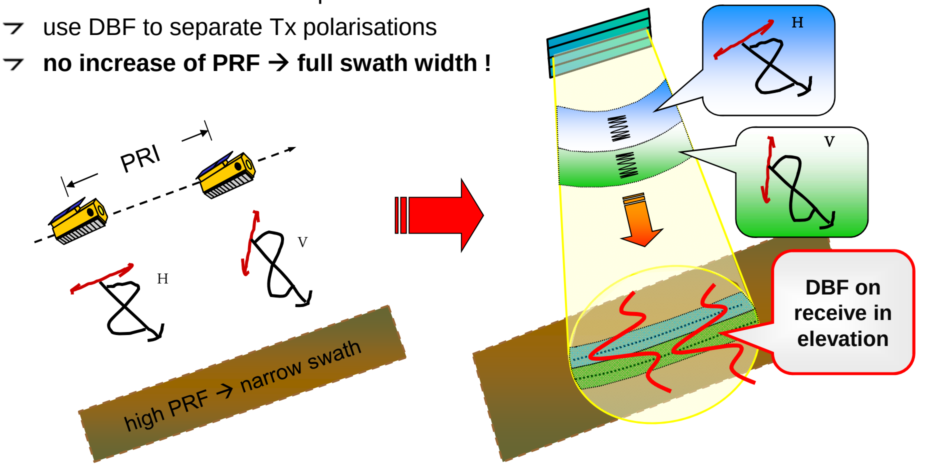

DLR

G. Krieger et al., Multidimensional waveform encoding for synthetic aperture radar remote sensing, Proc. IET Int. Conf. Radar Syst., Edinburgh, U.K., pp. 1–5, 2007.

IEEE TRANSACTIONS ON GEOSCIENCE AND REMOTE SENSING, VOL. 53, NO. 5, MAY 2015 2453

Spaceborne MIMO Synthetic Aperture Radar for Multimodal Operation

Jung-Hyo Kim, Marwan Younis, *Senior Member, IEEE*, Alberto Moreira, *Fellow, IEEE*, and Werner Wiesbeck, *Fellow, IEEE*

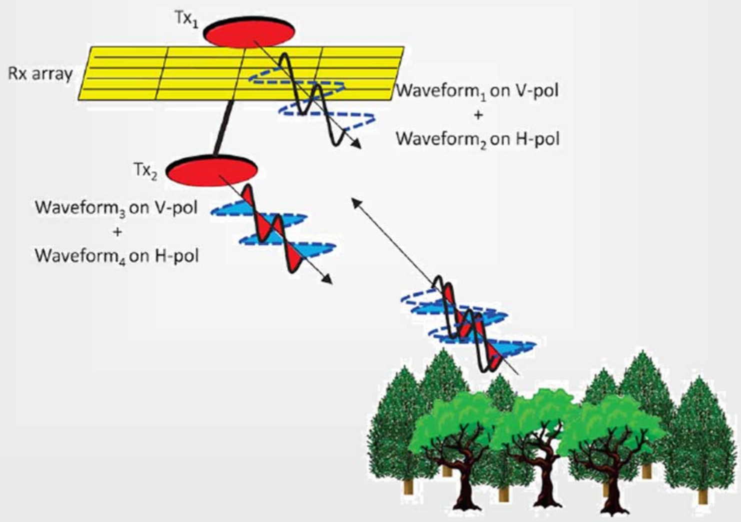

Orthogonal Waveforms for MIMO-SAR
(Examples from Recent IEEE Publications)

$$\int s_i(t)s_j^*(t+\tau)dt = 0, i \neq j, \forall \tau \in \mathbf{R}, i,j = 1,2,\cdots,L.$$

WQ Wang, IEEE AC 2007

$$S_i(f) \cdot S_j^*(f) = 0 \quad \forall \quad f \in \mathbb{R}$$

→ no coherence for interferometry, polarimetry, azimuth ambiguity suppression, GMTI, … ☹

Orthogonal Waveforms for MIMO-SAR
(Examples from Recent IEEE Publications)

$$\int s_i(t)s_j^*(t+\tau)dt = 0, i \neq j, \forall \tau \in \mathbf{R}, i,j = 1,2,\cdots,L.$$

WQ Wang, IEEE AC 2007

$$\int_0^{T_s} s_m(t)s_n^*(t)dt = \begin{cases} c_m, & m = n \\ 0, & m \neq n \end{cases}$$

WQ Wang, IEEE TGRS 2011

$$\int_{T_p} s_m(t)s_n^*(t)\mathrm{d}t = \delta(\cancel{t}), \qquad (m,n) \in [1,2,3,\ldots,K]$$

$$= \delta_{mn}?$$

WQ Wang, IEEE GRSL 2012

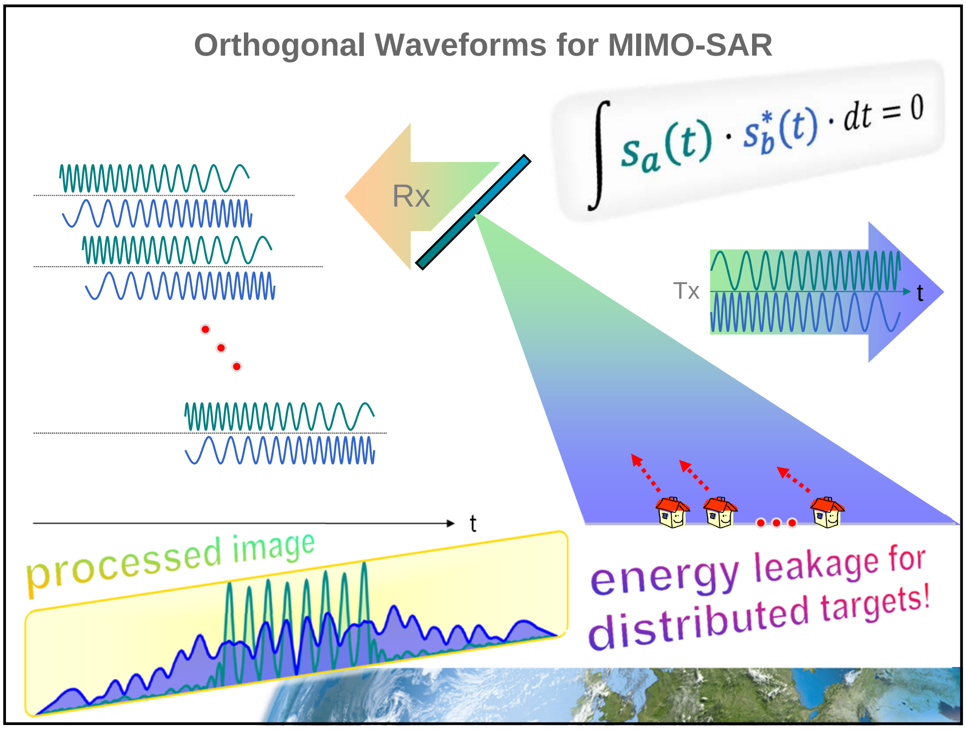

Orthogonal Waveforms for MIMO-SAR
$\int s_a(t) \cdot s_b^*(t) \cdot dt = 0$
Rx
Tx
t
t
processed image
energy leakage for distributed targets!

Orthogonal Waveforms for MIMO-SAR: Up & Down-Chirps
Original Scene
Matched Filter Result (only matched channel present)
Matched Filter Result (also orthogonal channel present)
azimuth
range

Orthogonal Waveforms for MIMO-SAR: Up & Down-Chirps

Original Scene

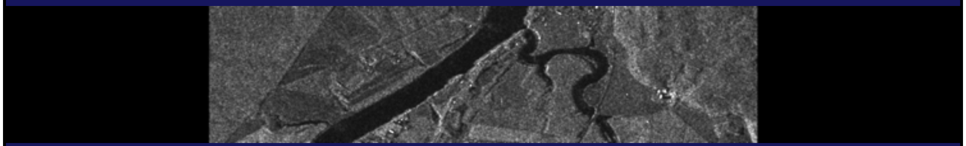

Matched Filter Result (only matched channel present)

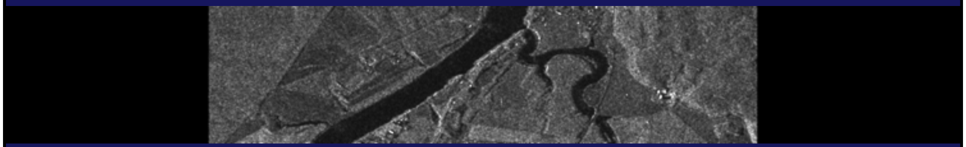

Matched Filter Result (also orthogonal channel present)

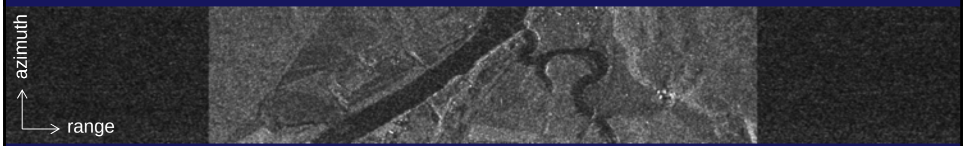

Orthogonal Waveforms for MIMO-SAR: Up & Down-Chirps

Original Scene

Matched Filter Result (only matched channel present)

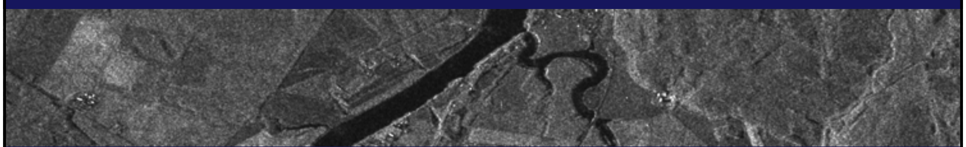

Matched Filter Result (also orthogonal channel present)

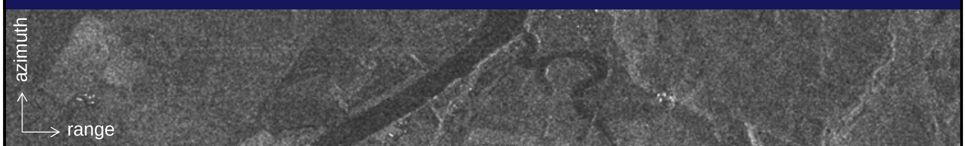

IEEE TRANSACTIONS ON GEOSCIENCE AND REMOTE SENSING, VOL. 53, NO. 3, MARCH 2015 1615

MIMO SAR OFDM Chirp Waveform Diversity Design With Random Matrix Modulation

Wen-Qin Wang, *Member, IEEE*

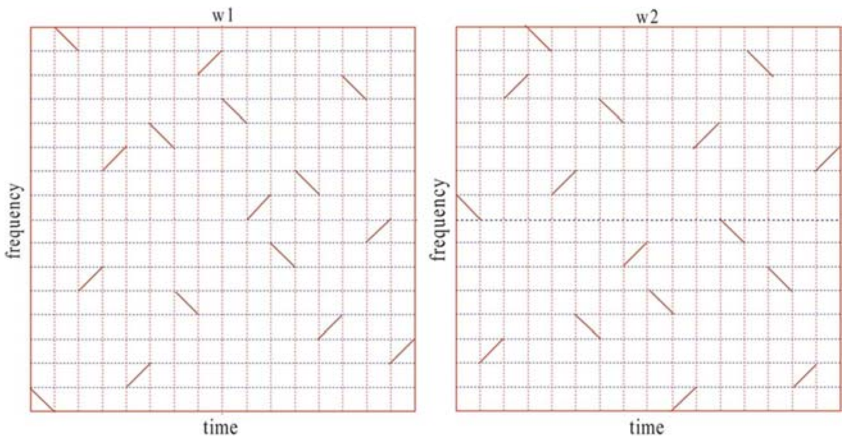

DLR

W. Q. Wang, MIMO SAR OFDM Chirp Waveform Diversity Design With Random Matrix Modulation, IEEE Trans. Geosci. Remote Sens., Vol. 53, pp. 1615-1625, 2015.

Autocorrelation and Crosscorrelation

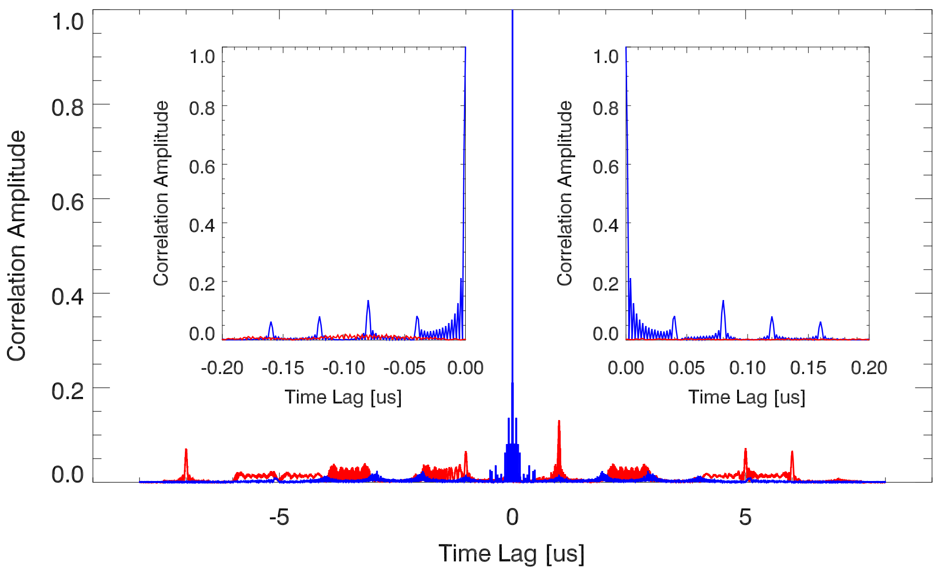

DLR

Orthogonal Waveforms for MIMO-SAR: Wen-Qin Wang 2015

Original Scene

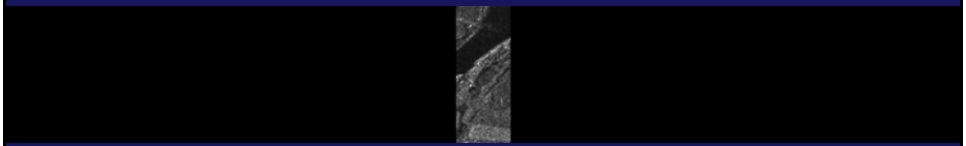

Matched Filter Result (only matched channel present)

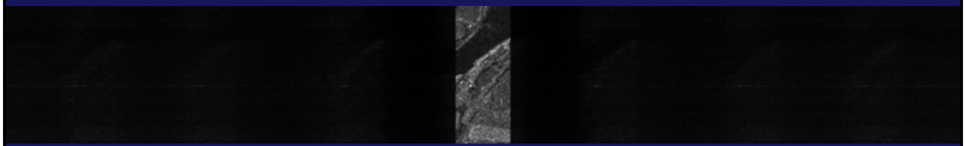

Matched Filter Result (also orthogonal channel present)

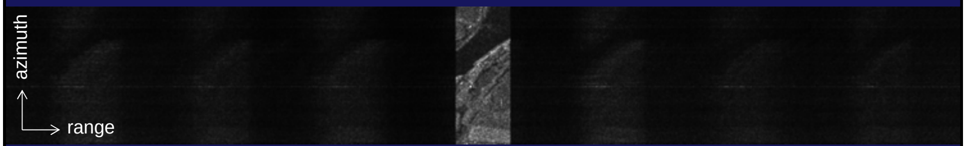

Orthogonal Waveforms for MIMO-SAR: Wen-Qin Wang 2015

Original Scene

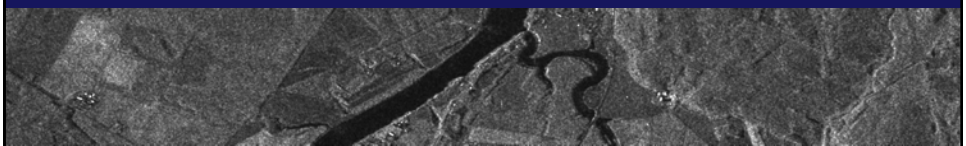

Matched Filter Result (only matched channel present)

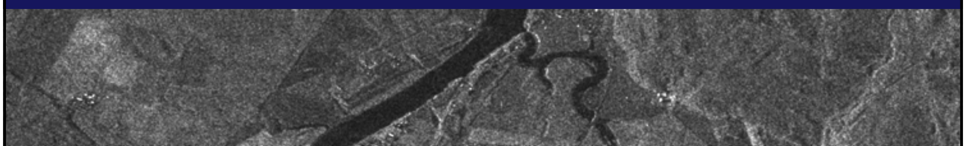

Matched Filter Result (also orthogonal channel present)

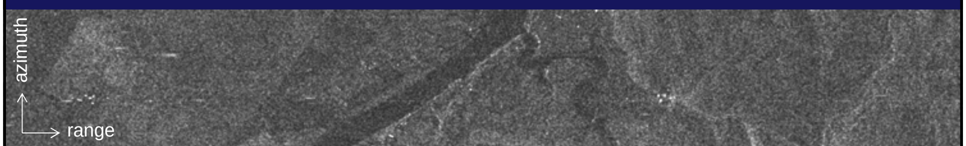

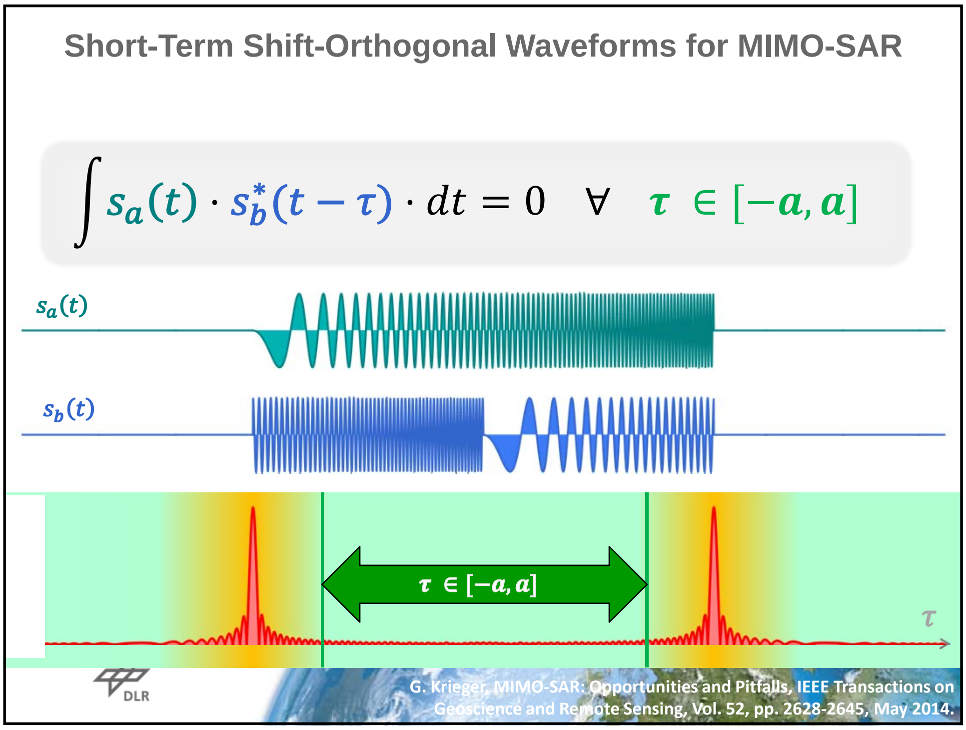
Short-Term Shift-Orthogonal Waveforms for MIMO-SAR
$\int s_a(t) \cdot s_b^*(t-\tau) \cdot dt = 0 \quad \forall \quad \tau \in [-a, a]$
$s_a(t)$
$s_b(t)$
$\tau \in [-a, a]$
τ
DLR
G. Krieger, MIMO-SAR: Opportunities and Pitfalls, IEEE Transactions on Geoscience and Remote Sensing, Vol. 52, pp. 2628-2645, May 2014.

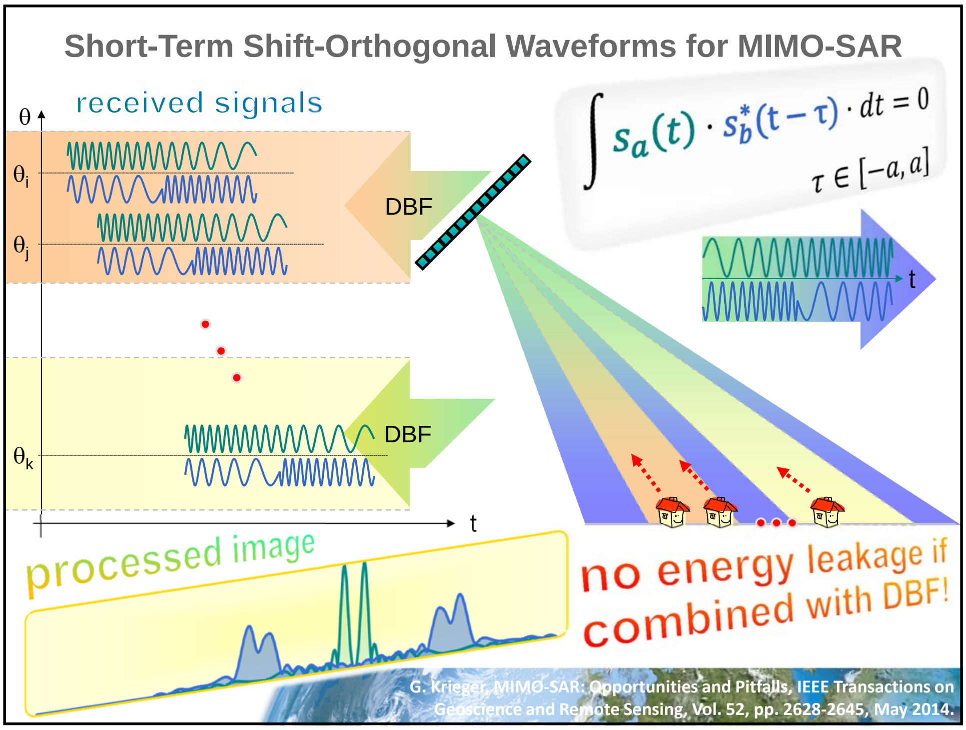
Short-Term Shift-Orthogonal Waveforms for MIMO-SAR
received signals
θ
θ_i
θ_j
θ_k
DBF
DBF
t
$\int s_a(t) \cdot s_b^*(t-\tau) \cdot dt = 0$
$\tau \in [-a, a]$
t
processed image
no energy leakage if combined with DBF!
G. Krieger, MIMO-SAR: Opportunities and Pitfalls, IEEE Transactions on Geoscience and Remote Sensing, Vol. 52, pp. 2628-2645, May 2014.

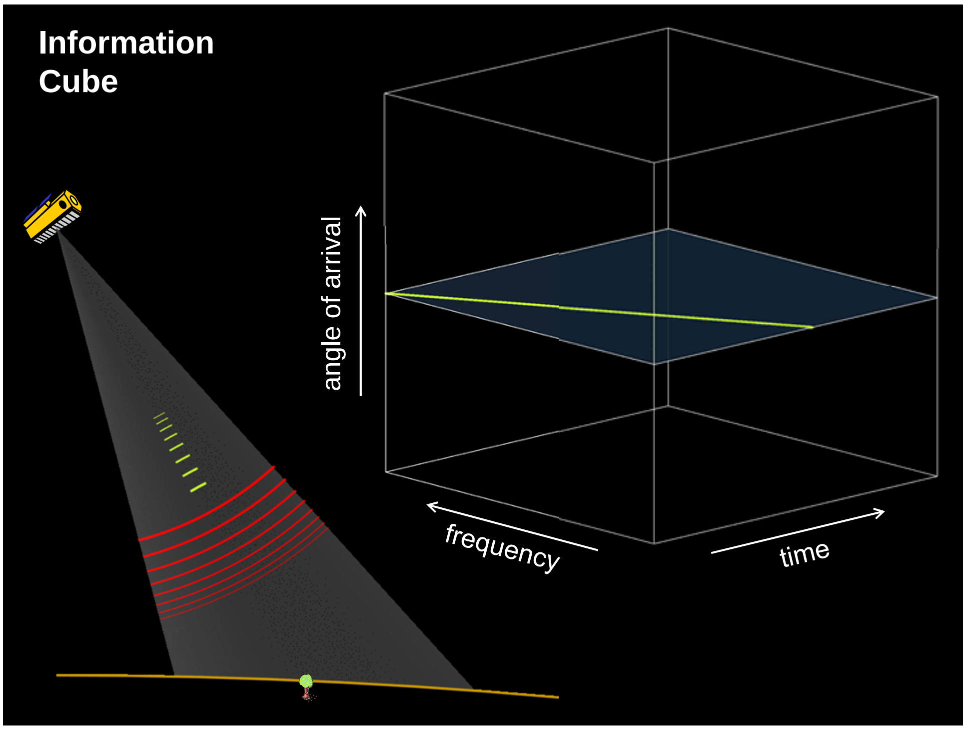
Information
Cube
angle of arrival
frequency
time

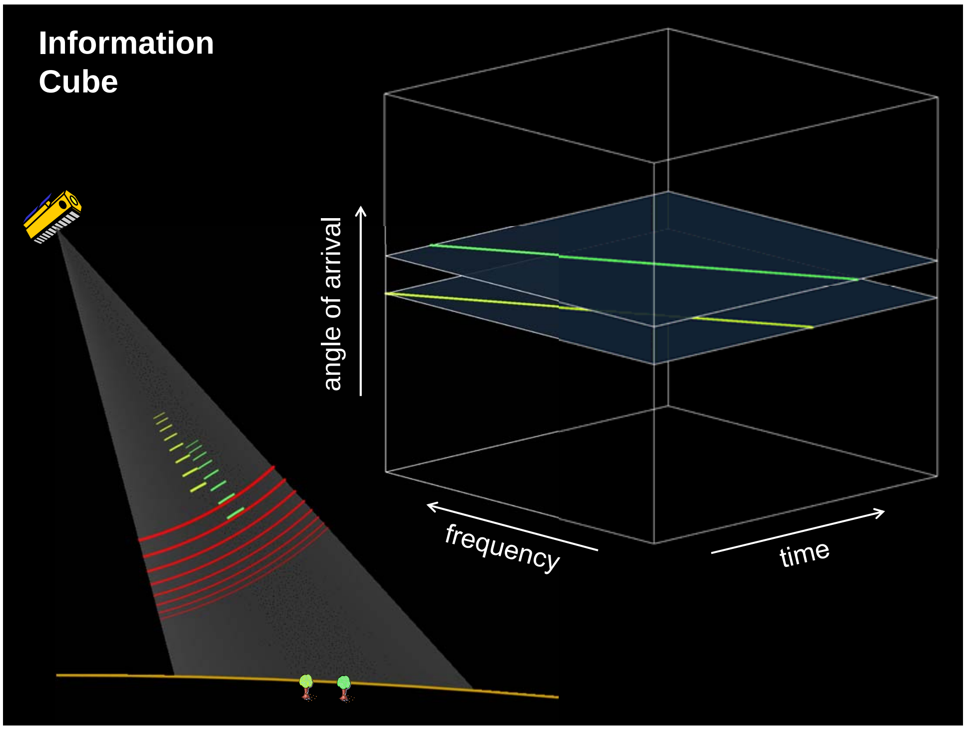
Information
Cube
angle of arrival
frequency
time

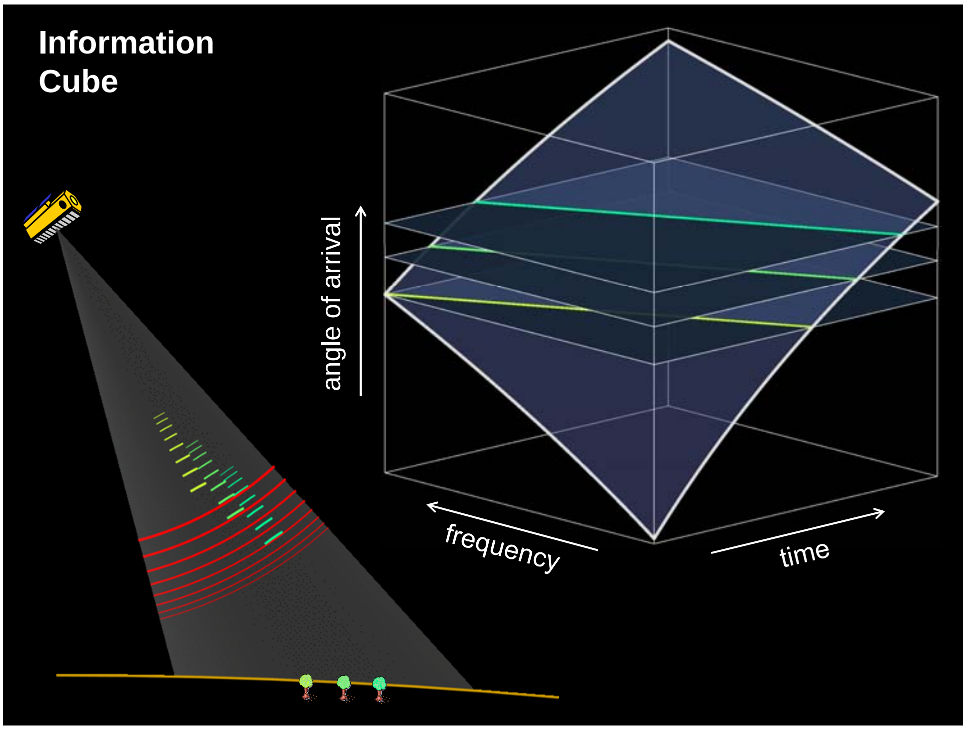
Information
Cube
angle of arrival
frequency
time

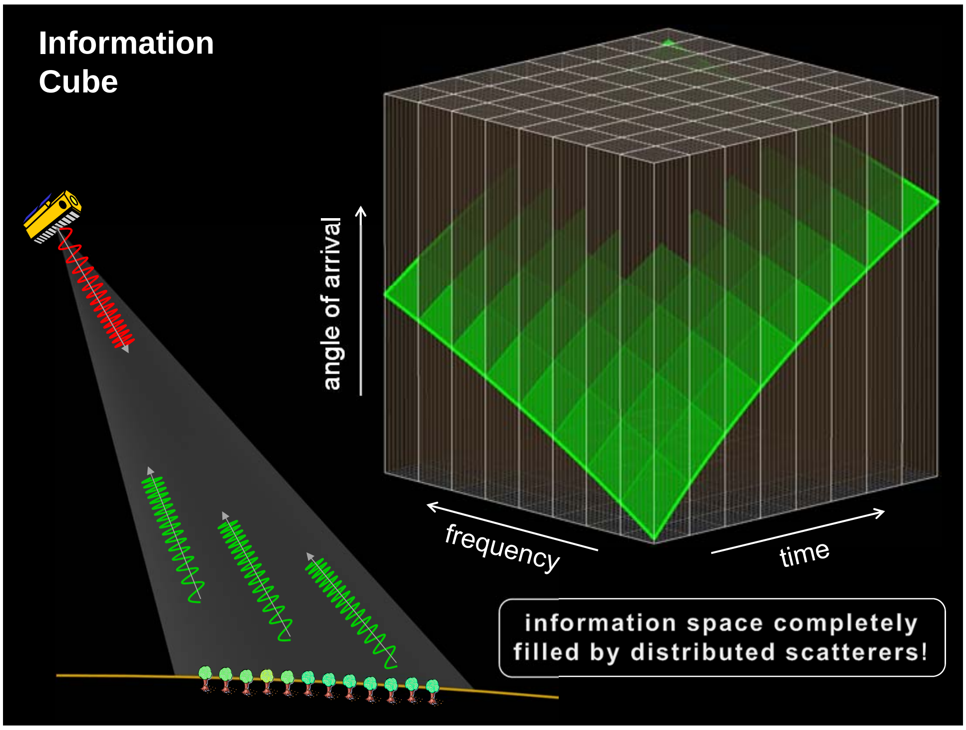
Information
Cube
angle of arrival
frequency
time
information space completely
filled by distributed scatterers!

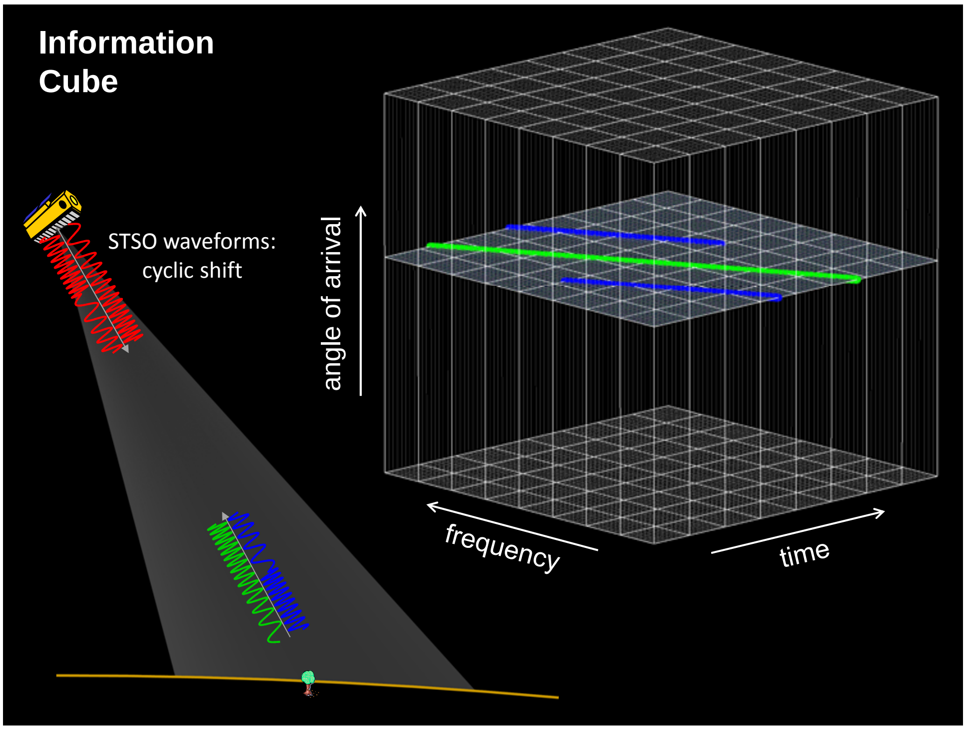
Information
Cube
STSO waveforms:
cyclic shift
angle of arrival
frequency
time

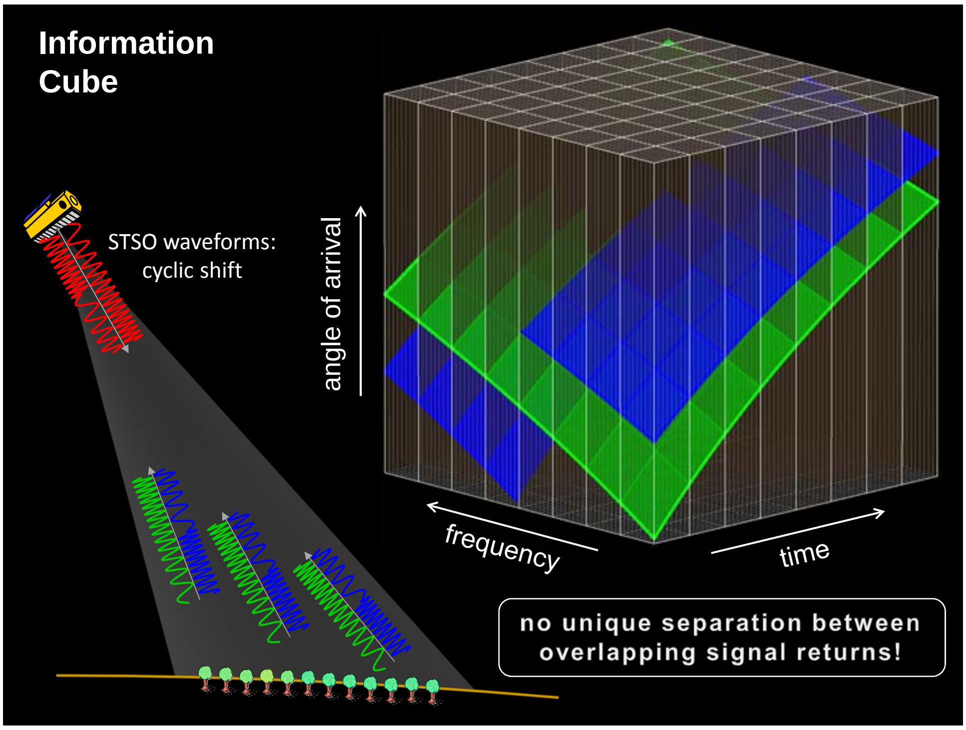
Information
Cube
STSO waveforms:
cyclic shift
angle of arrival
frequency
time
no unique separation between
overlapping signal returns!

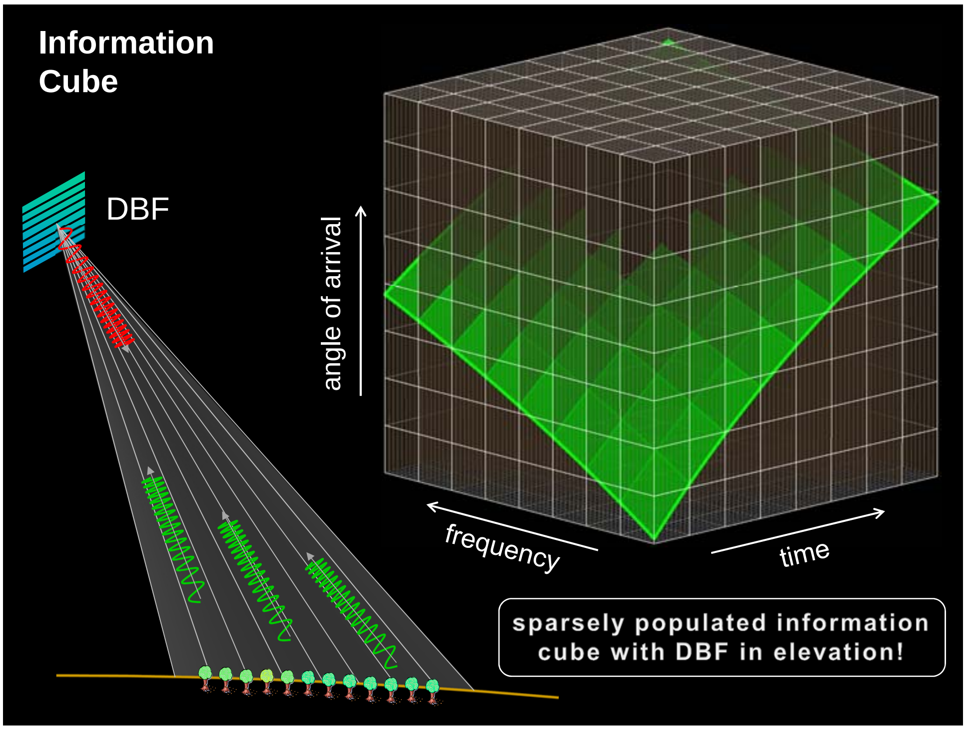
Information
Cube
DBF
angle of arrival
frequency
time
sparsely populated information
cube with DBF in elevation!

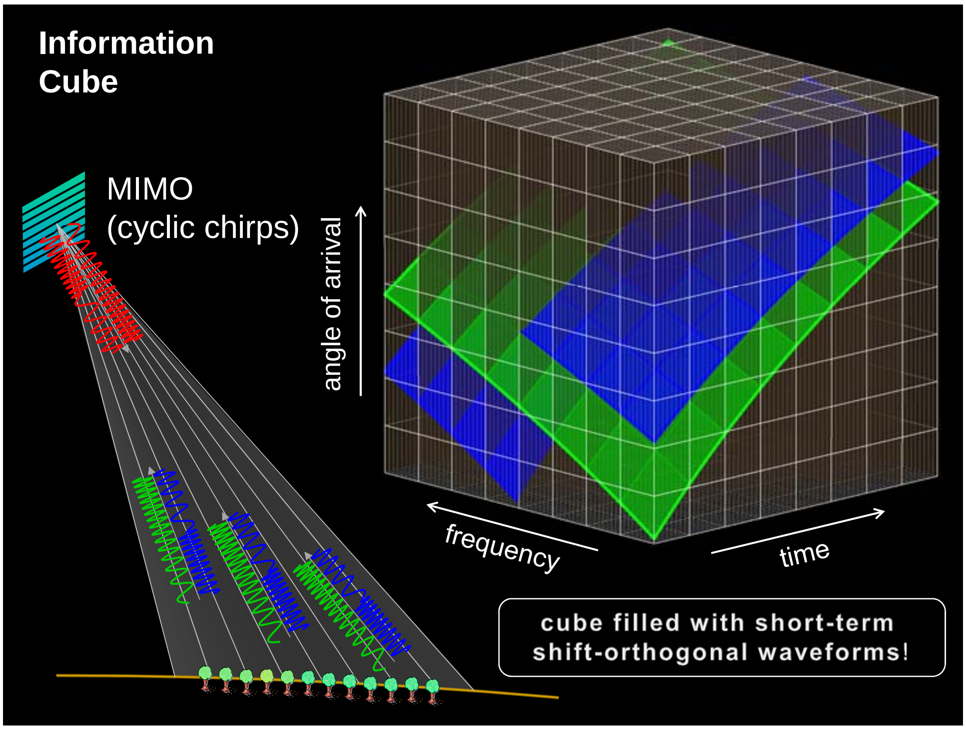
Information
Cube
MIMO
(cyclic chirps)
angle of arrival
frequency
time
cube filled with short-term
shift-orthogonal waveforms!

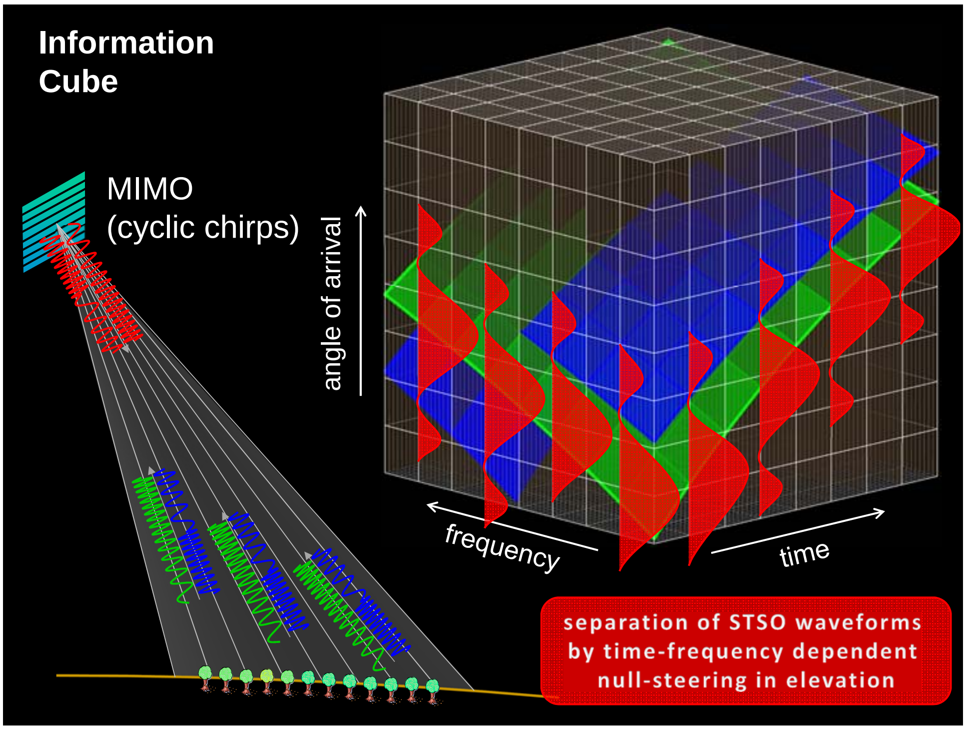

Echo Separation in Multidimensional Waveform Encoding SAR Remote Sensing Using an Advanced Null-Steering Beamformer

Fan Feng, Shiqiang Li, Weidong Yu, *Member, IEEE*, Pingping Huang, and Wei Xu

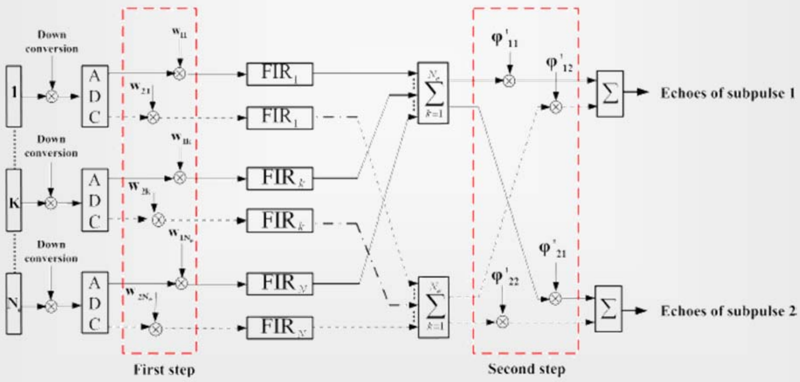

Fig. 8. Block diagram of advanced null-steering beamformer on the satellite. w_{mk} denotes the element of the matrix $\mathbf{V}^{H}$, where subscripts signify its position in the matrix, and ϕ'_{ij} represents the (i, j)th element of the matrix $N_e[(\mathbf{V}')^{H}\mathbf{V}']^{-1}$.

IEEE GEOSCIENCE AND REMOTE SENSING LETTERS, VOL. 11, NO. 12, DECEMBER 2014 2173

Digital Beamforming on Receive in Elevation for Multidimensional Waveform Encoding SAR Sensing

Feng He, Xile Ma, Zhen Dong, and Diannong Liang

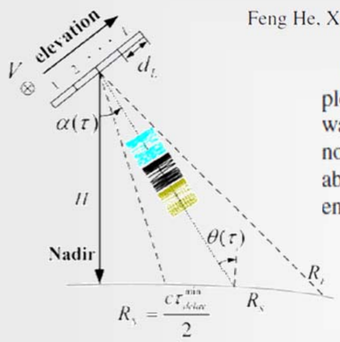

In this letter, the performance of the separation approach employing *a posteriori* DBF in elevation is investigated in detail. It was originally suggested in [2] and was employed in [9] with a novel full polarimetric SAR mode. This way, useful information about the spatial structure in elevation will be preserved to enable flexible and adaptive beamforming on the ground. An

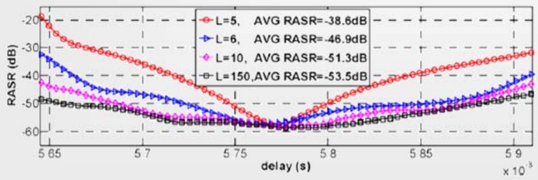

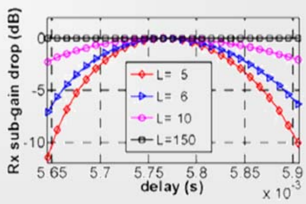

Fig. 3. RASR versus ground delay employing different elevation subapertures.

A Closer Look to Null-Steering

DLR

Example 1: Range Ambiguities for Planar Array

Antenna height	h_{ant}	2.5 m
Antenna height	l_{ant}	4 x 2.5 m
Wavelength	λ	0.031 m
Satellite height	z_{sat}	576 km
Height offset	dh	1.5 km
Satellite velocity	v_{sat}	7.5 km/s
Earth radius	r_e	6378 km
Look angle	θ_{look}	32.4°
Sub-pulse delay	$\Delta\tau$	50 µs

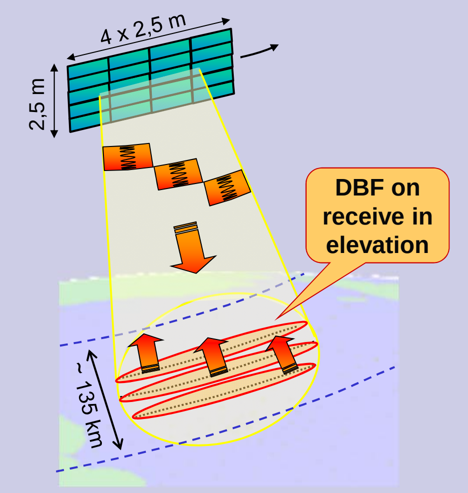

Iso-Range Contours on Earth Surface

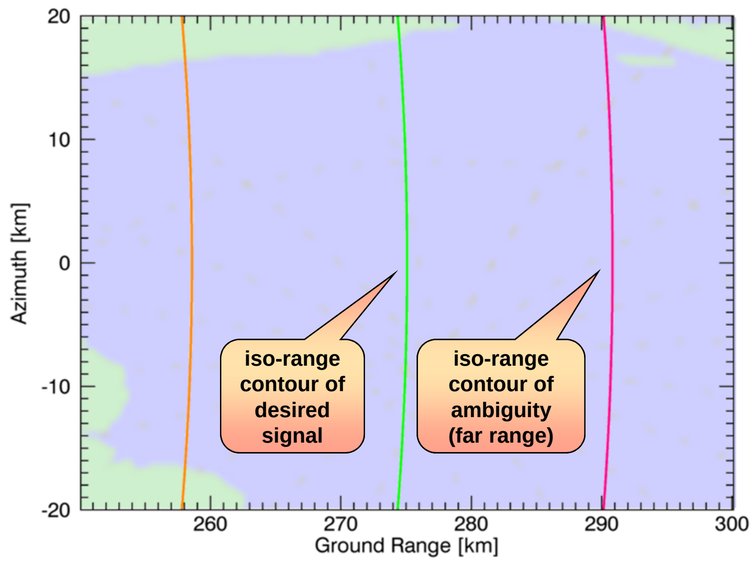

Null-Steering in Elevation for Zero-Doppler Position

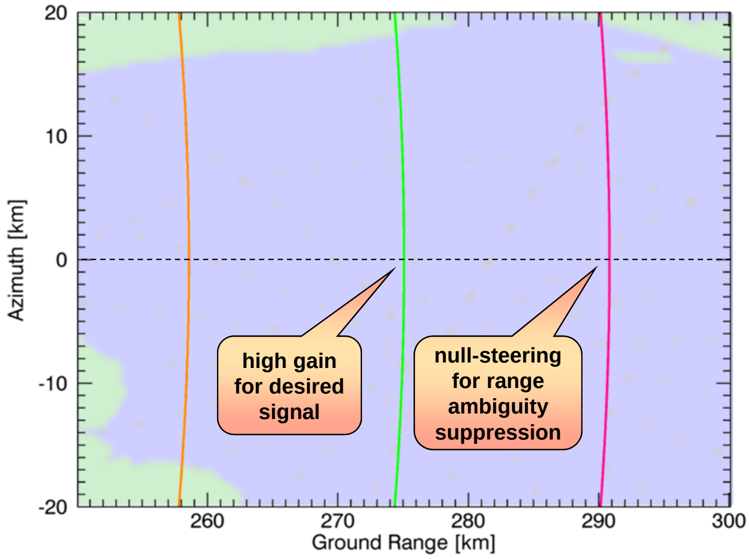

Null-Steering in Elevation for Zero-Doppler Position

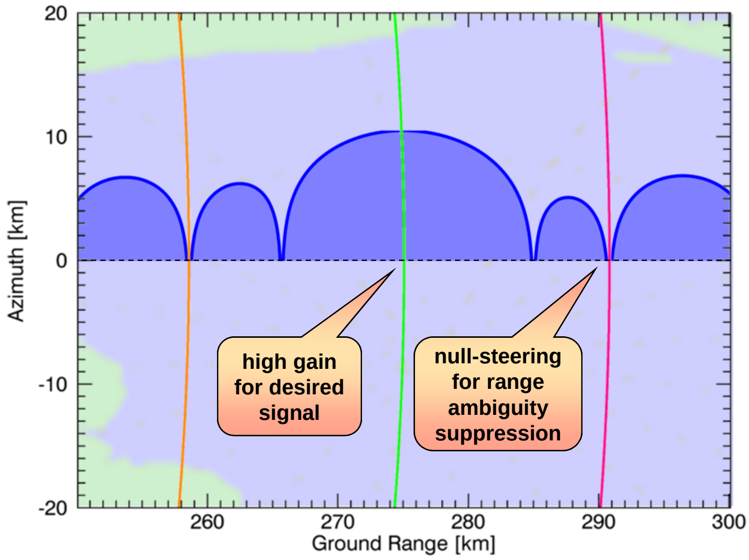

Null-Steering in Elevation: 2-D Pattern on Ground

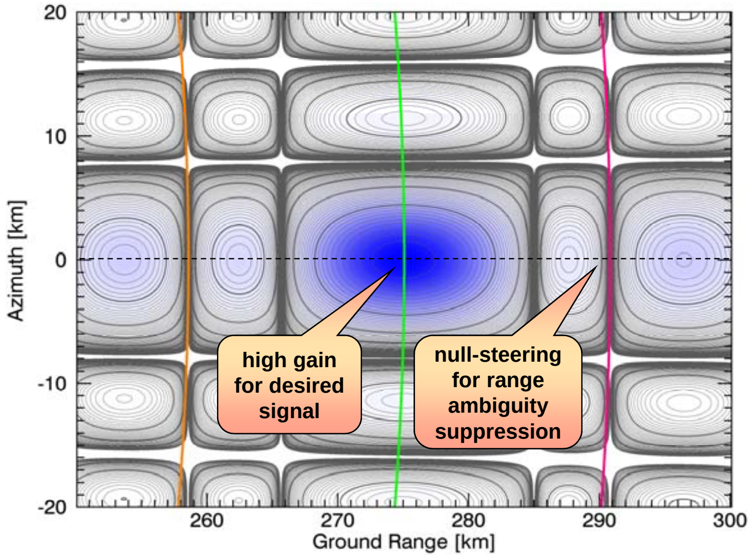

DLR

Null-Steering in Elevation: Azimuth Patterns

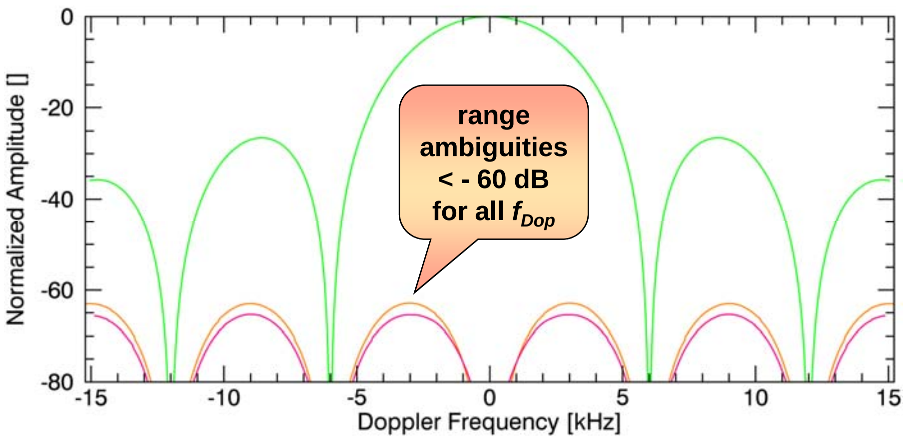

At nominal height:
- high gain for desired signal
- excellent suppression of ambiguities

DLR

Null-Steering in Elevation: Impact of Topography

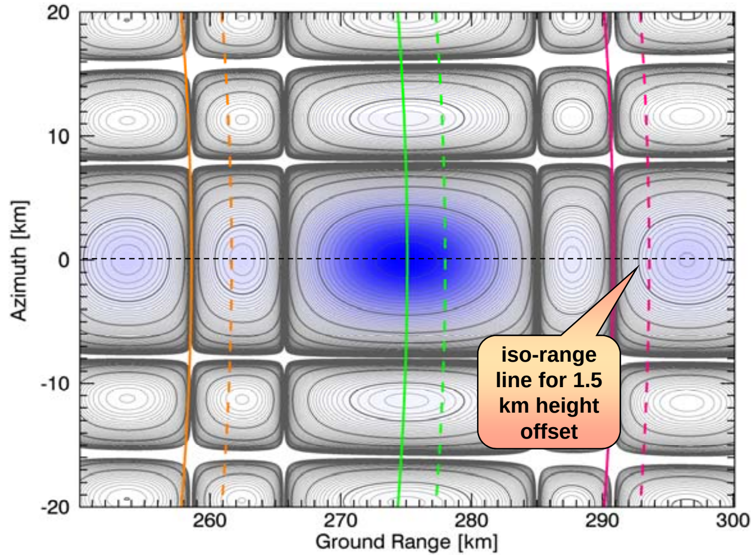

Null-Steering in Elevation: Impact of Topography

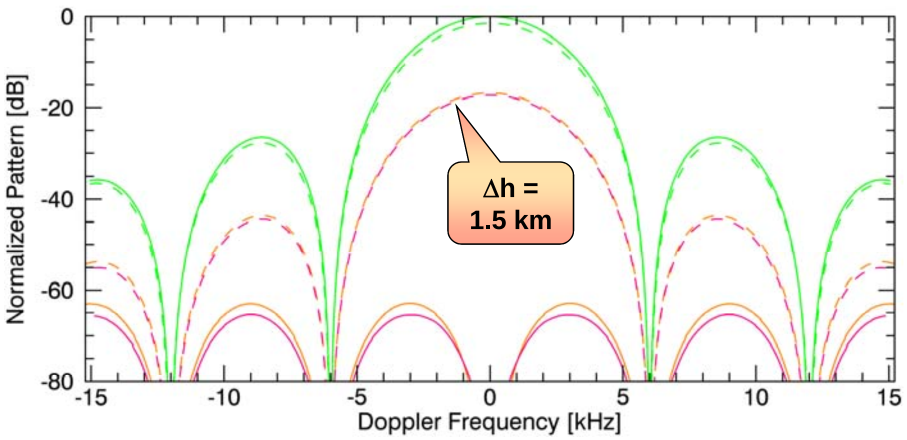

Height of 1.5 km has:
- ❑ minor impact on main beam (< 1.5 dB)
- ❑ strong impact on nulling (-60 → -17 dB)

Example 2: Range Ambiguities for Reflector DBF

Antenna diameter	d_{ant}	15 m
Feed elements	n_{el}	32
Wavelength	λ	0.236 m
Satellite height	z_{sat}	745 km
Height offset	dh	3 km
Satellite velocity	v_{sat}	7 km/s
Earth radius	r_e	6378 km
Steering angle	θ_{steer}	7.864°
PRI	$\Delta\tau$	150 μs

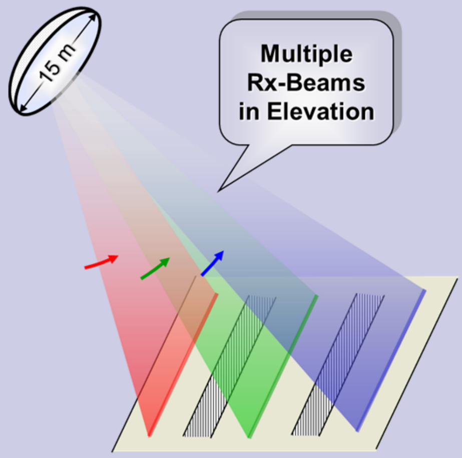

Null-Steering in Elevation: Pattern in Ground Plane

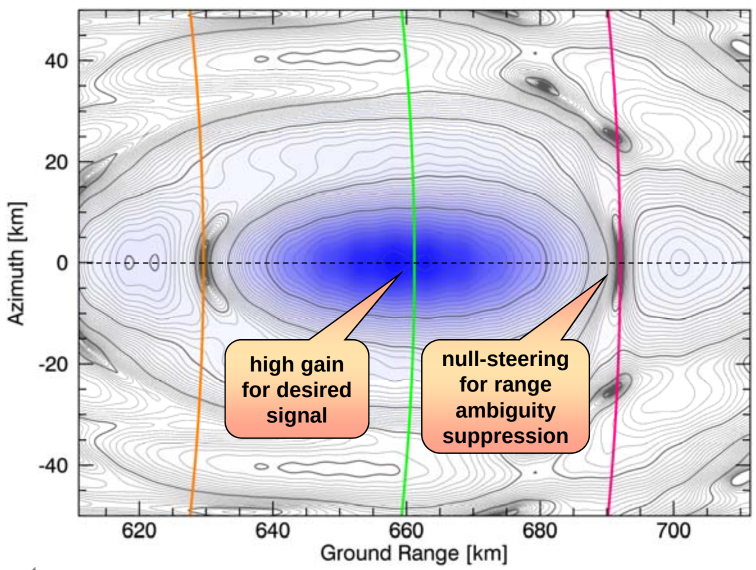

Null-Steering in Elevation: Azimuth Patterns

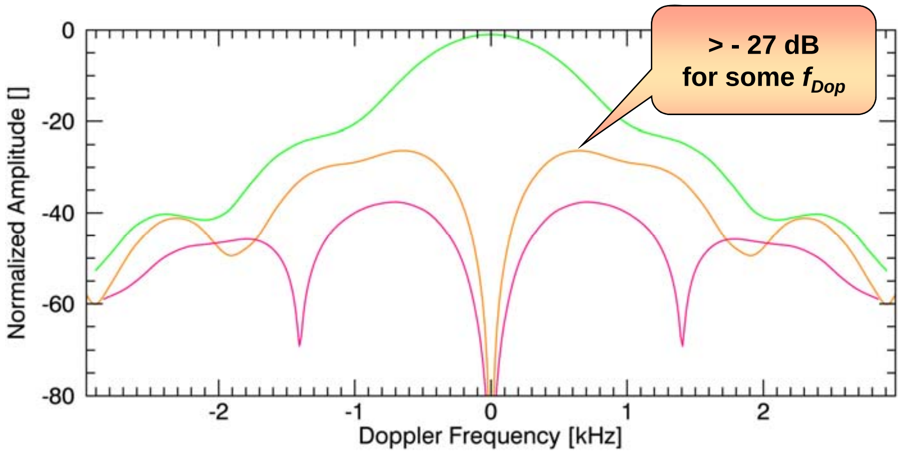

At nominal height:

- only -27 dB suppression for some f_{Dop}
- challenges fully polarimetric mode

DLR

Null-Steering in Elevation: Impact of Topography

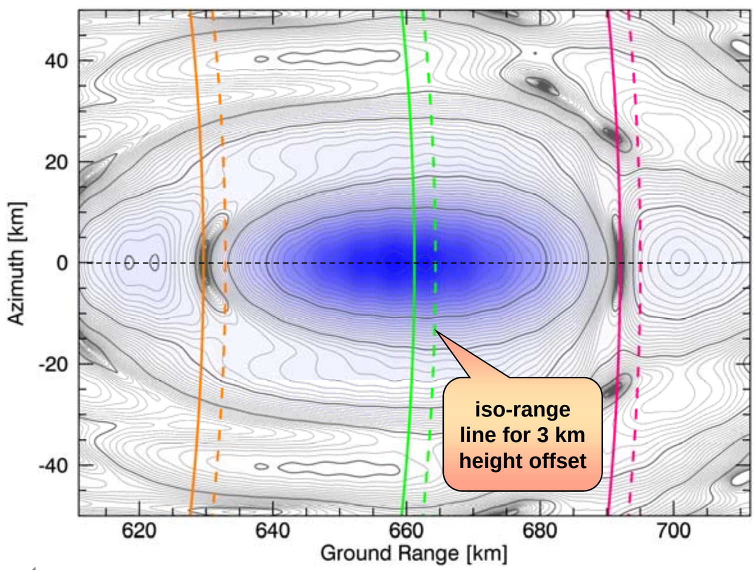

DLR

Null-Steering in Elevation: Impact of Topography

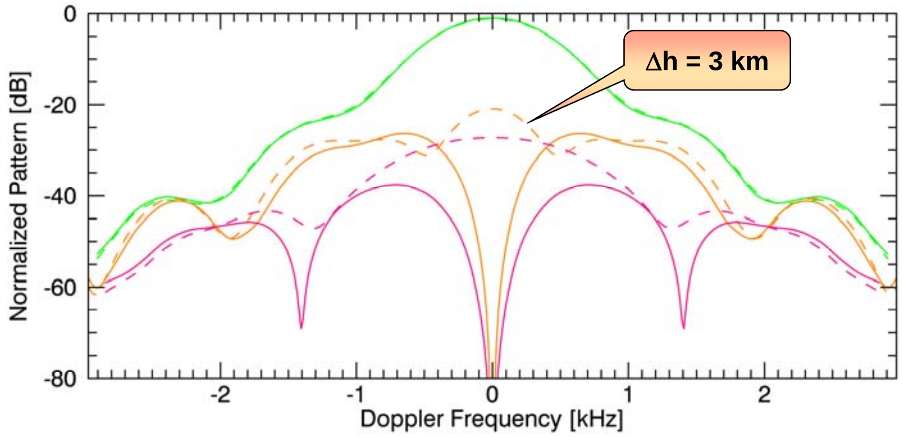

Height of 3 km has:
- negligible impact on main beam
- strong impact on nulling

CEBRAS

Cross Elevation Beam Range Ambiguity Suppression

- On-board scan-on-receive with multiple elevation beams
  - dispersive beams to account for extended pulses
  - beams follow topography (MVDR beamformer and coarse DEM)
- On-ground range ambiguity sup-pression by combining beam signals
  - beamforming in range-Doppler domain to account for topography changes in azimuth (based on high-res. DEM)
  - can take into account auxiliary data (platform orientation, calibration data, refined beam patterns, ...)

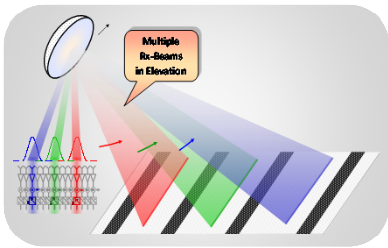

Down Link

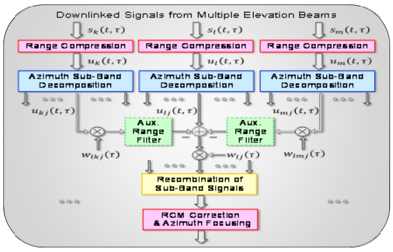

G. Krieger et al., CEBRAS: Cross elevation beam range ambiguity suppression for high-resolution wide-swath and MIMO-SAR imaging, IGARSS 2015.

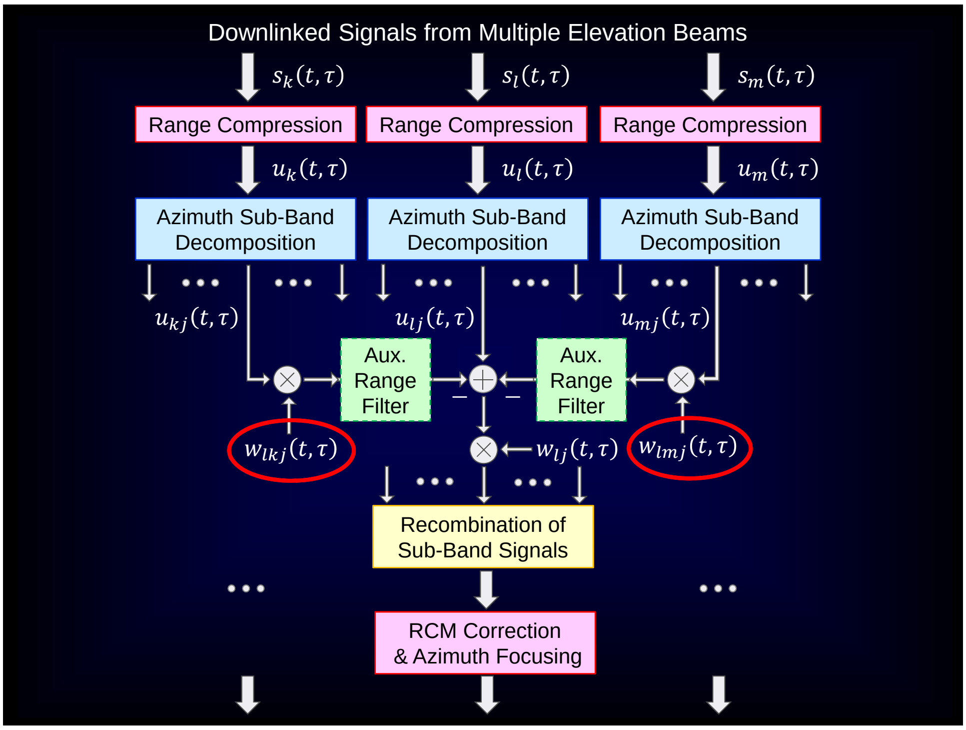

Beamforming Weights: Simple Solution

- Cancellation weights can be approximated by

$$w_{lkj}(t,\tau) = \frac{A_l(\theta_l(\tau+\tau_{kl},f_j),\varphi_l(\tau+\tau_{kl},f_j);t,\tau)}{A_k(\theta_k(\tau,f_j),\varphi_k(\tau,f_j);t,\tau)}$$

  with $\theta_k(\tau) = \theta_l(\tau+\tau_{kl})$

- Computation of beamforming weights $w_{lkj}(\tau)$ requires knowledge about
  - ❑ complex antenna patterns after real-time scan-on-receive beamforming $A_{\{k,l\}}(\theta,\varphi;t,\tau)$
  - ❑ antenna look angles $\theta_{\{k,l\}}$ and azimuth angles $\varphi_{\{k,l\}}$ of arriving wavefronts (derived from DEM together with a posteriori satellite attitude and position estimates)

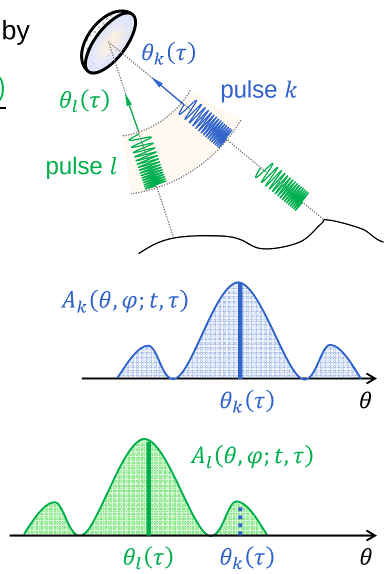

Estimation of Antenna Patterns / Cancellation Weights

- Option 1: A Priori Antenna Model
  - ❑ employ 2-D model for computation of beam patterns
  - ❑ accuracy may be challenging for reflector system
- Option 2: Calibration Data Takes
  - ❑ illuminate with low PRI and receive with multiple beams
  - ❑ topography can be emulated by varying beam trigger times
- Option 3: Cross-Correlation
  - ❑ cross-correlate signals from multiple beams
  - ❑ prone to „self-cancellation“
- Option 4: Blind Source Separation
  - ❑ unmix signals as in cocktail party effect
  - ❑ requires use of higher-order statistics

Option 2: Dedicated Calibration Data Takes

- Acquire multi-beam data without range ambiguities
  - MIMO-SAR: employ e.g. single Tx channel/sub-pulse

$$w_{12j}(t,\tau) = \frac{A_1(\theta_2,\varphi_2;t,\tau,f_j)}{A_2(\theta_2,\varphi_2;t,\tau,f_j)} = \frac{u_1(t;\tau,f_j)}{u_2(t;\tau,f_j)}$$

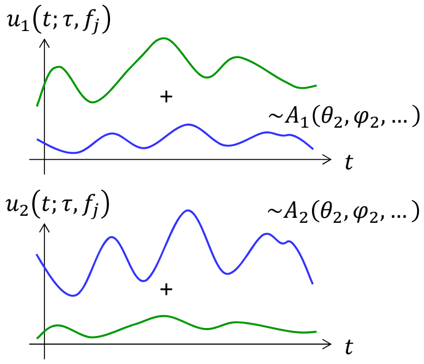

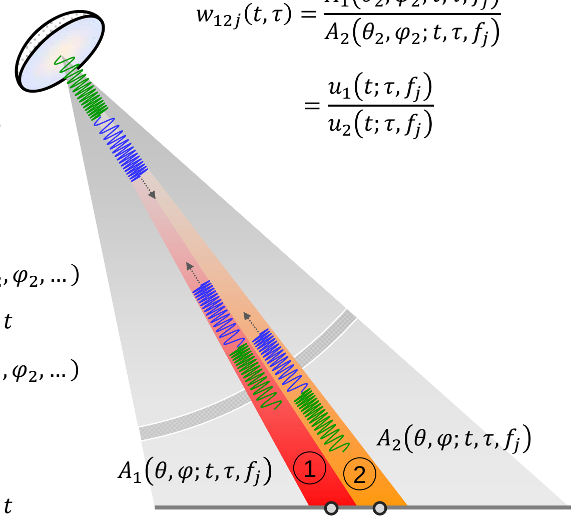

Option 3: Pattern Ratios from Cross-Correlation

- Operate SAR in nominal multiple beam mode

for all t where $|u_l(t,\ldots)| \gg |u_{\{k,m\}}(t,\ldots)|$ do

$$c_{lkj}(t;\tau) = \int u_l(t;\tau,f_j)\cdot u_k^*(t;\tau,f_j)\cdot dt$$

$\rightarrow w_{lkj}(t;\tau)$

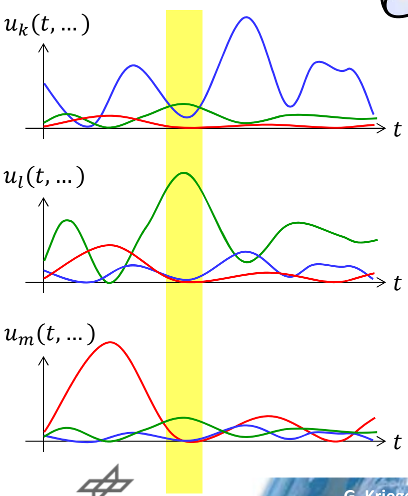

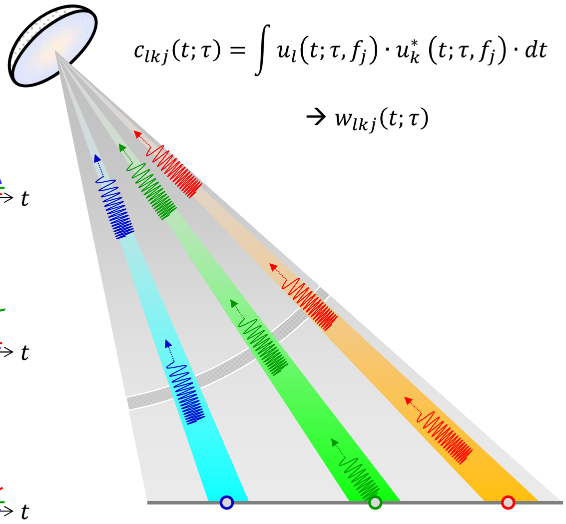

G. Krieger et al., CEBRAS: Cross-elevation beam range ambiguity suppression for high-resolution wide-swath and MIMO-SAR imaging, IGARSS 2015.

Option 4: Blind Source Separation

- Operate SAR in nominal multiple beam mode

$$\begin{bmatrix} u_1(t;\dots) \\ \vdots \\ u_N(t;\dots) \end{bmatrix} = \begin{bmatrix} a_{11} & \cdots & a_{1N} \\ \vdots & \ddots & \vdots \\ a_{N1} & \cdots & a_{NN} \end{bmatrix} \cdot \begin{bmatrix} s_1(t;\dots) \\ \vdots \\ s_N(t;\dots) \end{bmatrix}$$

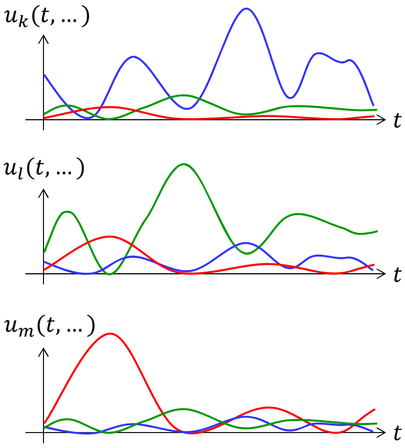

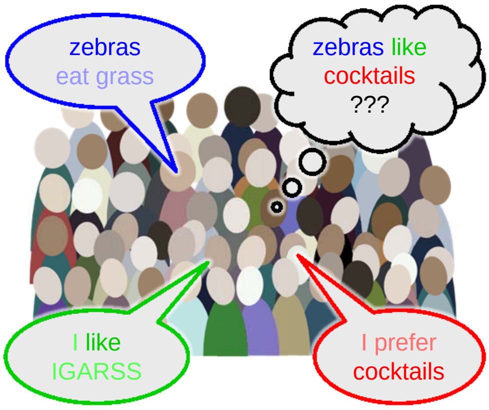

G. Krieger et al., CEBRAS: Cross-elevation beam range ambiguity suppression for high-resolution wide-swath and MIMO-SAR imaging, IGARSS 2015.

Option 4: Blind Source Separation

- Operate SAR in nominal multiple beam mode

$$\begin{bmatrix} u_1(t;\dots) \\ \vdots \\ u_N(t;\dots) \end{bmatrix} = \begin{bmatrix} a_{11} & \cdots & a_{1N} \\ \vdots & \ddots & \vdots \\ a_{N1} & \cdots & a_{NN} \end{bmatrix} \cdot \begin{bmatrix} s_1(t;\dots) \\ \vdots \\ s_N(t;\dots) \end{bmatrix}$$

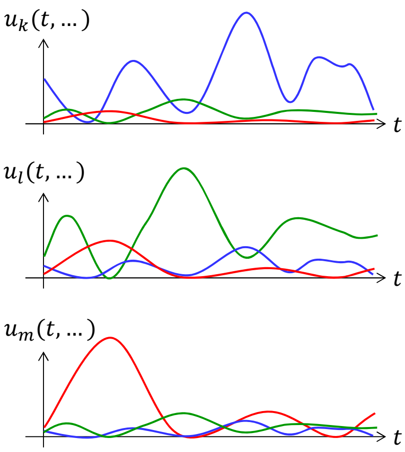

- Each recorded signal can be regarded as a linear superposition of statistically independent source signals
- Independent component analysis can be used to separate the source signals
  - entropy maximization
  - mimimize mutual information
  - higher-order decorrelation (cumulants)
  - infomax
  - ...

G. Krieger et al., CEBRAS: Cross-elevation beam range ambiguity suppression for high-resolution wide-swath and MIMO-SAR imaging, IGARSS 2015.

Option 4: Blind Source Separation

- Operate SAR in nominal multiple beam mode

$$\begin{bmatrix} u_1(t;\dots) \\ \vdots \\ u_N(t;\dots) \end{bmatrix} = \begin{bmatrix} a_{11} & \cdots & a_{1N} \\ \vdots & \ddots & \vdots \\ a_{N1} & \cdots & a_{NN} \end{bmatrix} \cdot \begin{bmatrix} s_1(t;\dots) \\ \vdots \\ s_N(t;\dots) \end{bmatrix}$$

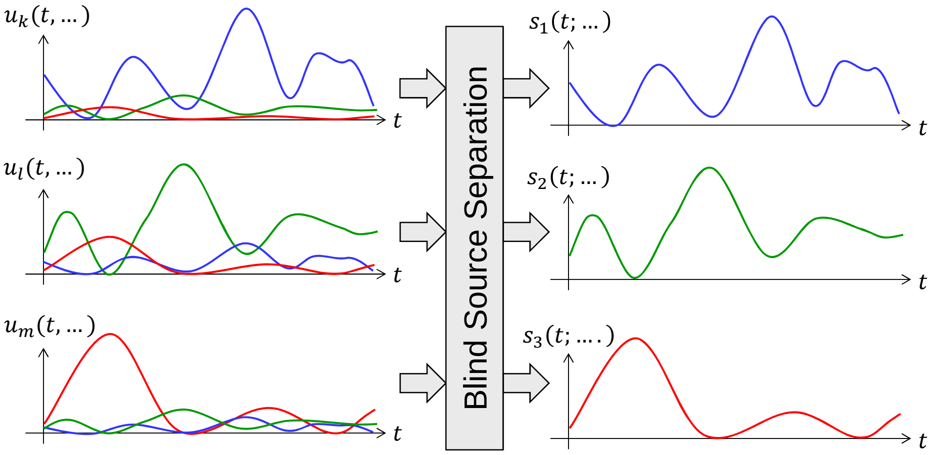

G. Krieger et al., CEBRAS: Cross elevation beam range ambiguity suppression for high-resolution wide-swath and MIMO-SAR imaging, IGARSS 2015.

MIMO SAR Design Example

MIMO-SAR Systems with Planar Arrays

MIMO-SAR	Acquisition of Additional Phase Centers for Each Tx-Pulse

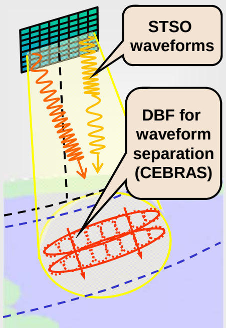

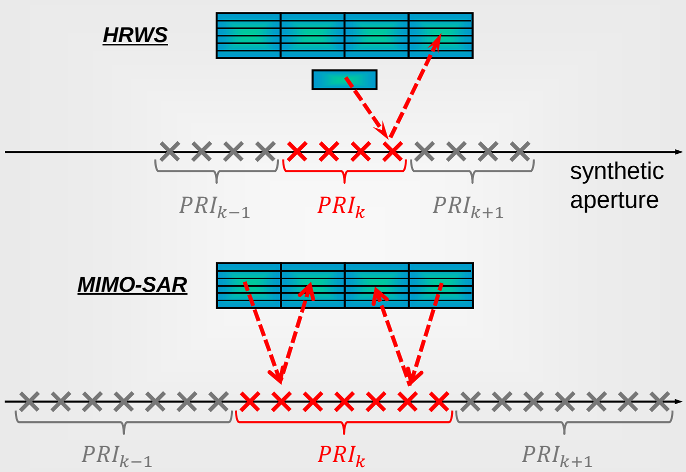

- additional phase centers for reduced antenna length
- requires high antenna to separate waveforms

DLR

MIMO-SAR Systems with Planar Arrays

MIMO-SAR	Acquisition of Additional Phase Centers for Each Tx-Pulse

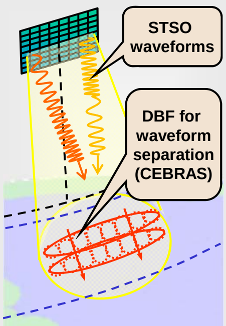

Parameter	Symbol	Value
Azimuth Resolution	δa	1 m
Swath Width	W	240 km
Orbit Height	h_{sat}	693 km

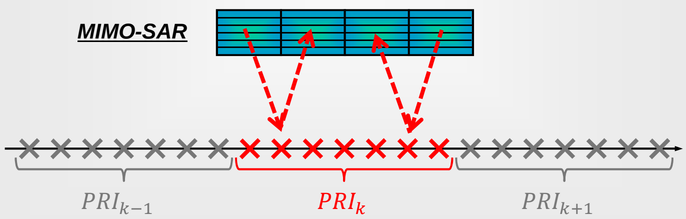

- additional phase centers for reduced antenna length
- requires high antenna to separate waveforms

DLR

MIMO-SAR Systems with Planar Arrays

MIMO-SAR	Acquisition of Additional Phase Centers for Each Tx-Pulse

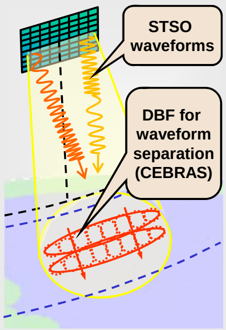

- additional phase centers for reduced antenna length
- requires high antenna to separate waveforms

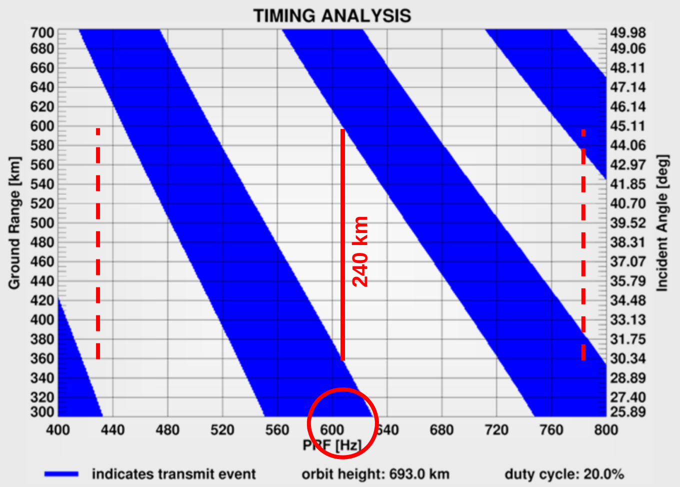

MIMO-SAR Systems with Planar Arrays

MIMO-SAR	Acquisition of Additional Phase Centers for Each Tx-Pulse

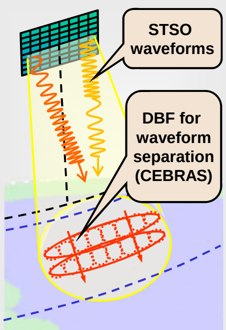

- additional phase centers for reduced antenna length
- requires high antenna to separate waveforms

Parameter	Symbol	Value
Azimuth Resolution	δa	1 m
Swath Width	W	240 km
Orbit Height	h_{sat}	693 km
Incident Angle	θ_i	30° - 45°
PRF	PRF	610 Hz

MIMO-SAR Systems with Planar Arrays

MIMO-SAR	Acquisition of Additional Phase Centers for Each Tx-Pulse

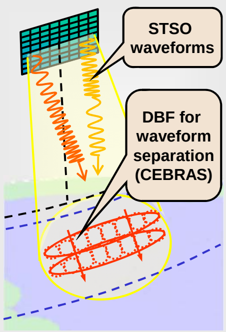

Parameter	Symbol	Value
Azimuth Resolution	δa	1 m
Swath Width	W	240 km
Orbit Height	h_{sat}	693 km
Incident Angle	θ_i	30° - 45°
PRF	PRF	610 Hz
Azimuth Channels	N_{az}	8
Antenna Length	l_{ant}	13.12 m

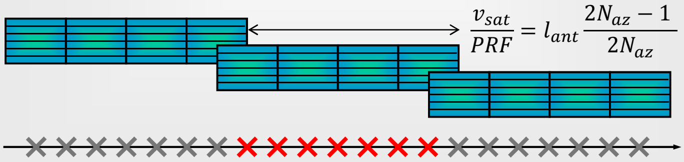

$$\frac{v_{sat}}{PRF} = l_{ant}\frac{2N_{az}-1}{2N_{az}}$$

- additional phase centers for reduced antenna length
- requires high antenna to separate waveforms

DLR

MIMO-SAR Systems with Planar Arrays

MIMO-SAR	Acquisition of Additional Phase Centers for Each Tx-Pulse

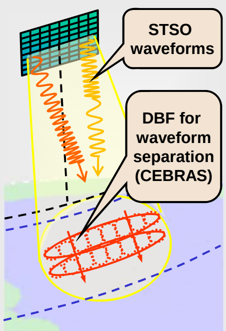

Parameter	Symbol	Value
Azimuth Resolution	δa	1 m
Swath Width	W	240 km
Orbit Height	h_{sat}	693 km
Incident Angle	θ_i	30° - 45°
PRF	PRF	610 Hz
Azimuth Channels	N_{az}	8
Antenna Length	l_{ant}	13.12 m
Sub-Aperture Length	l_{sub}	1.64 m
Duty Cycle	Δ_{duty}	20 %

- additional phase centers for reduced antenna length
- requires high antenna to separate waveforms

DLR

MIMO-SAR Systems with Planar Arrays

MIMO-SAR | **Acquisition of Additional Phase Centers for Each Tx-Pulse**

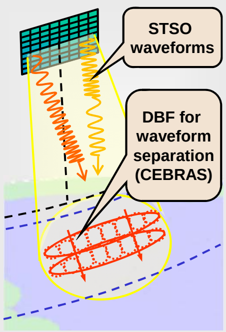

- additional phase centers for reduced antenna length
- requires high antenna to separate waveforms

Parameter	Symbol	Value
Azimuth Resolution	δa	1 m
Swath Width	W	240 km
Orbit Height	h_{sat}	693 km
Incident Angle	θ_i	30° - 45°
PRF	PRF	610 Hz
Azimuth Channels	N_{az}	8
Antenna Length	l_{ant}	13.12 m
Sub-Aperture Length	l_{sub}	1.64 m
Duty Cycle	Δ_{duty}	20 %
STSO Interval	τ_{STSO}	164 µs

$$\tau_{STSO} = (\Delta_{duty}/2) \cdot PRI$$

MIMO-SAR Systems with Planar Arrays

MIMO-SAR | ***Acquisition of Additional Phase Centers for Each Tx-Pulse***

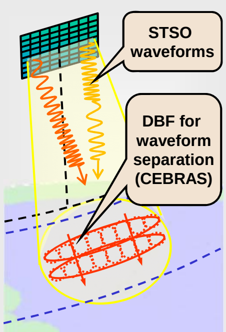

- additional phase centers for reduced antenna length
- requires high antenna to separate waveforms

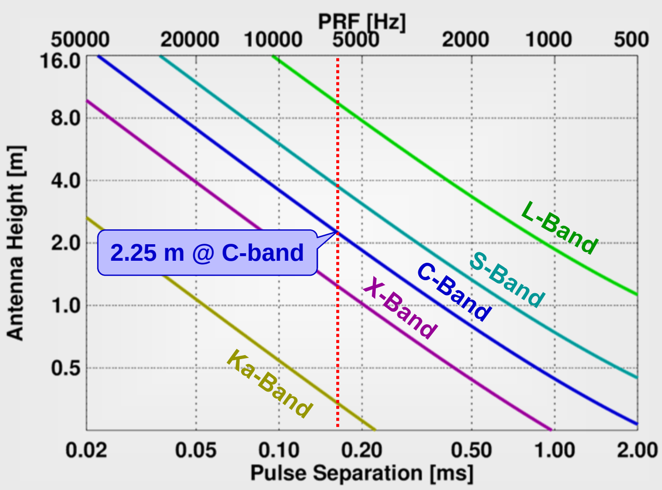

MIMO-SAR Systems with Planar Arrays

MIMO-SAR	Acquisition of Additional Phase Centers for Each Tx-Pulse

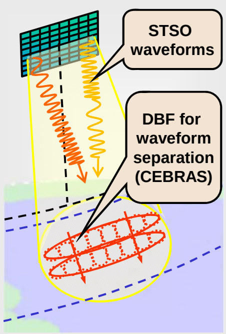

- additional phase centers for reduced antenna length
- requires high antenna to separate waveforms

Parameter	Symbol	Value
Azimuth Resolution	δa	1 m
Swath Width	W	240 km
Orbit Height	h_{sat}	693 km
Incident Angle	θ_i	30° - 45°
PRF	PRF	610 Hz
Azimuth Channels	N_{az}	8
Antenna Length	l_{ant}	13.12 m
Sub-Aperture Length	l_{sub}	1.64 m
Duty Cycle	Δ_{duty}	20 %
STSO Interval	τ_{STSO}	164 µs
Antenna Height (C-band)	h_{ant}	2.25 m

DLR

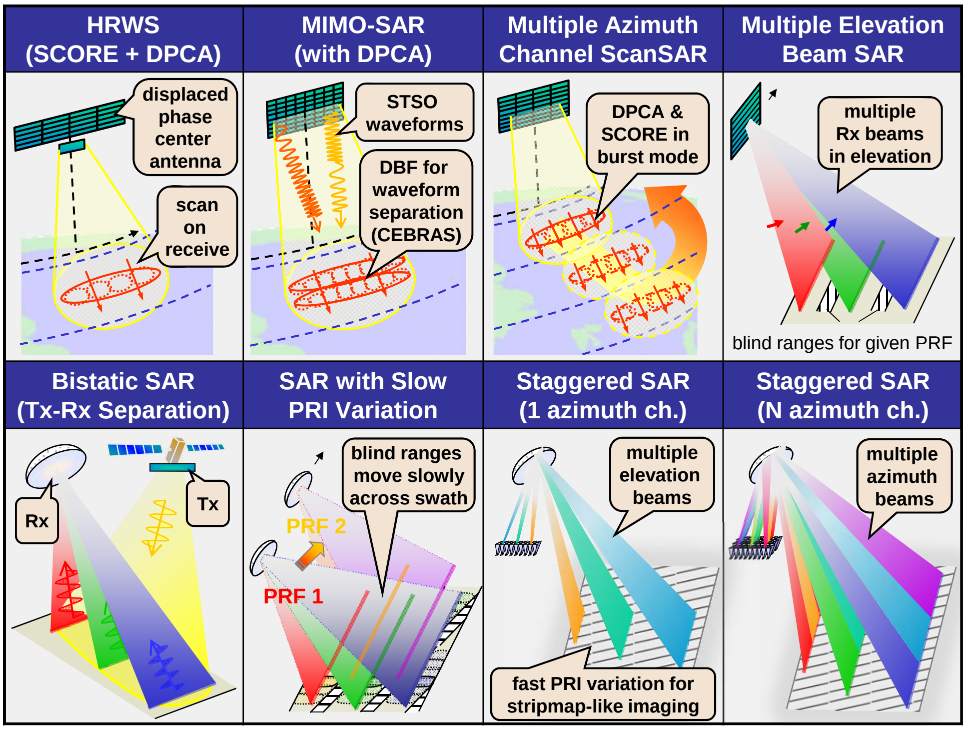

Outlook

Data Bottleneck

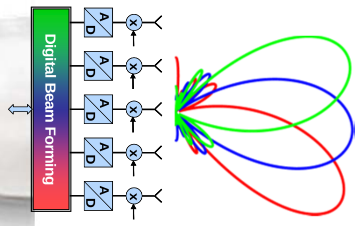

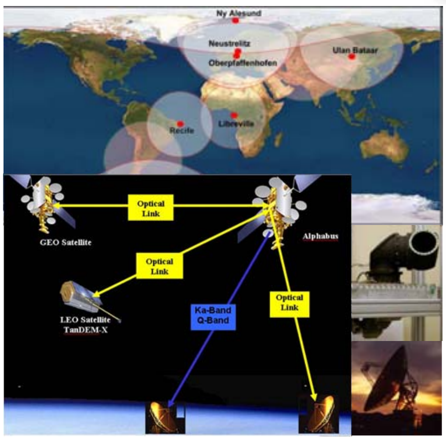

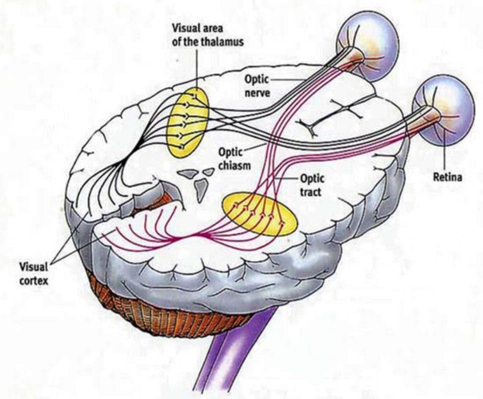

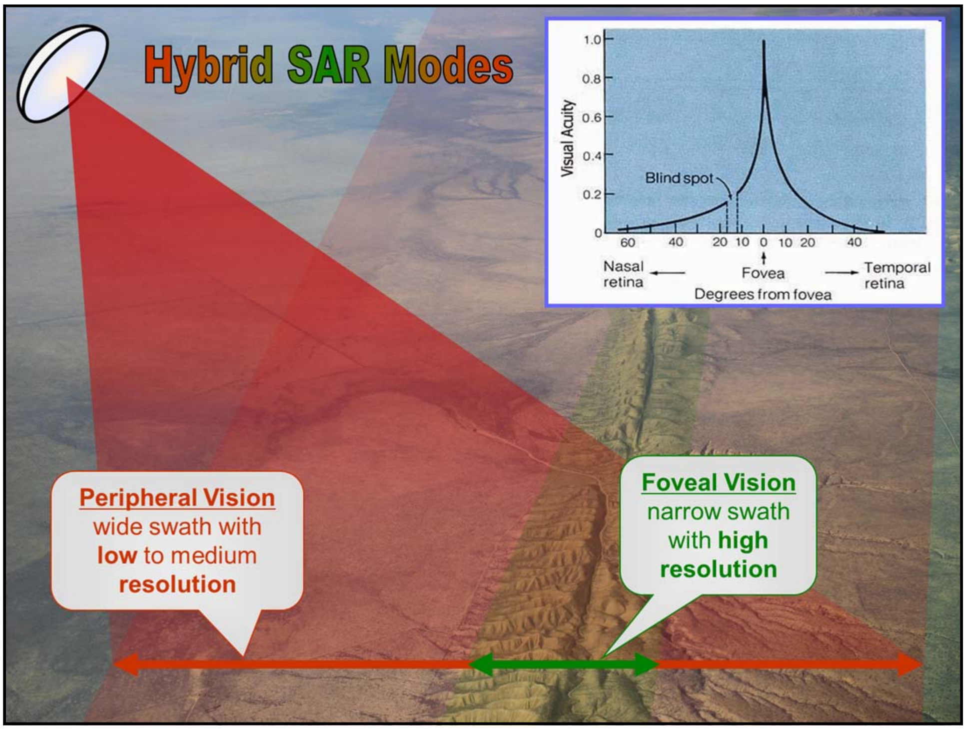
Hybrid SAR Modes
Visual Acuity
1.0
0.8
0.6
0.4
0.2
0
Blind spot
60 40 20 10 0 10 20 40
Nasal retina
Fovea
Temporal retina
Degrees from fovea
Peripheral Vision
wide swath with
low to medium
resolution
Foveal Vision
narrow swath
with high
resolution

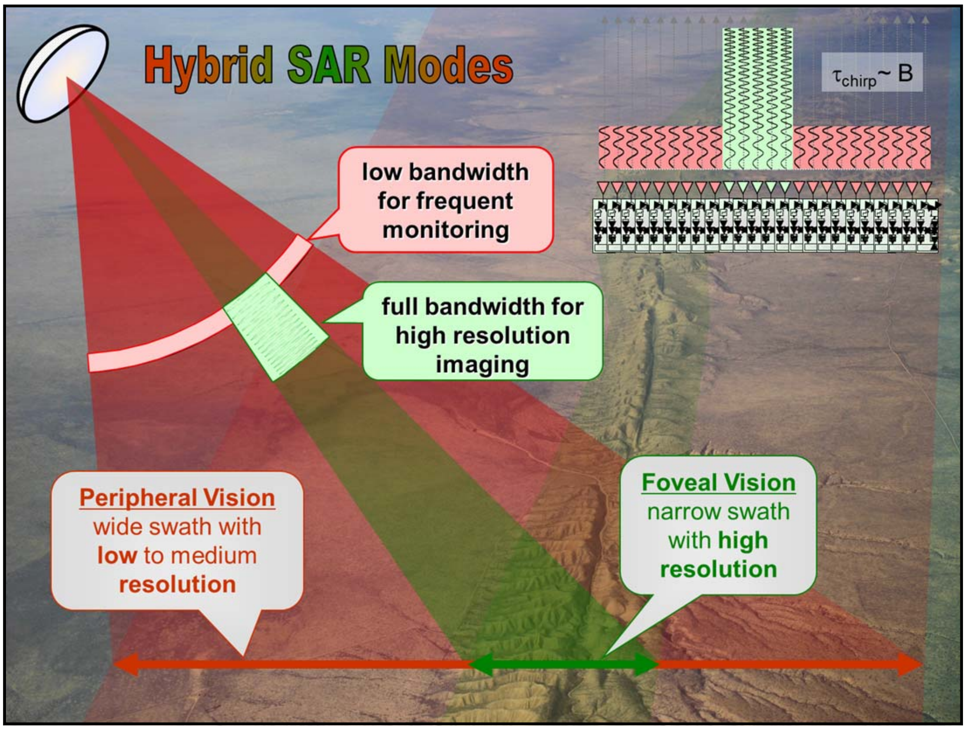
Hybrid SAR Modes
$\tau_{chirp} \sim B$
low bandwidth
for frequent
monitoring
full bandwidth for
high resolution
imaging
Peripheral Vision
wide swath with
low to medium
resolution
Foveal Vision
narrow swath
with high
resolution

Adaptive & Cognitive MIMO-SAR Systems

maximize information gain for a given power & data budget

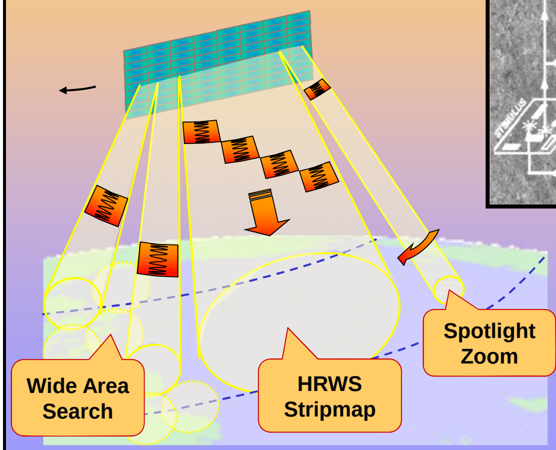

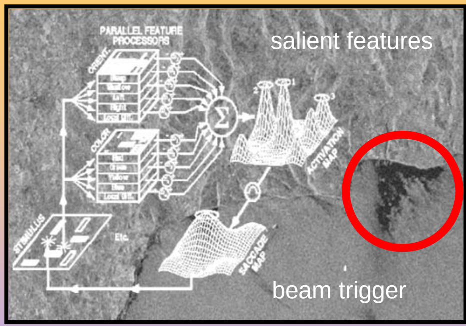

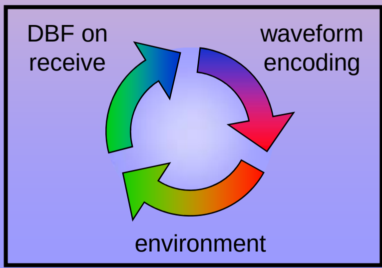

optimized distribution of system resources

Saccadic Eye Movements (Yarbus, 1967)

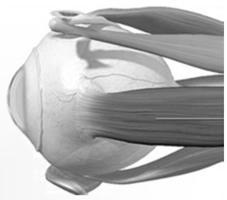

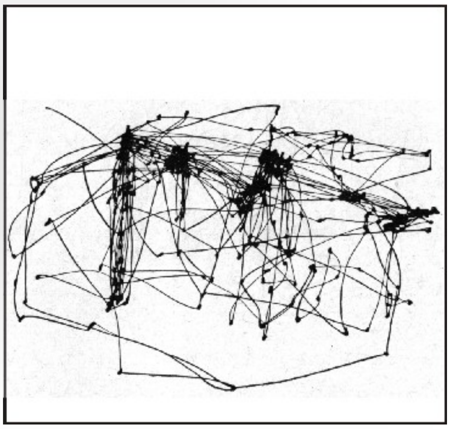

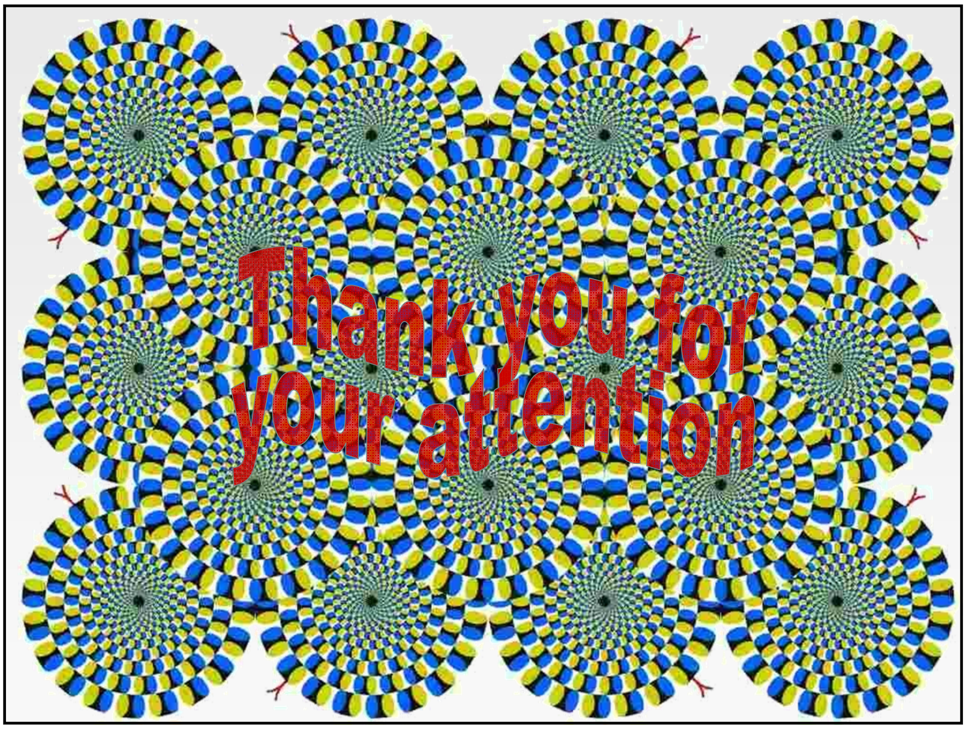
Thank you for
your attention